AD-A063 840 LOCKHEED-CALIFORNIA CO BURBANK F/G 1/2
DEVELOPMENT, EXPERIMENTAL VERIFICATION, AND APPLICATION OF PROG--ETC(U)
DEC 78 G WITTLIN DOT-FA75WA-3707
UNCLASSIFIED LR-28682 FAA-RD-78-119 NL

1 OF 2
AD A063 840

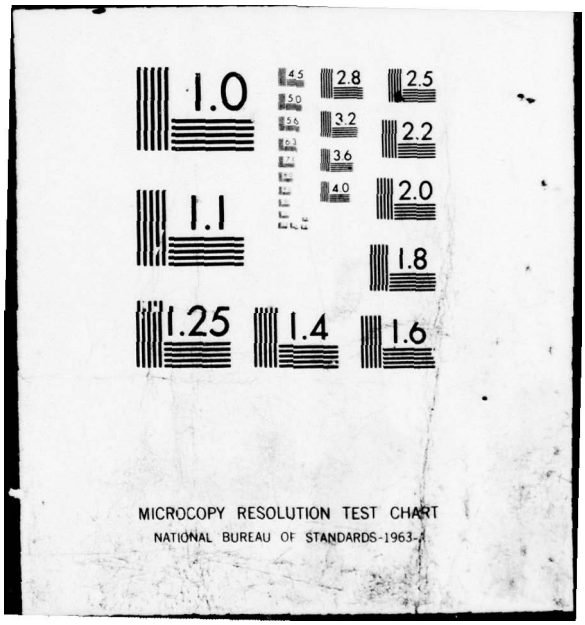
1.0
1.1
1.25
1.4
1.6
1.8
2.0
2.2
2.5
2.8
3.2
3.6
4.0
4.5
5.0
5.6
MICROCOPY RESOLUTION TEST CHART
NATIONAL BUREAU OF STANDARDS-1963-A

REPORT NO: FAA-RD-78-119

LEVEL II

Development, Experimental Verification and Application of Program 'KRASH' For General Aviation Airplane Structural Crash Dynamics

GIL WITTLIN

December 1978
Final Report

Prepared for

U.S. DEPARTMENT OF TRANSPORTATION
FEDERAL AVIATION ADMINISTRATION
Systems Research & Development Service
Washington, D.C. 20590

NOTICE

This document is disseminated under the sponsorship of the Department of Transportation in the interest of information exchange. The United States Government assumes no liability for its contents or use thereof.

Technical Report Documentation Page

1. REPORT NO.	2. GOVERNMENT ACCESSION NO.	3. RECIPIENT'S CATALOG NO.
FAA-RD-78-119		

4. TITLE AND SUBTITLE
DEVELOPMENT, EXPERIMENTAL VERIFICATION, AND APPLICATION OF PROGRAM 'KRASH' FOR GENERAL AVIATION STRUCTURAL CRASH DYNAMICS

5. REPORT DATE
December 1978

6. PERFORMING ORG CODE
L

7. AUTHOR(S)
GIL WITTLIN

8. PERFORMING ORG REPORT NO.
LR-28682

9. PERFORMING ORGANIZATION NAME AND ADDRESS
LOCKHEED-CALIFORNIA COMPANY
P.O. BOX 551
BURBANK, CALIFORNIA 91520

10. WORK UNIT NO. (TRAIS)

11. CONTRACT OR GRANT NO.
DOT-FA75WA-3707

12. SPONSORING AGENCY NAME AND ADDRESS
U.S. Department of Transportation
Federal Aviation Administration
Systems Research and Development Service

13. TYPE OF REPORT AND PERIOD COVERED
Final
Nov. 1977 - Dec. 1978

14. SPONSORING AGENCY CODE
Federal Aviation Adm.

15. SUPPLEMENTARY NOTES
Washington, D.C. 20590

The Cessna Aircraft Company participated as a subcontractor.

16. ABSTRACT

Included in this report are the results of a three-task effort to develop, experimentally verify, and apply digital computer program KRASH to structure of general aviation airplanes subjected to a survivable crash environment.

The Task I summary provides the essential results of: the evaluation of light fixed wing airplane, including operational velocity, weight, usage and occupant capacity; the evaluation of NTSB and CAMI accident data and an assessment of industry analytical requirements insofar as crash analysis is involved.

The Task II summary presents the highlights of the full-scale test preparation, the crash test condition, the crash test results, the mathematical models used to represent the crash test condition, the correlation between analysis and test results and an overview description of the KRASH User's Manual.

The Task III effort, including the parameter variation study and the application of program KRASH in the evaluation of structural design concepts during a survivable crash environment is presented in detail. The response of structure and occupants are obtained for different airplane configurations and impact condition and presented in the form of trend curves and time histories. Weight and implementation/operational cost penalties versus dynamic response changes are presented for different structural design changes.

Conclusions developed as result of the three-task effort are presented.

17. KEY WORDS (SUGGESTED BY AUTHOR(S))	18. DISTRIBUTION STATEMENT
Program KRASH, Structural Crashworthiness, Crash Dynamics, Light Fixed-Wing Aircraft, Mathematical Models, Cost-Weight Tradeoff, Full-Scale Crash Test, Trend Curves	Document is available to the public through the National Technical Information Service, Springfield, VA 22151.

19. SECURITY CLASSIF. (OF THIS REPORT)	20. SECURITY CLASSIF. (OF THIS PAGE)	21. NO. OF PAGES	22. PRICE*
Unclassified	Unclassified	166	—

Form DOT F 1700.7 (8-72) Reproduction of completed page authorized

METRIC CONVERSION FACTORS

Approximate Conversions to Metric Measures

Symbol	When You Know	Multiply by	To Find	Symbol
		LENGTH		
in	inches	*2.5	centimeters	cm
ft	feet	30	centimeters	cm
yd	yards	0.9	meters	m
mi	miles	1.6	kilometers	km
		AREA		
in^2	square inches	6.5	square centimeters	cm^2
ft^2	square feet	0.09	square meters	m^2
yd^2	square yards	0.8	square meters	m^2
mi^2	square miles	2.6	square kilometers	km^2
	acres	0.4	hectares	ha
		MASS (weight)		
oz	ounces	28	grams	g
lb	pounds	0.45	kilograms	kg
	short tons (2000 lb)	0.9	tonnes	t
		VOLUME		
tsp	teaspoons	5	milliliters	ml
Tbsp	tablespoons	15	milliliters	ml
fl oz	fluid ounces	30	milliliters	ml
c	cups	0.24	liters	l
pt	pints	0.47	liters	l
qt	quarts	0.95	liters	l
gal	gallons	3.8	liters	l
ft^3	cubic feet	0.03	cubic meters	m^3
yd^3	cubic yards	0.76	cubic meters	m^3
		TEMPERATURE (exact)		
°F	Fahrenheit temperature	5/9 (after subtracting 32)	Celsius temperature	°C

*1 in = 2.54 exactly). For other exact conversions and more detailed tables, see NBS Misc. Publ. 286, Units of Weights and Measures, Price $2.25, SD Catalog No. C13.10:286.

Approximate Conversions from Metric Measures

Symbol	When You Know	Multiply by	To Find	Symbol
		LENGTH		
mm	millimeters	0.04	inches	in
cm	centimeters	0.4	inches	in
m	meters	3.3	feet	ft
m	meters	1.1	yards	yd
km	kilometers	0.6	miles	mi
		AREA		
cm^2	square centimeters	0.16	square inches	in^2
m^2	square meters	1.2	square yards	yd^2
km^2	square kilometers	0.4	square miles	mi^2
ha	hectares (10,000 m^2)	2.5	acres	
		MASS (weight)		
g	grams	0.035	ounces	oz
kg	kilograms	2.2	pounds	lb
t	tonnes (1000 kg)	1.1	short tons	
		VOLUME		
ml	milliliters	0.03	fluid ounces	fl oz
l	liters	2.1	pints	pt
l	liters	1.06	quarts	qt
l	liters	0.26	gallons	gal
m^3	cubic meters	35	cubic feet	ft^3
m^3	cubic meters	1.3	cubic yards	yd^3
		TEMPERATURE (exact)		
°C	Celsius temperature	9/5 (then add 32)	Fahrenheit temperature	°F

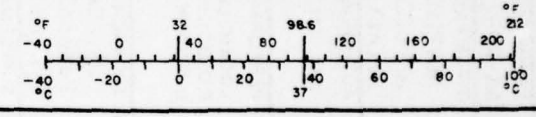

FOREWORD

This report was prepared by the Lockheed-California Company under Contract DOT-FA75-WA-3707. The report contains a summary of Task I and II effort, performed from June 1975 through December 1977 and the Task III effort covering the period from January 1978 to November 1978. The work was administered under the direction of the Federal Aviation Administration, with H. Spicer as Technical Monitor.

The project leader and principal investigator was Gil Wittlin of the Lockheed-California Company. W. L. LaBarge and M. A. Gamon of the Lockheed-California Company assisted with refinements to program KRASH. Important contributions were made to the program by the Cessna Aircraft Company under the direction of D. J. Ahrens and W. B. Bloedel.

The Lockheed effort was performed under the supervision of J. E. Wignot, Dynamic Loads Group; and R. F. O'Connell, Aeromechanics Department.

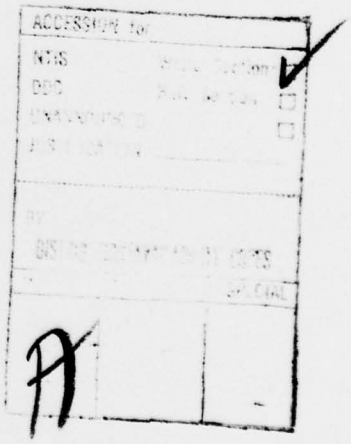

SUMMARY

Presented herein are the results of a three-task effort to develop, experimentally verify, and apply digital computer program KRASH to structures of general aviation airplanes subjected to a survivable crash environment and to show that it can be used as a design tool for predicting vehicle gross behavior, structural deformations, and structure and occupant responses for survivable crash conditions. The efforts described herein represent a significant step towards developing methods that can be used in the evaluation of future crashworthy designs.

Included are summaries of the previously documented Task I and Task II efforts. The Task I effort summary provides the essential results of: the evaluation of light fixed-wing airplanes, including operational velocity, weight, usage and occupant capacity; the evaluation of NTSB and CAMI accident data with regard to the various airplane categories; and an assessment of industry capability and needs insofar as computerized analytical requirements are concerned. The Task II effort summary presents the highlights of the full-scale test preparation, the crash test conditions, the crash test results, the mathematical models used to represent the crash test conditions, the correlation between analysis and test results, and an overview description of the KRASH User's Manual documentation.

Program KRASH modifications and refinements are briefly described for each of the three tasks in which the changes are applicable.

The Task III effort, including the parameter variation study and the application of Program KRASH in the evaluation of structural design concepts during a survivable crash environment is presented in detail. Three light fixed-wing airplanes representing different weight, usage, constructions, and category type are modeled and analyzed for comparable nose-up and nose-down impact conditions. One of the airplanes modeled is used as the basis for investigating

structural responses and deformations as a function of impact speed, angle, and terrain variation. The responses of the structure and occupants are obtained and trend curves established. The effect of structural design changes on the crashworthiness capability of an airplane is determined using program KRASH to evaluate airframe changes involving the underside of the fuselage, the wing fuselage attachment, the seat, and the engine installation design. The increased crashworthiness along with the associated weight and the implementation/operational cost penalties are used to assess the trade-offs between various concepts.

The KRASH Programmer's Manual, developed during Task III, and the Industry Workshop and Seminar, to be held during Task III, are also discussed.

Conclusions developed as a result of the three-task effort are presented.

LIST OF FIGURES

LIST OF FIGURES (Continued)

TABLE OF CONTENTS

TABLE OF CONTENTS (Continued)

LIST OF TABLES

LIST OF TABLES (Continued)

LIST OF FIGURES (Continued)

LIST OF TABLES (Continued)

SECTION 1

INTRODUCTION

1.1 BACKGROUND

This report summarizes the development, experimental verification and application of a mathematical model to predict structural dynamic response of general aviation airplane structures in a survivable crash environment and to facilitate the future development of improved structural crashworthiness designs.

The results of Task I and II, described in detail in References 1 and 2 show that program KRASH is a viable tool for assisting in the performance of structural crashworthiness analysis of light fixed-wing general aviation airplane configurations for which an analytical method for evaluating structural crashworthiness capabilities and improvements would be valuable. Via correclation of analytical results with test data obtained from four fully instrumented full-scale crash tests encompassing several crash impact conditions, Task II demonstrates that program KRASH is capable of assisting the general aviation industry in developing future improved structural crashworthiness designs. The highlights of Tasks I and II are briefly summarized in this report prior to describing the Task III achievements.

TASK III Effort

While both Task I and II efforts have helped to boost confidence in the use of an analytical tool to assist designers, neither effort demonstrated application of the program. Task III has as its objectives:

- Demonstrating the application of program KRASH in the evaluation of current and future general aviation airplane structural designs in a survivable crash environment.

- Demonstrating the manner in which program KRASH can assist in trade-off decisions involving weight, cost, and benefit.

- Transferring KRASH application experience and associated structural crashworthiness modeling guidelines to the general aviation industry.

To achieve the Task III objectives, program KRASH is used to perform parameter variation studies involving several current general aviation airplane configurations over a wide range of impact conditions and is applied to the evaluation of potential structural crashworthiness design improvements for which the associated weight and cost are available. In addition, several steps are taken in Task III to transfer the knowledge of the usage of and the experience gained with KRASH to the general aviation industry. This has been done in the following manner:

- A Programmer's Manual, developed during Task III and documented in Reference 3, has been made available to provide a better understanding of how program KRASH is organized. This document, combined with the KRASH User's Manual (References 4,5,6) gives the users a complete set of documentation, including theory, input-output format, usage guidelines, application techniques, programming details, and general design background.

- Assistance with the Cessna Aircraft Company in making a current version of KRASH operational at their facility.

- Indoctrination of industry members in the use of program KRASH as a tool in the support of crash analysis of airplane structural designs through the performance of a KRASH Workshop and Seminar at the conclusion of this FAA-sponsored effort.

SECTION 2

SUMMARY OF TASK I RESULTS

2.1 EVALUATION OF GENERAL AVIATION AIRPLANE CONFIGURATIONS

During Task I, a total of 61 general aviation basic airplane models, produced by the seven leading domestic manufacturers in the industry, were reviewed with regard to their operational usage and structural design characteristics. While not all-inclusive, the data is representative of more than 95 percent of the general aviation airplanes currently in operation. Pertinent information such as: probable usage, approximate maximum cruise (75 percent power) and stall speed (flaps down), number of engines, wing position, type of structure and passenger accommodations is noted. The data is compiled from Reference 7 and discussions with industry airplane design personnel. A complete list of airplane manufacturers and their respective models from which the data is compiled is presented in Reference 1 (Section 2.2).

Included in the review and evaluation of general aviation airplane characteristics are:

- A matrix of airplane configurations, maximum takeoff weight and usage
- A description of structural design characteristics of current general aviation airplanes
- A description of the various general aviation airplane types
- A categorization of airplanes as a function of configuration, maximum takeoff weight, stall speed, cruise speed, usage and accommodations.

The results of the study show that:

- There are four basic airplane configurations; single-engine low-wing, single-engine high-wing, twin-engine low-wing and twin-engine high-wing.
- With the exception of the agricultural airplane most airplanes have multiple uses.
- There is a trend, insofar as usage, accommodations, weight and speed characteristics are involved, which leads to a logical grouping of the airplanes by categories.
- While there are many manufacturers and airplane models and the design details of the structure may vary, there are only two basic structural designs: monocoque and tubular.

A plot of airplane maximum cruise and flaps down stall speeds as a function of maximum takeoff weight for the different airplane models reviewed during this effort, is presented in Figure 2-1. The envelope reflects a practical range of velocities that would emcompass most crash conditions which will aid in establishing the crash environment.

The categories of usage associated with general aviation airplanes are listed below:

- Agriculture.- Application of chemicals or seeding crops involving low-altitude flight maneuvering.
- Sport, aerobatic.- Performance of sporting and aerobatic functions usually involving high maneuvering load factors.
- Training.- Used for instructional purposes usually involving initial flight training. Some of the larger airplanes may be classified as trainers for instrument rating purposes which is not the usage that would lead to the accidents encountered in initial flight training operation.
- Business, executive.- This category may overlap into several areas, such as transport, cargo, and in a few cases testing and developing equipment. These airplanes in some cases may operate out of uncontrolled airfields.
- Commuter, transport, air taxi.- Used to carry people for commercial purposes in very short-range flights and may include operations from uncontrolled airfields.

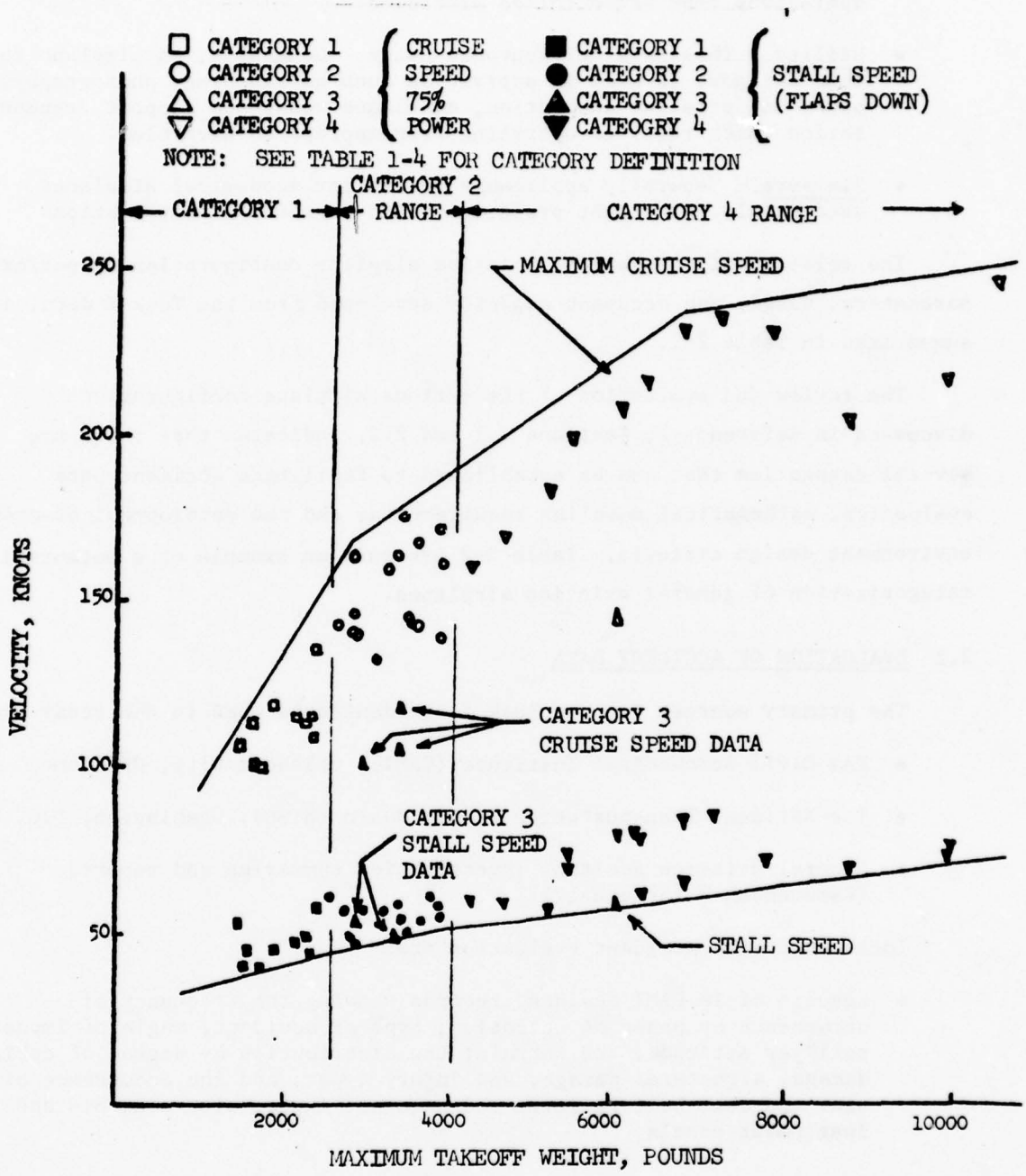

Figure 2-1. Operational Velocity/Weight Envelope for Current General Aviation Airplanes (Reference 1)

- Cargo, freight.- Hauling of freight or cargo which can include operations from uncontrolled airfields.

- Utility.- This is a multipurpose usage. Generally, an airplane in this category is used in activities such as ranching, photography, power and pipeline inspection, ambulance work, and support transportation which requires operating from unprepared airfields.

- Pleasure.- Generally applicable to smaller economical airplanes used mainly for flight proficiency and personal transportation.

The relationship of general aviation airplane configuration to performance parameters, usage, and occupant capacity developed from the Task I data, is summarized in Table 2-1.

The review and evaluation of the various airplane configurations discussed in Reference 1, Sections 2.1 and 2.2, indicates that there are several categories that can be established to facilitate accident data evaluation, mathematical modeling requirements, and the development of crash environment design criteria. Table 2-2 presents an example of a potential categorization of general aviation airplanes.

2.2 EVALUATION OF ACCIDENT DATA

The primary sources for the Task I accident data used in the study are:

- FAA Civil Aeromedical Institute (CAMI), Oklahoma City, Oklahoma

- The National Transportation Safety Board (NTSB), Washington, D.C.

- General aviation accident investigation summaries and reports (References 8 through 12)

Included in the accident evaluation are:

- Results of 18 CAMI accident records showing the frequency of occurrence by phase of operation, type of accident, angle of impact roll/yaw attitude, and terrain; the distribution by degree of cabin damage, structural damage, and injury types; and the occurrence of seat and seat belt failures and occupant impact with controls and instrument panels.

TABLE 2-1. RELATIONSHIP OF GENERAL AVIATION AIRPLANE CONFIGURATIONS TO PERFORMANCE PARAMETERS, USAGE AND OCCUPANT CAPACITY (REFERENCE 1)

Airplane Configuration	Maximum Takeoff Weight (Pounds)	Stall Speed Range, Flap Down (Knots)	Cruise Speed Range, 75 Percent Max. Power (Knots)	Primary Usage	Occupant Capacity
Single-Engine Low-Wing	< 2500	49-54	108-128	Training Pleasure	1-4
Single-Engine High-Wing	< 2500	38-45	100-114	Training Pleasure Aerobatics	2-4
Single-Engine Low-Wing	2500-4000	49-61	132-176	Business Commuting Training Utility	4-7
Single-Engine High-Wing	2500-4000	45-59	124-163	Business Utility Cargo	4-7
Single-Engine (a) Low-Wing	2900-6000	47-59	101-138	Agriculture	1
Twin-Engine Low-Wing	3700-10900	59-82	162-247	Commuting Business Cargo Commuting	4-17 (b)
Twin-Engine High-Wing	4600-10250	61-77	170-280	Business Cargo Commuting	4-11

(a) Includes one biplane

(b) 17 occupants for 1 airplane only, otherwise maximum is 11

TABLE 2-2. CATEGORIES FOR GENERAL AVIATION AIRPLANES (REFERENCE 1)

Category	Airplane Configuration	Maximum Takeoff Weight (Pounds)	Stall Speed Range, Flap Down (Knots)	Cruise Speed Range, 75 Percent Max. Power (Knots)	Primary Usage	Occupant Capacity
1	Single-Engine A. Low-Wing B. High-Wing	<2500	38-54	100-128	Training Sport Aerobatic Pleasure	1-4
2	Single-Engine A. Low-Wing B. High-Wing	2500-4000	45-61	124-176	Business Utility Commuting Training	4-7
3	(a) Single-Engine Low-Wing	2900-6000	50-53	101-122	Agriculture	1
4	Twin-Engine A. Low-Wing B. High-Wing	>4000-10900	59-82	162-280	Business Cargo Commuting	4-11 (b)

(a) Includes one biplane

(b) Except for 1 airplane accommodates 17

- A description of a Cessna Aircraft Company computer program, developed during this task, to sort and process selected pertinent crashworthiness accident data from NTSB data tapes.

- Results of 1971 through 1973 NTSB accident records, encompassing 8491 accidents, obtained from the accident computer program employing the airplane caterories established during this task.

The results of the accident data evaluation indicate that:

- The impact angle in a crash is predominantly ≤ 45 degrees.

- Stall, collisions with ground/water and collisions with obstacles are the prevalent types of accidents which result in serious or fatal injuries.

- In accidents wherein injuries are involved, light weight, single-engine airplanes have a greater number of stall accidents than accidents involving collision with ground/water or obstacles. Conversely, heavier weight single-engine and twin-engine airplanes experience more accidents involving collision with the ground.

- The personnel involved in agricultural type airplane accidents, wherein injuries occur, experience less fatalities per occupant in all types of accidents.

- The ratio of fatalities to number of occupants, for accidents involving injuries, is generally lower for the single-engine airplane than the corresponding ratio for twin-engine airplanes for the same type of accident.

The NTSB accident summary for 1971 through 1973 includes a survey of 8491 accidents of which 8030 (95%) involved airplane models that are used to establish the different airplane categories presented in Table 2-1.

Table 2-3 provides a summary of the accident data using the different categories of accidents, and the accident data pertinent to the models within each of the categories. Ratio No. 1 is for all accident types and relates the total number of occupants involved in all accidents. The ratio is defined below as:

$$\text{Ratio No. 1} = \frac{\text{total number of fatalities}}{\text{total number of occupants}} \quad \text{(all accidents)}$$

TABLE 2-3. SUMMARY OF ACCIDENT DATA EVALUATION (NTSB DATA 1971 THROUGH 1973) (REFERENCE 1)

Category (a)	Number of Accidents Surveyed	Ratio No. 1 (b)	Ratio No. 2 (c)			Order of Occurrence of Accident Type (Percent Distribution (d))		
			Stall	Collision with Ground	Collision with Obstacle	Stall	Collision with Ground	Collision with Obstacle
1 (<2500)	4502	.122	.428	.654	.325	1(37.5)	3(29.2)	2(33.3)
2 (>2500)	2245	.149	.422	.722	.523	3(22.3)	1(49.1)	2(28.6)
3 (Agriculture)	601	.081	.300	.222	.273	2(39.0)	3(6.5)	1(54.5)
4 (2 Engines)	682	.283	.733	.787	.697	3(21.3)	1(44.3)	2(34.4)
All Categories	8030	.147	.455	.707	.390	3(32.5)	2(33.6)	1(33.9)

(a) See Table 1-4 For Complete Definition of Categories

(b) Ratio No. 1 = (Total Number of Fatalities/Total Number of Occupants) All Accidents

(c) Ratio No. 2 =(Number of Fatalities/Number of Occupants) For a Particular Accident Type Involving an Injury

(d) Accident Types Involving an Injury. Percentage distribution is for the three types shown. Applicable to the Ratio No. 2.

Ratio No. 1 identifies the more crashworthy categories of airplanes, whether it be due to the structural design or the crash environment, to be those with lower ratios than that of the composite of all airplanes. On this basis the smaller lighter weight airplanes and the agricultural airplanes appear to be more crashworthy than the other airplanes.

The data presented in Table 2-3 indicates that the most probable accident for the lighter weight airplanes (<2500 pounds) is a stall condition. The most fatal accidents for heavier weight airplanes (>2500 pounds) are associated with collisions with ground or water. This particular type of accident can be either controlled or uncontrolled in nature. The NTSB information does not provide sufficient data with which to delineate between the two situations. Miscellaneous accidents, such as a hard landing, undershoot, overshoot, ground swerve, generally do not result in fatalities. The 1971 through 1973 NTSB data indicates that less than 5 percent of the occupants involved in these types of accidents received fatal injuries. This value is extremely low by comparison to the overall average of 45.5, 70.7, and 39 percent, respectively, for all categories of airplanes involved in the three major accident types shown in Table 2-4.

Of the three major accident types, the most survivable appears to be an accident which is initiated by contact with some obstacle. One possible reason for this is that this type of accident occurs close to the ground at reduced airplane operating speeds (i.e. landings, approaches, and takeoffs) and the impact angle usually is flat. The least chance of occupant survival occurs in collisions with the ground. With the exception of agricultural airplanes, at least 62 percent of the occupants that are involved in this type of accident sustain a fatal injury. While collisions with the ground represent a wide range of accidents (e.g. forced landings, bad weather, misjudged altitude and/or clearance), most of the accidents generally occur at speeds approaching that of cruise.

The agriculture airplanes (Category 3) which have a takeoff weight comparable to that of the single-engine airplanes used primarily for business, utility, commuter and cargo purposes (Category 2), demonstrate

TABLE 2-4. SUMMARY OF ACCIDENT DATA FATALITIES TO OCCUPANTS INVOLVED BY SUBCATEGORIES AND ACCIDENT TYPES (NTSB DATA 1971 THROUGH 1973) (REFERENCE 1)

Subcategory (a)	Number of Accidents Surveyed	Ratio No. 2 (b), Percent			Deviation from Mean Average Value of Ratio No. 2 (c) for Category (Percent)		
		Stall	Collision with Ground	Collision with Obstacle	Stall	Collision with Ground	Collision with Obstacle
1A Low-Wing	1595	38.6	66.3	38.3	±8.5	±1.1	±15
1B High-Wing	2907	45.7	64.5	28.3			
2A Low-Wing	933	43.	56.8	35.3	±5.4	±8.5	± 1.4
2B High-Wing	1312	38.5	67.4	34.2			
4A Low-Wing	583	74.3	78.3	66.1	±2.6	±1.5	±11.5
4B High-Wing	99	70.4	80.8	83.3			

(a) See Table 4 for definition of subcategories

(b) Ratio No. 2 = (Number of fatalities/number of occupants) (for a particular accident type involving an injury and/or a fatality)

(c) Based on average of low and high-wing ratio values for each type of accident

considerably more crashworthiness capability for all the three major accident types. Factors that most likely account for this difference are:

- Agricultural airplanes are designed with specific crashworthy features (overturn pylon, long fuselage, harness, isolated cockpit) that are compatible with their mission.
- Agriculture airplanes may crash under more controlled conditions, usually after hitting some obstacle.
- The pilots of agricultural airplanes generally are more experienced in emergency conditions than the average general aviation pilot.

While the agricultural airplanes provide a greater chance of occupant survivability during a crash, the pilot will sustain a fatal injury in about 30 percent of the accidents in which injuries occur.

The data presented in Table 2-4 indicate that benefits due to improvements in crashworthiness design for the twin-engine airplanes may provide the biggest payoff in reducing the degree of severe or fatal injuries that are sustained relative to the number of people involved. However, on an absolute basis there have been substantially more fatalities in single-engine airplane accidents than in twin-engine airplanes because there are substantially more single-engine airplanes in operation. Therefore, from a life-saving point of view, if a priority is to be assigned, emphasis should be placed on upgrading the crashworthiness characteristics of single-engine airplanes.

Table 2-4 sets forth the accident data for the categories wherein a distinction is made between a low-wing configuration and a high-wing configuration and indicates that:

- With the exception of the comparisons between high-wing and low-wing configurations for both light airplanes (<2500 pounds) and two-engine airplanes in accidents involving collision with obstacles, the deviation from the mean value does not exceed ± 8.5 percent for all accident types and airplane categories noted in Table 2-4. This trend indicates that for the airplane and accidents considered and the period of time covered (1971-73) the location of the wing, for a particular category of airplane, is not very significant with regard to fatality potential in injury incurred accidents.

- The low-wing, single-engine airplane experiences approximately the same rate of fatalities in accidents involving stall as do the high-wing, single-engine configurations. The data for the lower weight (<2500 pounds) airplane indicate a slightly higher fatality rate for the high-wing airplane (45.7 versus 38.6 percent). This trend is reversed for the higher weight (2500-4000 pound) category (38.5 percent versus 43 percent).

- The lower weight (< 2500 pounds) low-wing, single-engine airplanes experience approximately the same rate of fatalities in accidents involving collision with ground/water as do the high-wing, single-engine airplanes (66.3 versus 64.5 percent). For the heavier weight (2500 to 4000 pounds) single-engine airplanes, the fatality rate for the ground/water type of accident is slightly in favor of high-wing configurations (67.4 versus 56.8 percent).

- The heavier weight (2500 to 4000 pounds) low-wing, single-engine airplanes experience approximately the same rate of fatalities in collision with obstacle-type accidents as compared to the high-wing configuration (35.3 versus 34.2 percent). The lower weight (< 2500 pounds) low-wing, single-engine airplanes exhibit higher rates of fatalities for this type of accident when compared to the high-wing configuration (38.3 versus 28.3 percent). However, a closer examination of the lower weight category shows that for airplanes weighing between 2000 and 2500 pounds the rate of fatality for this type of accident is relatively close (38.9 for the low-wing configuration and 32.5 percent for the high-wing configuration). The rate of fatalities for the extremely light-weight airplanes (< 2000 pounds) for this type of accident is 27 percent for the low-wing configuration and 24.4 percent for the high-wing configuration. The low fatality rate for these light-weight airplanes may be attributed to the lower impact speeds of these airplanes as a result of their lower flight speeds. The fatality rate associated with the agricultural airplane for this type of accident is 27.3 percent (Table 2-3). Since there are very few low-wing airplanes weighing less than 2000 pounds in the accident data as compared to 2000 to 2500 pound low-wing airplanes, the 38.9 percent shown in Table 2-4 is due to the fact that the weighted value is based on relative number of accident cases included.

- The comparison of the number of fatalities by accident types for twin-engine high-wing and low-wing airplanes is generally within ± 3 percent of their mean average except for the case of impact with an obstacle. However, the sample of this type accident in the data bank for the twin-engine high-wing airplane is inadequate for a true comparison.

Ratio No. 2 (Tables 2-3 and 2-4) is used in an effort to provide a level of severity of an accident by only including accidents in which injuries occur. (Accordingly, the data does not indicate the chances of survival in accidents which do not involve injuries). Ratio No. 2 defines the number of fatalities relative to the number of occupants involved for a particular accident type. This ratio is established for accident types such as the stall, collision with ground/water and collision with obstacle.

$$\text{Ratio No. 2} = \frac{\text{number of fatalities}}{\text{number of occupants}} \quad \begin{matrix}\text{(for a particular accident type)} \\ \text{(involving an injury)}\end{matrix}$$

Obviously, larger airplanes, which carry more passengers, will have a higher ratio of fatalities to accidents than the smaller airplanes. In dividing by the number of occupants involved for each particular accident type, a more rational manner of comparing different size and weight airplanes on an equal basis can be used.

Ratio No. 2 indicates that collision with the ground consistently results, except for the agricultural airplanes, in a high fatality rate. The impact velocities associated with this type of accident are higher and will require the absorption of a greater amount of energy than that of the stall and the obstacle collision types of accidents. Although it may not be practical from weight and cost effectiveness considerations to provide crashworthiness capabilities to fully cover this type of accident, the use of a consistent crash design philosophy in the design of a new airplane should provide a reduction in potential fatalities.

The results of the CAMI and NTSB data review and evaluation indicates that work should be performed to evaluate the effectiveness of incorporating shoulder harnesses along with seat and safety belt installations that are consistent with the present structural crashworthiness capabilities of each of the general aviation airplane models now in operation.

2.3 MATHEMATICAL MODELING REQUIREMENTS

During Task I, seven members of the General Aviation Manufacturer's Association (GAMA) were sent an inquiry regarding their current and anticipated

computer capability. Their responses indicate that the industry computer capability will be sufficient to use reasonably large ($\geq$ 500,000 bytes) computer programs.

The Task I review and evaluation of general aviation airplane characteristics, industry design practices, and industry computer capabilities, indicates that the use of a computerized analytical technique for performing crash analysis would be an asset to the industry if it contained certain features. The development of a general aviation airplane industry crash analysis computer program must take into consideration the need to analyze realistic crash conditions, yet not impose unwarranted and costly investments in specialized manpower and/or equipment to facilitate improved future crashworthy designs.

Ideally, the computer program should have the capability to:

- Provide sufficient information which can be used to assess an occupant's chances for survival. As a minimum this information should consist of defining floor acceleration pulses and evaluating cabin damage and cabin geometry change.
- Define forces, accelerations, velocities and displacements in three directions.
- Treat multidirectional impact forces, angles, and angular rates representative of the probable crash conditions associated with the different airplane usages and operational characteristics.
- Represent various types of structural behavior for a wide range of structural element types, particularly wherein post-failure large deflections occur.
- Treat structural failures and the consequences of the failures on surrounding structure.
- Represent different airplane configurations such as high-wing, low-wing, single-engine, twin-engine, tandem engines, individual and multiple seating accommodations, weights up to at least 12,500 pounds, and retracted or extended landing gear.

- Provide the means to treat differences in terrain (level, hilly, water, dirt, concrete) using available data for describing the properties of the terrain.
- Treat the significant phases of multiple impact crashes wherein the effect of an initial impact is accounted for in subsequent impacts during the same crash.
- Define acceleration magnitude, shape, duration and direction for selected masses.
- Provide data as part of the analysis which can be used to assess energy flow, member stresses, and structure rupture.

Furthermore, the program should be written in Fortran IV and be applicable for use on the larger size computers (i.e. IBM 360, IBM 370, CDC 6600) having at least 375,000 bytes of core storage.

2.4 ASSESSMENT OF PROGRAM KRASH

The capability of program KRASH, refined during Task I, to meet the general aviation airplane modeling requirements was assessed with the use of two different sets of limited controlled crash test data for two different airplane configurations (single-engine, high-wing, and low-wing). The comparison of test and analysis was performed for the following three impact conditions:

a. 45 feet per second longitudinal velocity impact on to a 45-degree dirt barrier.

b. Cg velocity of 1.6 feet per second down, 21.6 feet per second forward, and a pitch attitude of 38.5 degrees nose down.

c. Cg velocity of 8.5 feet per second down, 3.8 feet per second forward, a pitch attitude of 19.6 degrees nose down in inverted position.

Condition a. is a test representing a stall spin accident while conditions b. and c. are the primary and secondary impacts, respectively, during a test representing an overturn accident.

During Task I, Program KRASH was shown to be capable of defining:

- Spatial and temporal energy distribution including mass kinetic and potential, member strain and damping, structural crushing and ground friction.
- Large nonlinear behavior into the post-failure region including cabin deformation.
- Acceleration pulses at the floor in regions where occupants are located for the purpose of determining occupant response using an available occupant-seat-restraint system math model.
- Forces, accelerations, velocities, and deflections resulting from multidirectional impacts.
- Structural behavior for a wide range of structural element types associated with general aviation airplane design.
- Large motion rigid-body behavior wherein ground contact forces can be defined.
- Mathematical model requirements for two different airplane configurations (high-wing, low-wing).

SECTION 3

SUMMARY OF TASK II RESULTS

3.1 TEST PREPARATION

The four fully instrumented full-scale airplane crash tests performed during Task II were for the purpose of obtaining data for:

- Correlating with digital computer program KRASH
- Using as a basis for improving the computer program
- Subsequent use in occupant-seat-restraint system math models
- Developing improvements for future airframe and seat-restraint system design.

All full-scale crash tests were performed at the NASA-Langley Research Center (LRC) Impact Dynamics Research Facility (IDRF). The basic structure (gantry) of the IDRF is 241 feet high, 403 feet long and 270 feet wide at the ground. Aircraft are crashed into the impact surface as free bodies by use of a pendulum swing method to obtain desired flight paths and velocities. The crash test facility and testing technique are fully described in Reference 13.

The crash test impact conditions are shown in Table 3-1. All the tests were performed on a concrete impact surface, except Test 4 which was performed on a bed of soil.

A minimum of forty-four accelerometer channels were employed to record the dynamic response of the structure and the occupants during each crash test. Figure 3-1 shows a typical layout for accelerometers. Depending on the impact conditions, some accelerometer locations were altered. For each test there were two instrumented dummies. The pilot was represented by a 95th percentile anthropomorphic dummy weighing 224 pounds. The anthropometric dummy representing the co-pilot weighed 202 pounds (≈80th percentile by weight).

TABLE 3-1. SUMMARY OF CRASH TEST IMPACT CONDITIONS (REFERENCE 2)

	Test Number			
	1	2	3	4
Impact Velocities (MPH)				
along flight path	55.5	50.8	58.1	55.9
longitudinal	47.4	48.6	47.6	48.4
vertical	28.7	14.8	33.2	31.9
Angles (degrees)				
flight path (γ)	-30.72	-17	-34.86	-32.
impact (θ)	-30.17	+13.5	-39.4	-34.8
attack (α)	.57	+30.5	- 4.54	- 2.8
roll (ϕ)	+ 4.13	+ 3.25	+18.75	< 1.0
yaw (ψ)	- 3.27	-11.5	- 7.9	< 1.0
Rotational Velocities (deg/sec)				
pitch ($\dot{\theta}$)	46.4	6.9	14.3	18.2
roll ($\dot{\phi}$)	negligible	negligible	negligible	negligible
yaw ($\dot{\psi}$)	negligible	negligible	negligible	negligible

γ is negative in dive

$\theta, \dot{\theta}$ are positive nose up relative to ground

α is positive nose up relative to flight path

$\phi, \dot{\phi}$ are positive right wing down

$\psi, \dot{\psi}$ are positive tail left

and $\theta = \gamma + \alpha$

ft/sec = 1.467 x MPH

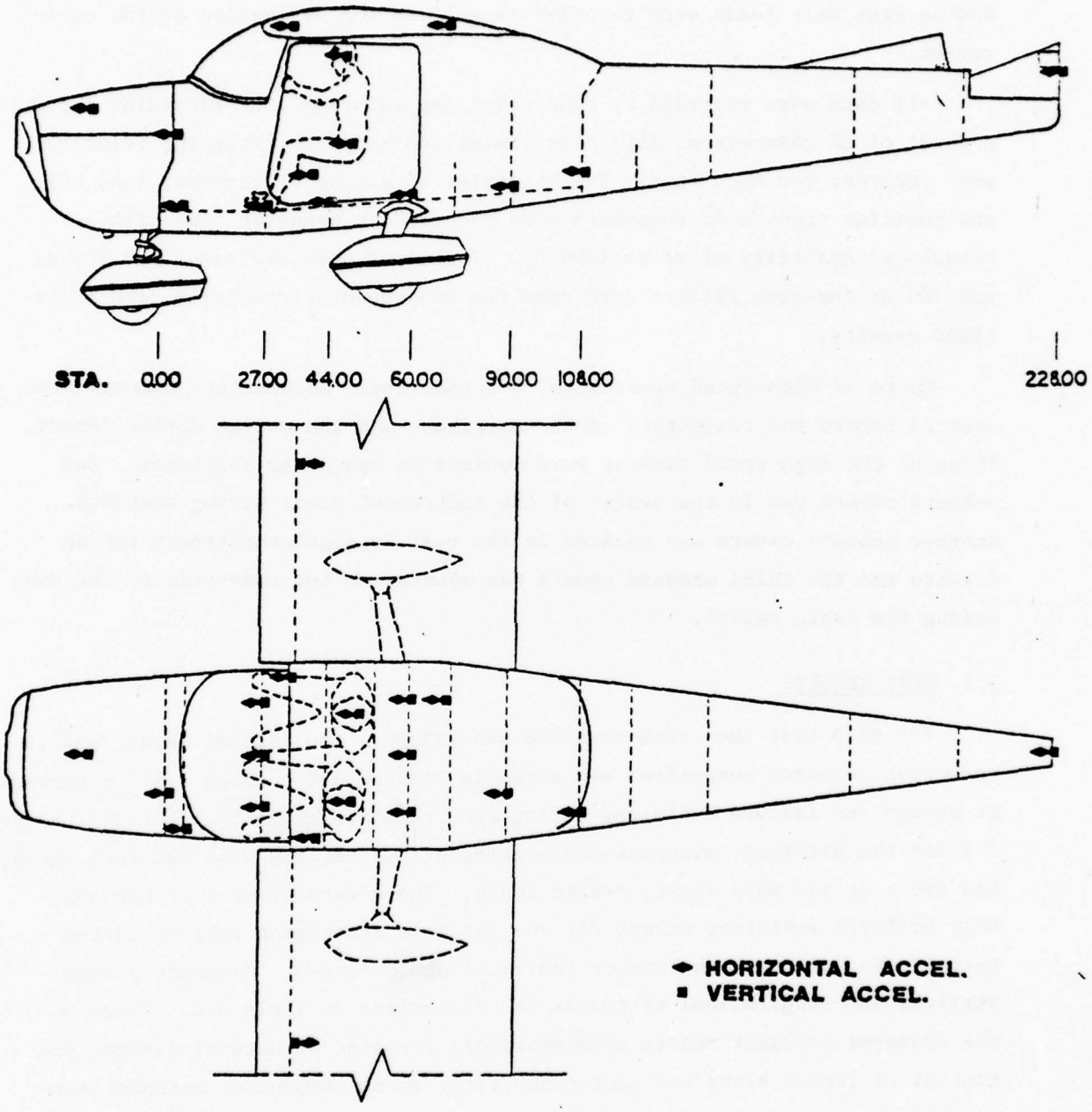

Figure 3-1. Accelerometer Locations, Single-Engine, High-Wing Airplane, Crash Tests 1 and 2 (Reference 2)

The restraint systems were compatible with the airplanes that were used for test vehicles. Consequently, each dummy had a lap belt and shoulder harness and no inertia reel. The pilot dummy chest deflection and both dummy lap and harness belt loads were recorded as well as the deflection of the cabin region.

All data were recorded by NASA using the existing IDRF recording system. A total of 52 channels of data plus timing and radar to determine velocity were recorded for each test. The histories of all accelerometer, load cell, and position transducer responses were recorded on magnetic tape with a frequency capability of up to 1000 Hz. The tapes were digitized and 100 Hz and 300 Hz low-pass filters were used for subsequent correlation with analytical results.

Up to 17 high-speed cameras and 3 normal-speed documentary cameras were used to record the trajectory of the airplanes and the action during impact. Three of the high-speed cameras were located on board the airplanes. One onboard camera was in the center of the instrument panel facing rearward. Another onboard camera was mounted in the rear luggage compartment facing forward and the third onboard camera was mounted on the underside of the wing facing the cabin region.

3.2 TEST RESULTS

For each test the crash sequence was filmed. The initial impact position and crash sequence composites are shown in Figures 3-2 through 3-5. Summaries of damage and failure sustained during each test are given in Table 3-2 through 3-5 for the airframe, occupant-seat-restraint system, the wing and fuel tanks, and the nose and main gears, respectively. There were no seat-or harness-belt failures sustained except for one lap-belt attachment failure during test 4. No fuel tank rupture or fuel spillage occurred. Occupant pelvis vertical and longitudinal responses are summarized in Table 3-6. Based on the measured occupant pelvis accelerations, airplane structural damage, potential of lethal blows and post-crash fire, an assessment of occupant survivability was made for each test.

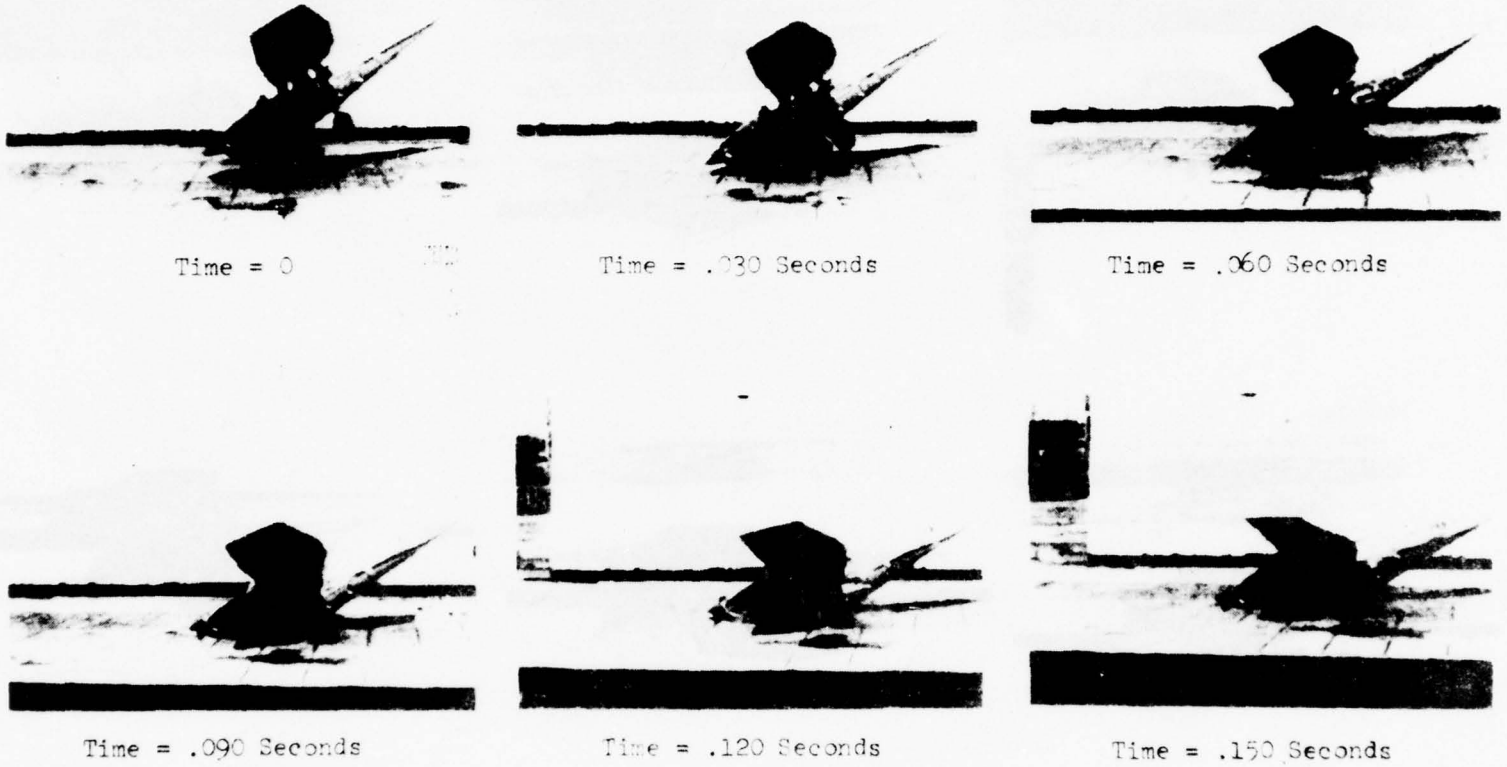

Figure 3-2. Crash Test 1, Impact Sequence (Reference 2)

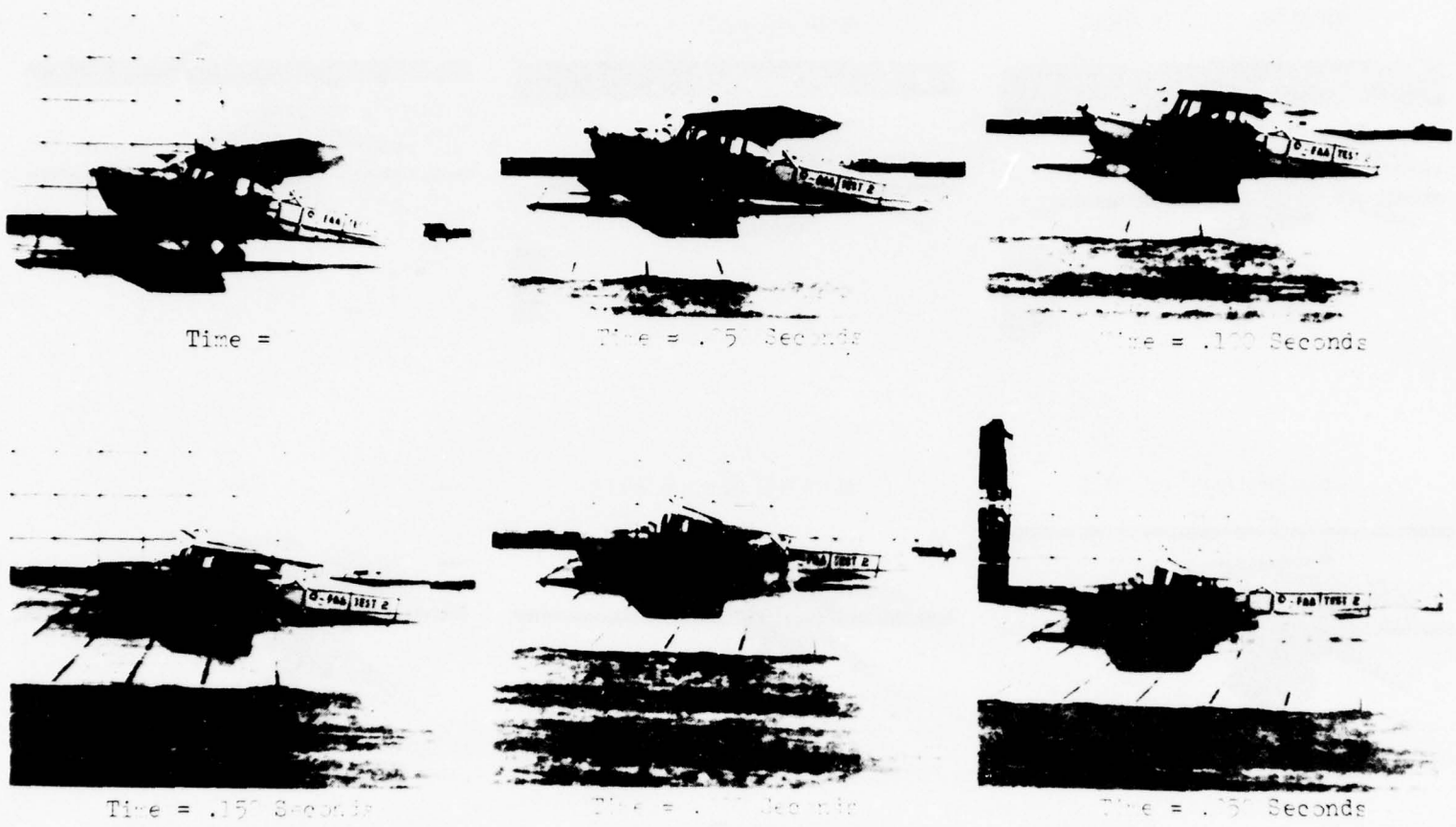

Figure 3-3. Crash Test 2, Impact Sequence (Reference 2)

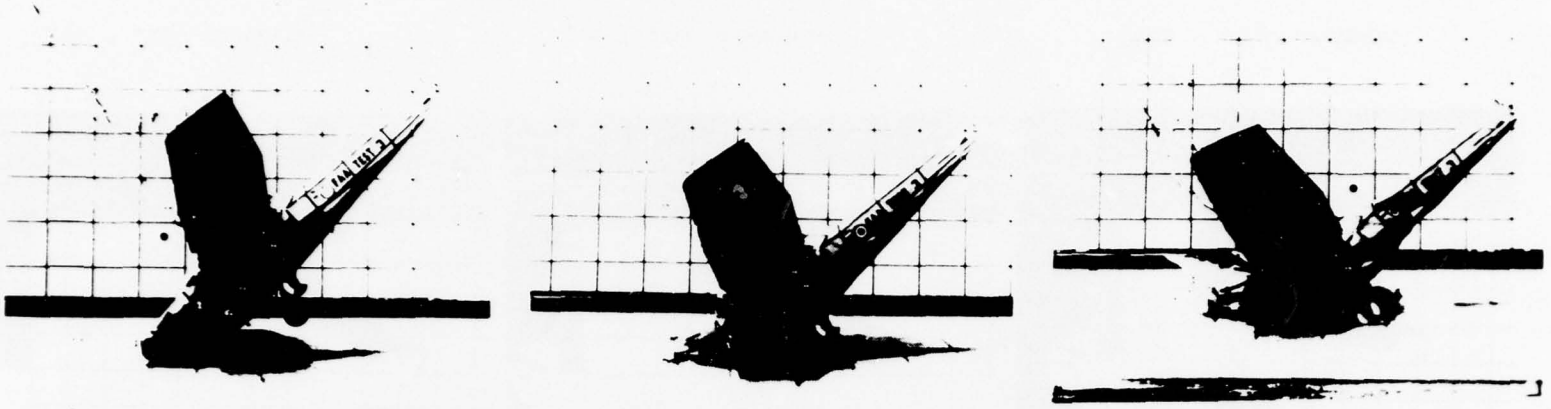

Time = 0

Time = .050 Seconds

Time = .100 Seconds

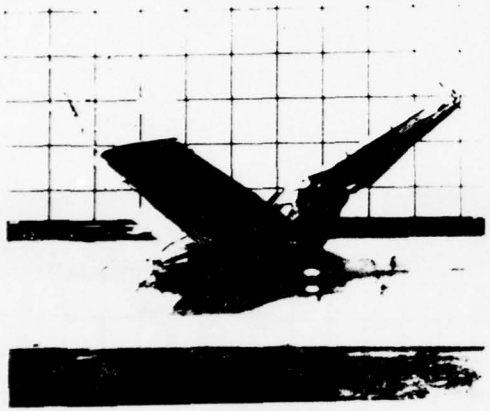

Time = .150 Seconds

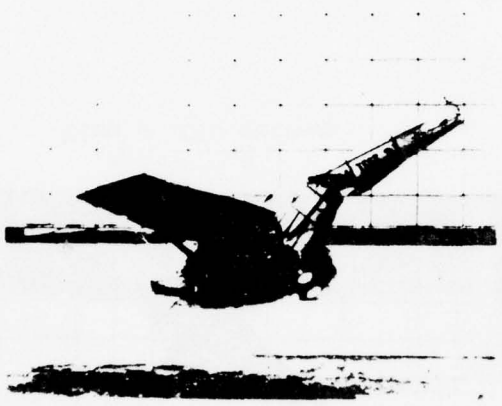

Time = .200 Seconds

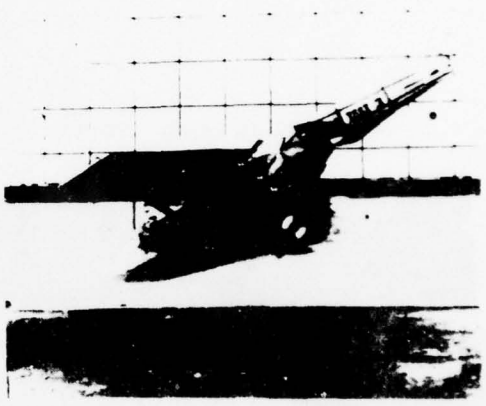

Time = .250 Seconds

Figure 3-4. Crash Test 3, Impact Sequence (Reference 2)

Time = 0 Time = .050 seconds Time = .100 seconds

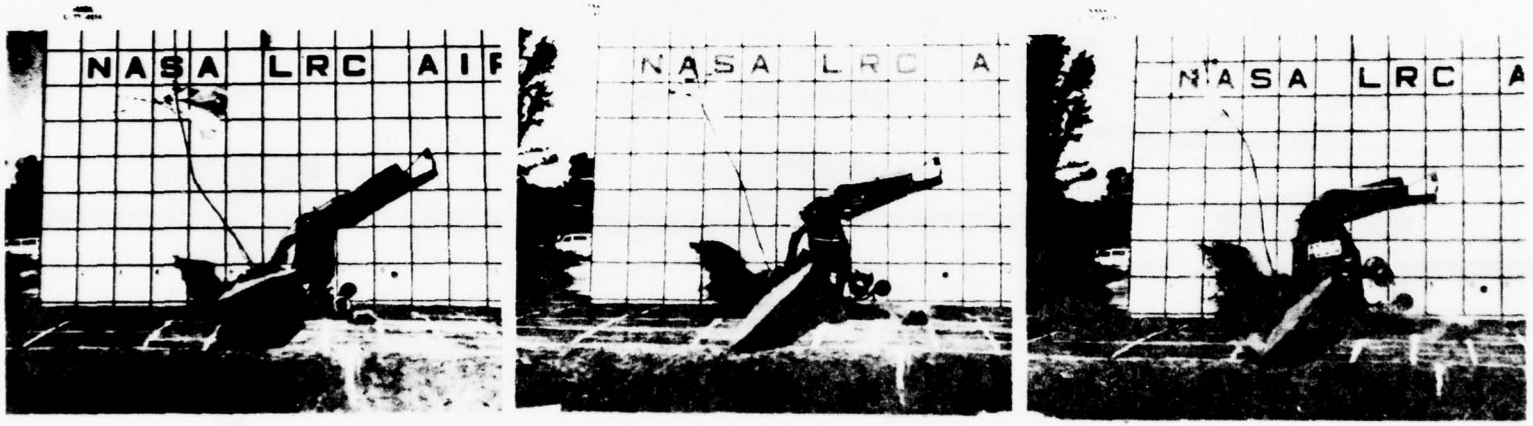

Time = .150 seconds Time = .200 seconds Time = .250 seconds

Figure 3-5. Crash Test 4, Impact Sequence (Reference 2)

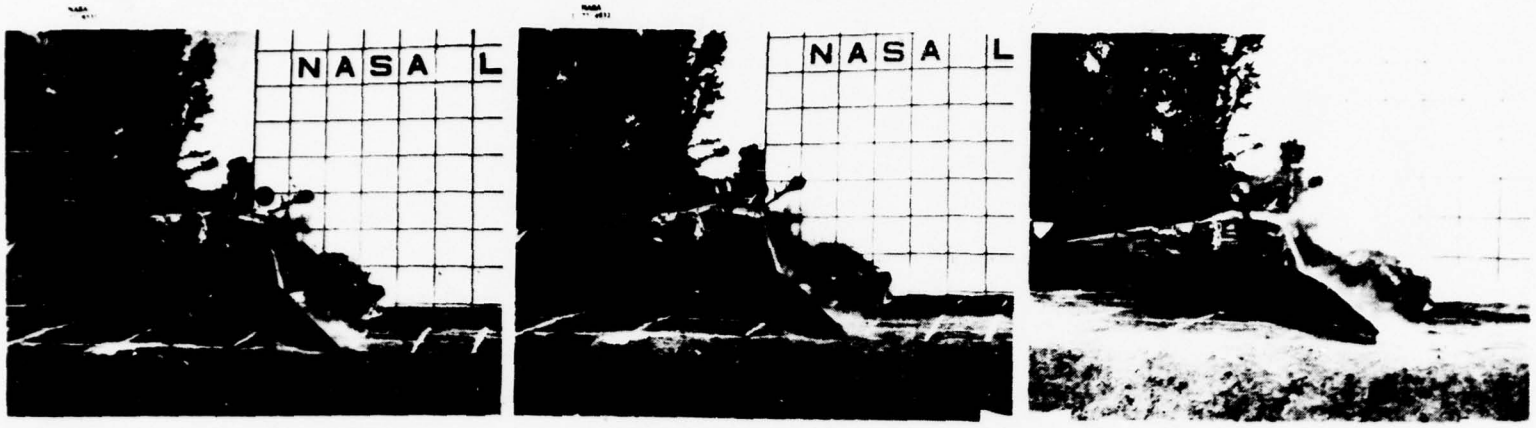

Time = .900 seconds Time = .950 seconds Time = 1.00 seconds

Time = 1.05 seconds Time = 1.1 seconds Time = 1.15 seconds

Figure 3-5. Crash Test 4, Impact Sequence (Reference 2)(Continued)

TABLE 3-2. SUMMARY OF AIRFRAME DAMAGE AS A RESULT OF THE CRASH TESTS (REFERENCE 2)

Location	Test Number			
	1	2	3	4
Engine and Firewall	Mounts buckled Firewall buckled	Firewall Buckled in Lower Region	Severe buckling, engine shoved back into firewall	Engine Torn Loose From Mounts -
Forward Fuselage	Lower Fuselage Crushed several inches	Slight damage to underside aft of firewall	Severe crushing of lower fuselage	Lower fuselage completely crushed
Passenger Cabin Compartment	Moderate Deformation	No damage	Left and right front door posts buckled forward and outboard. Substantial deformation of cabin area Cabin top structure ruptured	Door posts severed. cabin volume substantially compressed
Floor	Severely buckled at F.S. 27 and F.S. 65	No damage	Severely buckled at base of floorboard. Moderate buckling near landing gear bulkhead	Base of instrument panel completely crushed
Tail Section	Slight buckle aft of F.S. 108	Buckled between F.S. 205-208	Moderate buckling aft of F.S. 108	Severely buckled aft of F.S. 108

TABLE 3-3. SUMMARY OF OCCUPANT-SEAT-RESTRAINT SYSTEM FAILURES AND OCCUPANT IMPACTS EXPERIENCED DURING THE CRASH TESTS (REFERENCE 2)

Location	Test Number			
	1	2	3	4
Pilot				
Seat leg failure				
forward	X		X	
rear				
Seat leg pulled from floor tracks				
forward			X	X
rear	X			
Shoulder harness or attachment failure				
Lap belt or attachment failure				
Occupant contact with Instrument Panel			X	X
Co-Pilot				
Seat leg failure				
forward	X			
rear				
Seat leg pulled from floor tracks				
forward			X	X
rear	X		X	
Shoulder harness or attachment failure				
Lap belt or attachment failure				X
Occupant contact with Instrument Panel			X	X

X Denotes occurrence

TABLE 3-4. SUMMARY OF WING DAMAGE EXPERIENCED AS A RESULT OF THE CRASH TESTS (REFERENCE 2)

Location	Test Number			
	1	2	3	4
Left Wing				
torsional failure	X			
rear spar failure			X (b)	X (b)
column strut buckle			X	
fuel tank rupture				
fuel spillage				
wing tip damage				X
Right Wing				
torsional failure				
rear spar failure			X (c)	
column strut buckle				
fuel tank rupture				
fuel spillage				
wing tip damage			X	X

(a) X denotes occurrence
(b) tension failure
(c) compression failure

TABLE 3-5. NOSE AND MAIN GEAR FAILURES AS A RESULT OF THE CRASH TESTS (REFERENCE 2)

Location	Crash Test Number			
	1	2	3	4
Nose Gear				
Lower Support Failure	X	X	X	X
Upper Support Failure	X		X	X
Gears Failed Aft	X		X	X
Gears Failed Forward		X		
Right Main Gear				
Inboard Bolt Failure	X		X	
Gear Failure				
Left Main Gear				
Inboard Bolt Failure				
Gear Failure				

X denotes occurrence

TABLE 3-o. SUMMARY OF OCCUPANT PELVIS VERTICAL AND LONGITUDINAL RESPONSES, CRASH TESTS 1 THROUGH 4 (REFERENCE 2)

Location	Direction	Test Number 1		2		3		4	
		Acceleration (a)	Duration (b)	Acceleration (a)	Duration (b)	Acceleration (a)	Duration (b)	Acceleration (a)	Duration (b)
Pilot	Up	40	.007	10	.008	40	.010	60	.015
	Down	(d)	(d)	(d)	(d)	(d)	(d)	80	.005
	Forward	20	.003	8	.010	(d)	(d)	40	.015
	Aft	10	.015	(d)	(d)	12	.020	10	.017
Copilot	Up	45	.008	10	.005	(c)	(c)	80	.002
	Down	(d)	(d)	(d)	(d)	(c)	(c)	20	.003
	Forward	15	.002	3	.020	10	.010	60	.006
	Aft	12	.015	(d)	(d)	20	.013	10	.007

(a) g's
(b) seconds
(c) not recorded
(d) low value

The assessment indicates that for Tests 1 and 2 there will be an extremely high probability of occupant survival. Occupants exposed to the conditions of Tests 3 and 4 can be expected to receive serious fatal injuries.

The dramatic difference between Test 1 and Test 4 results where only the impact surface was changed, indicates the need for additional research on the effects of terrain-structure interaction.

A complete detailed discussion of the test results is presented in Sections 3 and 7 of Reference 2.

3.3 MATHEMATICAL MODEL

Digital computer program KRASH was used to model the high-wing, single-engine type airplane used in the crash tests. The analysis for Tests 1, 2, and 3 was performed using a full airplane representation. For Test 4, a symmetrical impact condition (no roll or yaw) was used. The math models used for each of the four tests are identical except for:

- Weight and cg representation
- Initial impact condition
- Lift consideration for Test 2
- Soil representation for Test 4
- Post-failure representation of nose gear structure

Figure 3-6 depicts the basic mathematical model used throughout the analysis and correlation. Table 3-7 presents the airplane math model size data. A detailed description of the math model is presented in Section 5 of Reference 2.

3.4 CORRELATION OF ANALYSIS AND TEST RESULTS

The analysis and test results were correlated for the following range of impact conditions:

- Flight-path velocity: 74.5 to 85.2 ft/sec
- Longitudinal velocity: 69.5 to 71.3 ft/sec

NOTES:

(a) ONLY LEFT SIDE SHOWN
(b) BEAMS 6-7, 7-9, 6-10 NOT SHOWN FOR CLARITY
(c) OCCUPANT-SEAT – RESTRAINT SYSTEM MODEL NOT SHOWN
(d) NODE POINT 13-4 NOT SHOWN FOR CLARITY

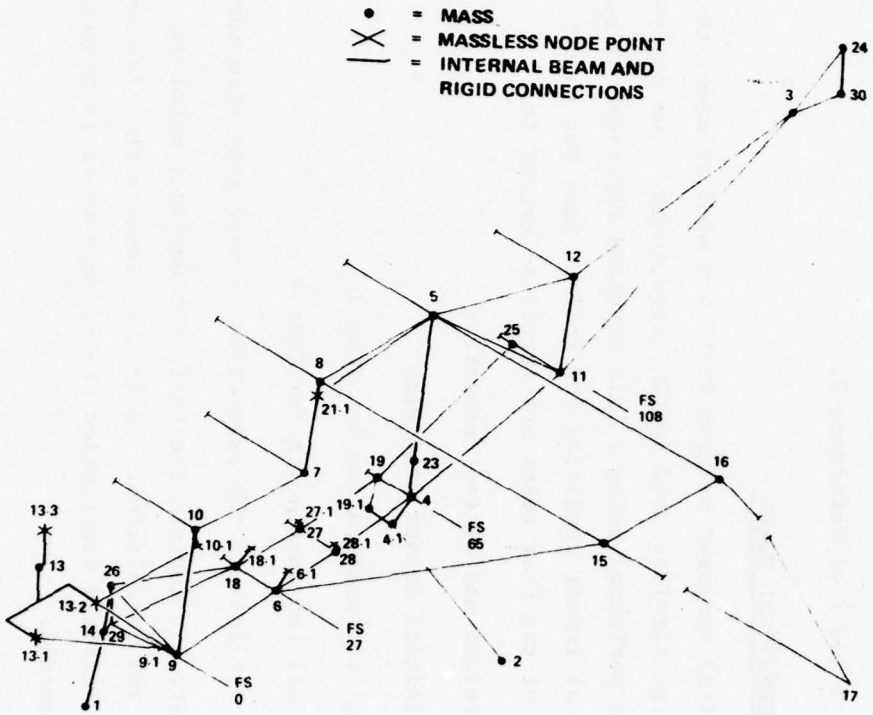

Figure 3-6 Single-Engine, High-Wing Symmetrical Math Model (Reference 2)

TABLE 3-7. SUMMARY OF MATH MODELS (REFERENCE 2)

Full (F) or Half-Model (H)[a]	TEST 1 F	TEST 2 F	TEST 3 F	TEST 4 H
Number of:				
Masses	48	48	48	30
Node Points	32	32	32	17
External Springs	32	32	32	22
Linear Beams	100	100	100	59
Nonlinear Beams	118	118	118	68
DRI Elements	2	2	2	1
Pin-Pin Beams	2	2	2	1
Pin-Fixed Beams	4	4	4	2
Unsymmetrical Elements	7	7	7	4
Lift/Weight Ratio	0	.65	0	0
Impact Conditions:				
Vertical Velocity (fps)	42.3	21.8	48.7	43.4
Longitudinal Velocity (fps)	68.9	71.3	70.	69.6
Pitch Angle (degrees	-30.	13.5	-39.4	-34.8
Roll Angle (degrees)	4.1	3.3	18.7	0.
Yaw Angle (degrees)	-3.3	-11.5	-7.9	0.
Pitch Rate (degrees/second)	46.4	6.9	14.3	18.2
Weight (lb)	2370	2390	2370	2370
C.G. Position (Fuselage Station-in)	44.1	47.2	44.1	44.1
Inertias ($lb\text{-}in\text{-}sec^2$)				
Roll	1.84 E04	1.84 E04	1.84 E04	1.84 E04
Pitch	1.77 E04	2.10 E04	1.77 E04	1.77 E04
Yaw	2.96 E04	3.25 E04	2.96 E04	2.96 E04

(a) Refers to the analysis. Airplane data input as a half model in all four cases with the program computing full airplane data for Tests 1, 2 and 3.

- Vertical Velocity: 21.8 to 48.7 ft/sec
- Flight-Path Velocity: -17 to -34.9 degrees
- Pitch angle: 13.5 to 39.4 degrees
- Attack angle: 0.5 to 30.5 degrees
- Roll angle: 0.0 to 18.7 degrees
- Yaw angle: 0.0 to 11.3 degrees

Figures 3-7 and 3-8 provide a summary of the composite comparison of analysis and test structure response results at several locations for all four tests. Figure 3-7 shows the peak accelerations in the vertical direction. The percentage differences are shown in parentheses. In some individual comparisons a substantial percentage difference exists. However, the overall trend of the analysis considering all four conditions is in good agreement with the trend exhibited by the four crash test results. From Figure 3-7 it can be seen that the location at which the predominant response occurs varies as a function of the test condition. Similarly, Figure 3-8 presents a composite comparison of responses in the longitudinal direction. As in the case of the vertical direction, the analysis results for the longitudinal direction are in good agreement with the test data. In 75 percent of the comparisons shown in Figures 3-7 and 3-8, the time difference between analysis and test response is 20 milliseconds or less.

Figure 3-9 shows a comparison of analysis versus test cabin deformation for Tests 1, 3, and 4. While the analysis does not show the degree of mid-cabin deformation that is observed in the tests, it does show a trend to more deformation from Test 1 to Test 3 to Test 4. Test 2 experienced no cabin deformation during the test, nor does the analysis indicate any significant deformation.

In Table 3-8 the analysis results are compared to the test results on the basis of how they would rank with regard to severity. The comparison takes into consideration energy, structure damage, failures, cabin deformation, occupant response and structure response. The analysis and test results are in agreement with regard to the severity rank that should be applied to the test conditions.

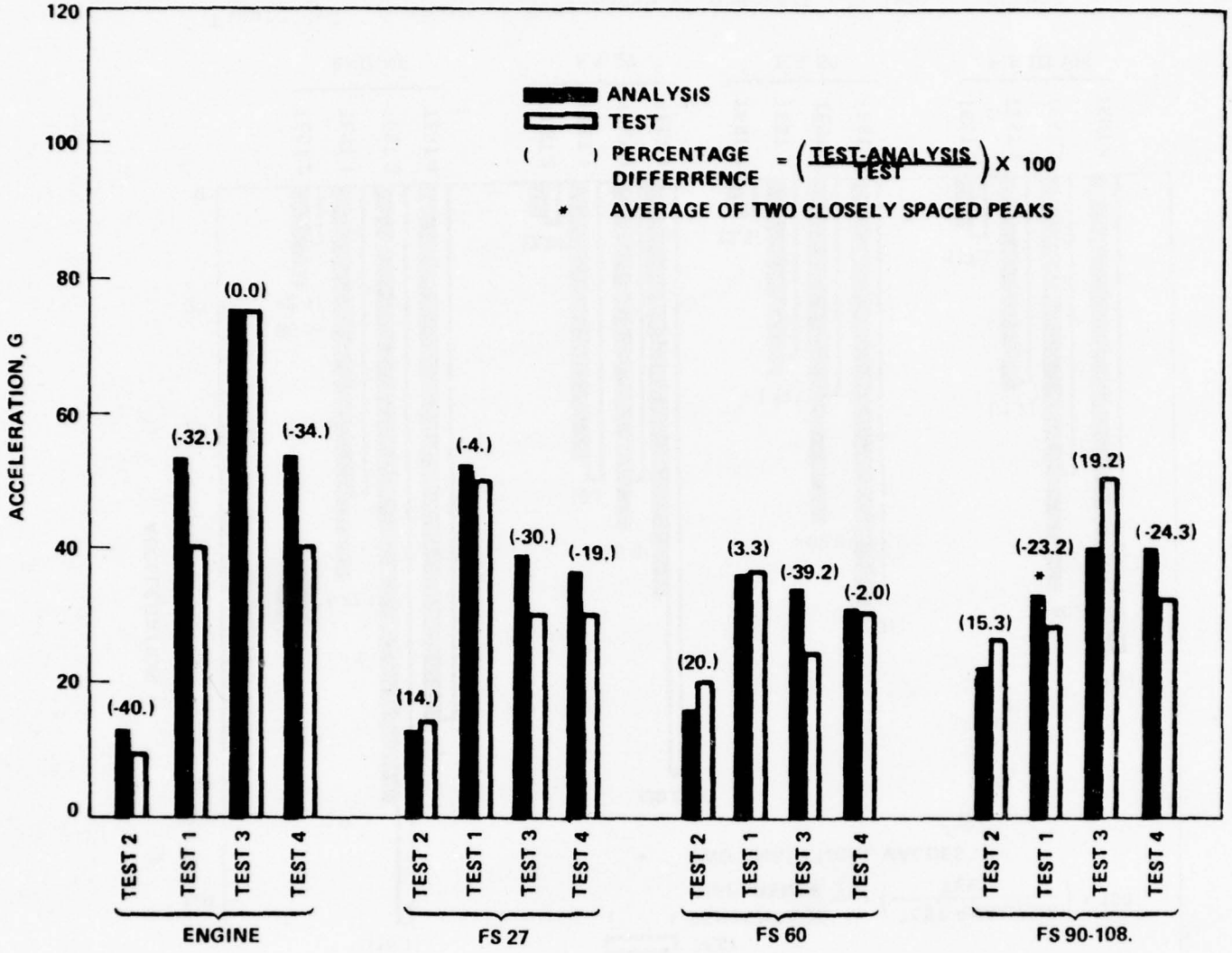

Figure 3-7. Summary of Comparison of Analysis and Test Structure Vertical Responses, Crash Tests 1 through 4 (Reference 2)

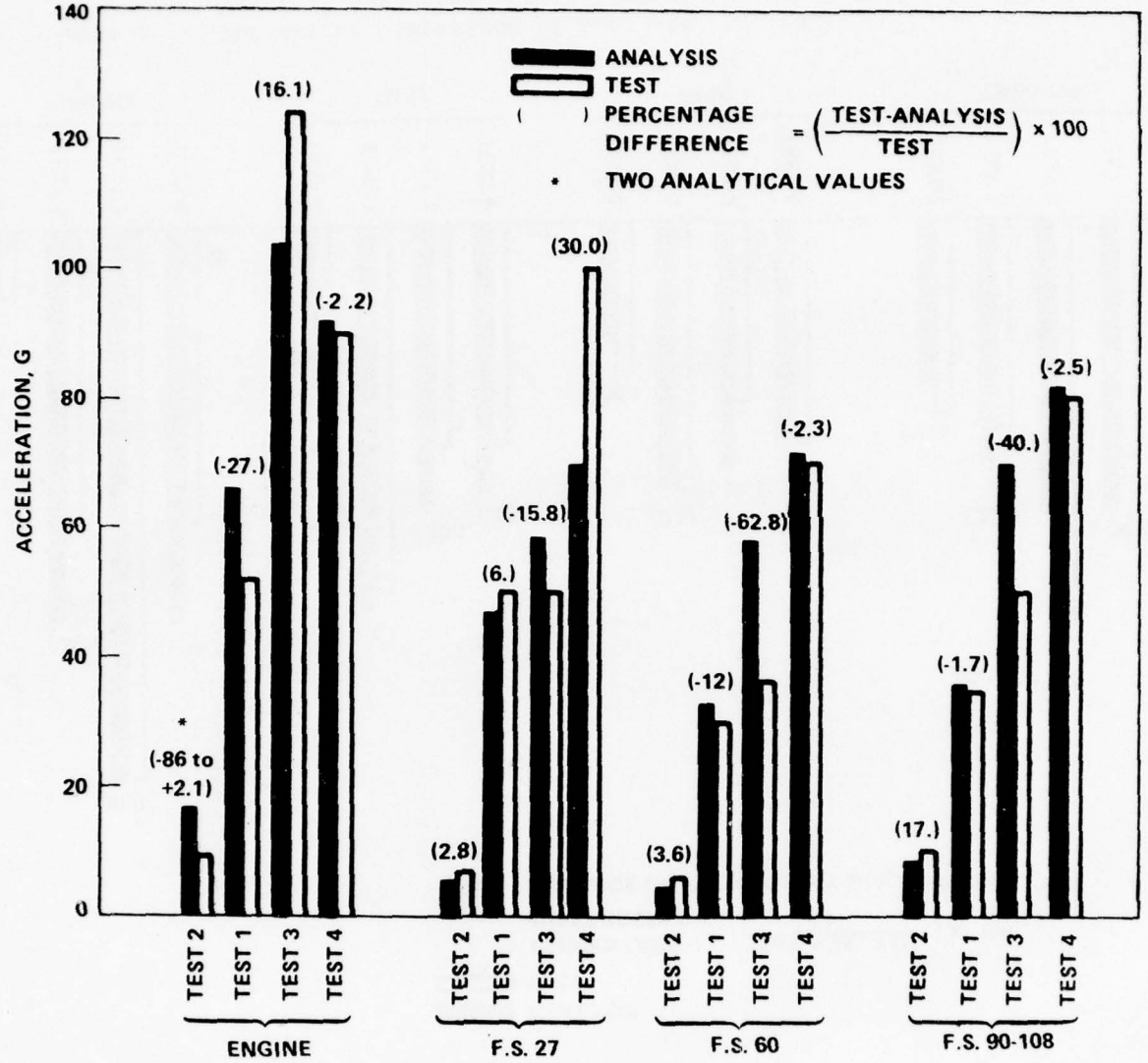

Figure 3-8. Summary of Comparison of Analysis and Test Structure Longitudinal Responses, Crash Tests 1 through 4 (Reference 2)

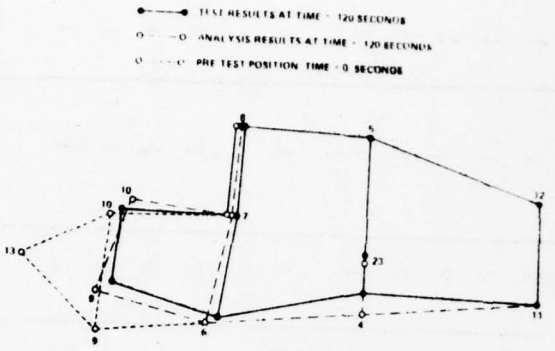

TEST 1

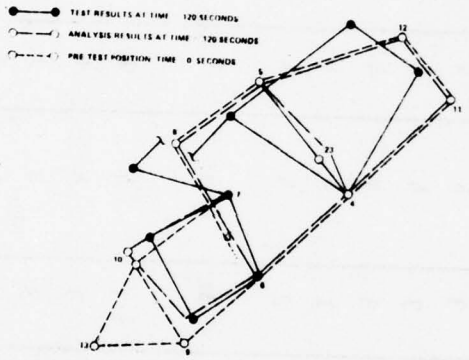

TEST 3

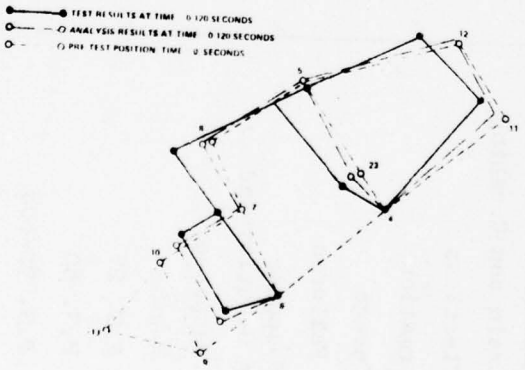

TEST 4

Figure 3-9. Comparison of Cabin Deformations, Crash Tests 1, 3 and 4 (Reference 2)

TABLE 3-8. COMPARISON OF TEST SEVERITY RANKING BASED ON ANALYSIS AND TEST RESULTS, CRASH TESTS 1 THROUGH 4 (REFERENCE 2)

Consideration	Test Numbers							
	1		2		3		4	
	Analysis	Test	Analysis	Test	Analysis	Test	Analysis	Test
Energy; Strain and Crushing	3	3	4	4	2	2	1	1
Member Deflections	2	3	4	4	3	2	1	1
Cabin Deformation	3	3	4	4	2	2	1	1
Seat Leg Damage	1	1	4	4	2	2	3	3
Structure Failures	1	2	4	4	1	1	3	2
Occupant Response (including Severity Index)	2,3	3	4	4	2,3	2	1	1
Structure Response								
Engine	3	3	4	4	1	1	2	2
F.S. 27	3	3	4	4	2	2	1	1
F.S. 60	3	3	4	4	2	2	1	1
F.S. 90-108	3	3	4	4	2	2	1	1
Landing Gear Bulkhead Damage	1	1	4	4	2	2	3	3
Landing Gear Failure Potential	2	2	1	1	3	3	4	4

Ranking: 1. most severe
2. 2nd most severe
3. 3rd most severe
4. least severe

Individual tests detailed correlation results and a comprehensive composite summary of correlation results are presented in Sections 6 and 7 of Reference 2.

3.5 KRASH USER'S MANUAL

A three-volume KRASH User's Manual was issued in conjunction with the Task II effort. The first volume (Reference 4) presents the program theory and listing. Volume II (Reference 5) provides input-output format, techniques, and applications to facilitate the program usage. Included in this volume are descriptions of math model development procedures, KRASH data requirements and typical model arrangements. The third volume (Reference 6) presents related design information in such areas as:

- General aviation airplane operational and structural characteristics
- Crash environment
- Occupant injury assessment
- Structural data and methods
- Structural crash design and compliance methods

3.6 CRASH ENVIRONMENT

The results of the accident review and evaluation (Reference 1), the full-scale crash tests and analysis of the crash test conditions described in Reference 2, as well as the on-going crash test programs discussed in Reference 13, indicate that a preliminary survivable crash environment for light-fixed aircraft can be suggested. For example, the CAMI accident data, summarized in Reference 1, indicated that for approximately 60 percent of eighteen light fixed-wing airplane accidents for which detailed analysis was available the impact angle was determined to be 30 degrees or less. The controlled crash tests of single-engine, high-wing and twin-engine low-wing light-fixed-wing airplanes showed little or moderate damage when the airplane with a -30-degree impact angle and 50 to 60 mph flight path velocity impacted on a rigid surface.

Furthermore, the full-scale crash test results show that the lower the impact angle the less severe the expected damage and occupant responses. In addition, for flared nose-up impact conditions onto a rigid surface at around the airplane stall speed, the airplane showed little or no liklihood of severe injury to the occupant or substantial damage occurring to the structure for current airplane designs. However, the controlled crash test program also showed that an impact onto a flexible surface is far less predictable and possibly far more severe than on a rigid surface. When considering flexible terrain in the development of a crash design criteria the major problem is representing a "typical" terrain. The wide range in variation of soil properties presents a significant problem for prediction techniques given the current state of the art in structure-soil interaction analysis and available test data for crash type conditions. The idealization of the impact surface as "rigid" eliminates the many variables associated with a flexible surface and allows the designer to concentrate on the design concepts and structural behavior.

On the basis of the foregoing discussion, two potential crash environment conditions to be considered for future crash survivable design criteria of light-fixed-wing airplanes are:

1. Pitch angle = -30 degrees

   Flight-path angle = -30 degrees

   Flight-path velocity = minimum airplane stall speed (flaps down) but not less than 42 mph

   Lift/weight ratio = 0.0

   Impact surface = rigid

2. Pitch angle = +15 degrees

   Flight-path angle = -15 degrees

   Flight-path velocity = minimum airplanes stall speed (flaps down) but not less than 42 mph

   Lift/weight ratio = 0.0 to .65

   Impact surface = rigid

The potential procedure that can be followed in analytically assessing crashworthiness capability is as follows:

- Determine the response characteristics of the structure and occupants for the basic nose-down and nose-up crash conditions using a rigid impact surface.

- Perform a qualitative evaluation of the airplane's structural crashworthiness capability for soil (flexible ground) impacts by assessing the airplane airframe design characteristics with regard to the guidelines for desirable airframe design to minimize detrimental earth gouging (plowing) effects, as outlined in Reference 17 (section 2.7).

- Perform limited component impact tests to determine load-deflection characteristics to support analytical procedures.

- Combine the results of the quantitative and qualitative assessments of occupant survivability to ascertain the structural design capability in a survivable crash environment.

- Update analytical models as additional post-linear structure load-deflection behavior and structure-flexible ground interaction data is obtained.

SECTION 4

PROGRAM KRASH MODIFICATIONS

4.1 TASK I MODIFICATIONS

Program KRASH was developed for the purpose of providing a practical engineering analytical approach to assist in the determination of the structural crashworthiness capabilities of vehicles.

KRASH was originally verified using experimental data obtained from a fully instrumented full-scale helicopter crash test involving a combined vertical and lateral impact velocity (Reference 14). There are similarities in the requirements for the crash analysis of helicopters and general aviation airplanes, including:

- Exposure to multidirectional forces during a crash
- Comparable takeoff weights for certain classes of each
- Similar structure in many areas
- Multiple impact for certain crash conditions
- Comparable crash durations

Prior to the initiation of the Task I effort, program KRASH had the capability to:

- Define a six-degree-of-freedom (DOF) response at each representative location, including three translations and three rotations (accelerations, velocities, and displacements are computed).
- Determine mass accelerations, velocities and displacements, and internal member loads and deformations at each time interval.
- Provide for general nonlinear stiffness properties in the plastic regime, including different types of load-limiting devices, and determine the amount of permanent deformation.

- Determine how and when rupture of an element takes place and redistribute its load-carrying capability over the other structural elements involved.
- Define mass penetration into an occupiable volume.
- Provide for ground contact by external structure including sliding friction.
- Include viscous damped internal elements.
- Include a measure of injury potential to the occupants; for instance, the probability of spinal injury indicated by the Dynamic Response Index (DRI).
- Determine the distribution of kinetic and potential energy by mass item, the distribution of strain and damping energy by element, and the crushing energy associated with each external spring.
- Determine the vehicle response to an initial condition that includes linear and angular velocity about three axes and any arbitrary vehicle attitude.
- Treat up to 80 masses (480 DOF), 100 internal (6 x 6) beam elements and 120 nonlinear degrees-of-freedom.

A comprehensive description of KRASH prior to the general aviation airplane effort is presented in References 14 and 15.

The results of the Task I effort regarding the general aviation airplane types, operational and structural characteristics, the crash environment, and mathematical modeling requirements indicated the following modifications would enhance program KRASH usage.

4.1.1 Generalized Impact Surface Capability

This modification allows the user to specify a surface which makes an angle with the horizontal of up to 90 degrees. The airplane represented by the math model can be positioned relative to the surface with the proper input data selection, or, if the user chooses, the program will automatically position the vehicle in the proper attitude relative to the surface using the existing external spring input data. This is a practical feature and requires only one additional input term, the angle of the slope. The generalized impact

surface was applied in the analysis of a stall-spin crash test that impacts into a 45 degree slope which is described in Section 5, Reference 1. The generalized surface capability is useful for analyzing crash conditions involving hillsides, mounds and possibly trees.

4.1.2 Cabin Volume Change

The prime concern in a crash is the protection of the occupant. As noted earlier, one of the design goals is to have the structure crush and deform in such a manner that a survivable cabin volume will be maintained for the occupant and that the occupant is kept from impacting structure or hardware in such a manner as to receive serious or fatal injuries. Consequently, coding is added to KRASH wherein any eight masses are specified for a particular volume. The original coordinate positions of the masses are used to compute an initial volume. The new coordinates of the specified masses are computed at each integration. The ratio of the new volume to the original volume is calculated and printed out along with the regular output print. Although usually only one volume (occupiable region) is of concern, the program allows the user to specify up to eight distinct volumes. This modification in no way alters the program's basic computations. Since there will be an occupant-seat-restraint system model available later in the program, a refinement for future consideration would involve combining the volume history from KRASH and the occupant model history to ascertain relative positions and velocities of the structure and occupant extremities.

4.1.3 Member Directional Stresses

The determination of member directional stresses is obtained using the material property data used by the program to computer linear stiffnesses. The procedure the program follows to compute stresses with the required input data is as follows.

- Using member forces computed in the program and the member properties, the element stresses acting at the top, bottom, right, and left side on each of the selected members is determined. The method of calculating the member forces is unchanged; stresses are calculated only for output information and are not used internally in the force calculations.

- Combined stresses due to bending, axial, shear and torsional forces are computed.
- The principal and maximum shear stresses are computed.
- The maximum shear failure theory and the theory of constant energy of distortion for a combined axial and shear stress condition are applied.
- Ratios of element stress to yield stress are computed during the entire analysis (A ratio of >1.0 indicates yield has been exceeded).

The above approach is simple and consistent with the techniques used in KRASH and, as such, has limitations. The incorporation of the stress check offers the advantage of being able to monitor selected elements to determine if they have reached a yield condition. Once the element has yielded the failure theories are invalid and, consequently, the most meaningful use of the stress data is to identify which elements yield and at what time during the crash analysis. The stress data can help assess the validity of results with regard to the data used in modeling some of the structure. However, the computed stresses should not be used to verify structural designs because they do not provide sufficiently accurate data with which to make critical design decisions. For example, the effect of stress concentrations, unique geometry shapes and detail attachment practices at joints, are not included. Furthermore, care should be exercized in using this option since many times a complex structure is idealized with beam properties.

4.1.4 Internal Computation of Element Linear Stiffnesses

The internal computation of element linear stiffnesses involves providing the following input data for each member:

E = modulus of elasticity

G = shear modulus

J = polar moment of inertia

A = cross sectional area

L = member length

I_y, I_z = area moment of inertia about the y and z axis

The data is used in the program to formulate the linear stiffness matrix for each element. One line (card) of imput data per internal element member is required instead of six cards of stiffness terms as was formerly required. Since stiffnesses are often obtained from the member properties prior to input to the program, this change can result in a substantial saving in effort. Wherein stiffnesses are known from available data, material properties representative of the section can still be readily obtained since the beam stiffness terms are related to the member properties in a relatively straightforward manner. The formulation of linear stiffness within the program does not alter any of the basic computations. Direct input of the stiffness matrices is still available as an option.

4.1.5 Internal Computation of Nonlinear Curves

The determination of the exact nonlinear behavior of structural elements is very difficult, particularly when interaction of loads is involved. By the use of linear stiffness reduction curves, KR, different types of nonlinear behavior can be represented. By programming the typical nonlinear curve shapes, as shown in Figure 4-1, the need to input all KR tables is obviated.

A type 1 (Figure 4-1) curve uses five data points (NP=5)*

A type 2 (Figure 4-1) uses six data points (NP=6)*

A type 3 (Figure 4-1) uses seven data points (NP=7)*

A type 4 (Figure 4-1) uses eight data points (NP=8)*

A type 5 (Figure 4-1) uses nine data points (NP=9)*

*Coding is self-contained in KRASH

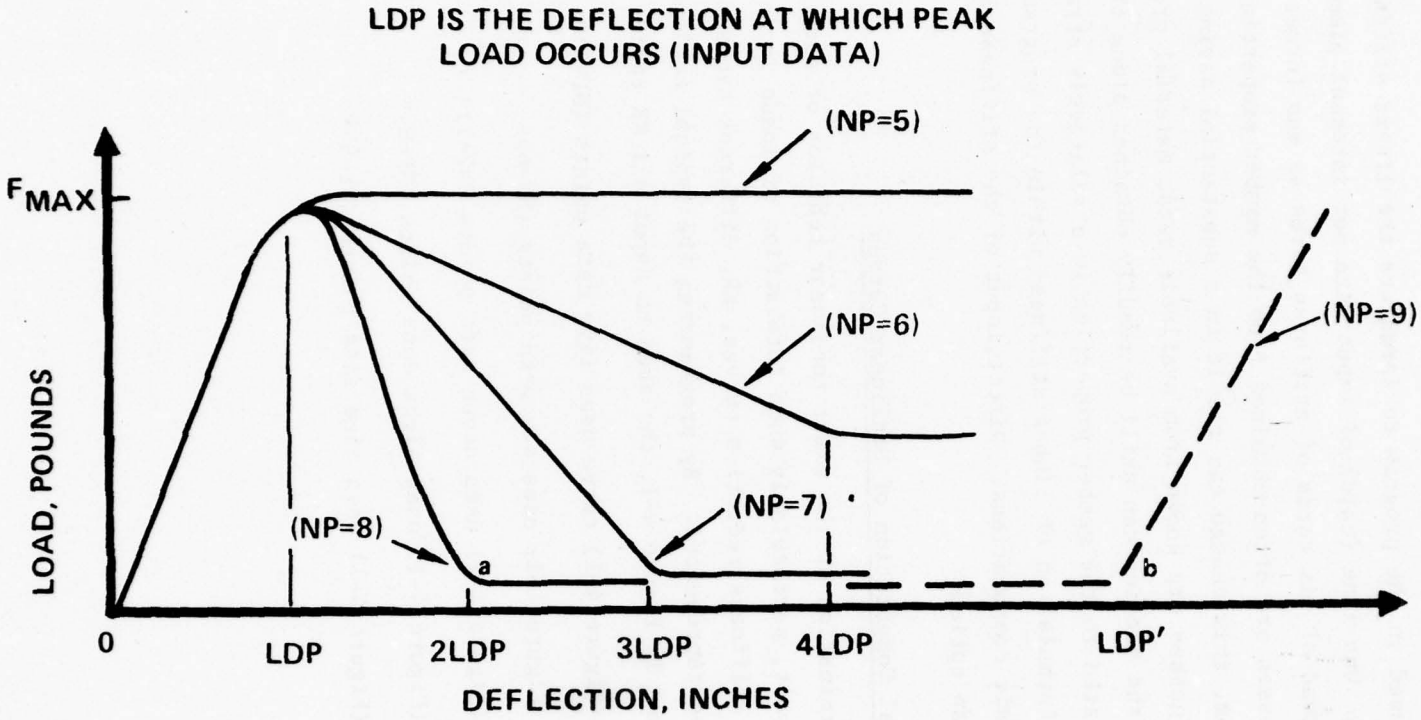

Figure 4-1. Load-Deflection Type Curves in KRASH

The input requirements to use the nonlinear curves consist of the identification of the member for which nonlinear behavior is desired, the deflection (LDP) at which inelastic behavior occurs, the direction of interest (3 translation and 3 rotations are possible), and the number of points (NP) defining the curve. When NP = 5, 6, 7, 8 or 9, the program computes the nonlinear curve. When a 9-point curve is used, the user also specifies the deflection corresponding to point b in Figure 4-1. When NP ≥10 a series of KR versus deflection data points is required. This allows the user to retain the capability to define an arbitrary load-deflection curve. The relationship between KR versus deflection and the load versus deflection is defined in the User's Manual (Reference 5, Section 4).

4.1.6 Addition of External Spring Force and Compression Data

The program prints out the external spring forces along with the spring compression in both ground and mass axis coordinates. The directions in which the forces act are identified. The added external spring force data is conveniently located with the external spring deflection data and provides useful information to help the user assess the results. The data allows the user to distinguish between crushing and friction forces.

4.1.7 Separation of Crushing and Friction Energy

The crushing and friction energy terms are separated in the program. Previously both were included under the heading "crushing energy". The user can now assess the relative effect of the structure crushing and ground friction employed in the analysis.

Other changes incorporated into KRASH during Task I included

- Revised Input-Output Formats
- Addition of Subroutine Echo which prints out the input in card image format
- Addition of 'Model Parameter Data'
- Provisions for specifying an acceleration pulse magnitude, shape, duration, and direction for a mass
- Miscellaneous standardization of terms and coding changes

The KRASH Task I modifications are discussed in Section 4 of Reference 2.

4.2 TASK II MODIFICATIONS

As a result of the Task II effort, additional refinements to KRASH were made to provide more versatility and to facilitate its usage.

4.2.1 Symmetrical Model Coding

Program KRASH has been recoded to allow the input of model data for only one-half of the airplane for cases in which both the airplane (normally the case) and the impact condition (no lateral, roll or yaw velocities and no initial roll or yaw attitude) are symmetrical. Previously, KRASH required input data for the full airplane; for the symmetrical impact condition the program uses only the half-airplane model.

Thus, either a more detailed model can be used as compared with a complete model within the limits of the allowable number of masses and beam elements, or the same modeling detail can be maintained as used in the complete model which will reduce computer run time and cost. As an example, for the single-engine, high-wing airplanes modeled during Task II, the symmetrical half-airplane model involved in a symmetrical impact can achieve the same modeling detail with 30 masses as that of the complete airplane model with 48 masses. The half-airplane model requires more than half the masses of the complete airplane model because some of the masses are on the airplane plane of symmetry and are common to both models. In the above example, the symmetrical model yields a reduction in computer run time of 38 percent from that of the complete airplane model involved in the same symmetrical impact.

4.2.2 Massless Node Capability

KRASH allows the user to define node points which are massless. These points are rigidly connected to mass points. With this capability the user can attach internal beams and external springs at points other than the cg of each lumped mass.

While KRASH has the capability to model 80 masses, mass locations cannot be arbitrarily assigned, particularly in regions wherein lightweight structure is located. Experience in modeling light fixed-wing airplane structure has indicated that reasonable care must be taken in selecting mass locations such that element response frequencies are compatible with the integration interval. The higher the element frequency, the smaller the integration interval (and higher the cost to perform an analysis) that is required to maintain a stable system. Two areas that are particularly vulnerable in this regard are:

(1) The rigorous modeling of a finite mass (engine) which has several attach points

(2) The rigorous modeling of a seat system.

The massless node feature is particularly helpful in modeling the types of structure wherein a network of extremely lightweight members (struts, seat legs) is involved.

4.2.3 Revised Stiffness and Damping Formulation

The calculation of the internal beam forces was revised. Previously, the forces at one end of the beam were calculated using the relative deflections of one end with respect to the other ($\Delta X_j - \Delta X_i$, etc), and a 6 x 6 stiffness matrix for a cantilevered beam. Now the forces are calculated using the absolute deflections of each end of the beam and a 12 x 12 stiffness matrix. In the actual computations, the full 12 x 12 k matrix is not employed. If the coupled z-θ bending portion of the full 12 x 12 k matrix is expanded and terms recombined, it can be shown that the forces and moments at the i and j ends of the beam are given by

$$\begin{Bmatrix} \Delta F_{zi} \\ \Delta M_i \\ \Delta F_{zj} \\ \Delta M_j \end{Bmatrix} = \begin{bmatrix} -k_z & & -k_{z\theta} & \\ k_{z\theta} & -k_{\theta/4} & 3k_{z\theta/4} & \\ k_z & & k_{z\theta} & \\ k_{z\theta} & k_{z\theta} & 3k_{\theta/4} & \end{bmatrix} \begin{Bmatrix} \Delta z_j - \Delta z_i \\ \Delta\theta j - \Delta\theta i \\ \Delta\theta j + \Delta\theta i \end{Bmatrix}$$

The Δ's indicate incremental forces and deflections for the numerical integration time interval being considered. The elements k_z, $k_{z\theta}$ and $k\theta$ are the terms of the 6 x 6 cantilever beam stiffness matrix originally used. Notice that the relative deflections and rotations are still used (Δz_j, $-\Delta z_i$, $\Delta\theta_j$, $-\Delta\theta_i$), but that the rotational sum terms ($\Delta\theta_j + \Delta\theta_i$) are also included. A similar equation is written for the coupled (y, $-\psi$) bending, while the axial and torsional modes (x and ϕ) are uncoupled. All forces and moments are expressed in a beam axis coordinate system. This is now a time-varying system whose x axis is always pointing from mass i to mass j.

The damping forces were previously calculated using a diagonalized damping coefficient matrix. They are now calculated as the product of the coupled stiffness matrix times the velocity vector times a damping constant $2\zeta/\omega_n$, where a separate natural frequency ω_n is used for each of the 6 directions. This model yields an approximation of structural-type damping as opposed to the viscous damping previously used. The expression for damping forces and moments is shown below for the couplex z and θ damping forces. A similar expression applies to the y, ψ terms. The axial and torsional terms are uncoupled.

$$\begin{Bmatrix} F_{zDi} \\ M_{\theta Di} \\ F_{zDj} \\ M_{\theta Dj} \end{Bmatrix} \quad 2\frac{\zeta_{ij}}{\omega_n} \quad \begin{bmatrix} k \end{bmatrix} \quad \begin{Bmatrix} \dot{z}_j - \dot{z}_i \\ \theta_j - \theta_i \\ \theta_j + \theta_i \end{Bmatrix}$$

where

ζ_{ij} = internal beam structural damping factor

ω_n = internal beam natural frequency

$\dot{z}, \dot{\theta}$ = beam end point velocities

subscript i = i^{th} end of beam

subscript j = j^{th} end of beam

subscript D = damping term

Strain and damping energy calculations have been revised to be consistent with the new strain and damping force calculation schemes.

4.2.4 Flexible Ground Coding

Provision is made for modeling a simplified representation of soil characteristics. For each external spring, an elastic model of the soil surface may be specified. Separate soil characteristics for each external spring may be input. The linear ground load-deflection model is combined in series with the nonlinear external spring load-deflection model to arrive at a combined nonlinear characteristic curve. This is then used as before in the analysis. Unloading of the soil is not allowed. A separate plowing force may be specified in the input; this force acts in the direction of the ground drag force due to friction.

4.2.5 Restart

Program KRASH is revised to allow the option of starting a case from an intermediate time cut from a previous case. For example, an analysis may be run from 0 to 150 milliseconds, and then restarted from the 50 millisecond point with revised data. The type of data changed would generally be the characteristics of nonlinear beam load-deflection curves that have not yet gone nonlinear, so that the early portion of the analysis would be valid even for the revised data. This feature allows the program user to explore the influence of parameter variations without having to rerun long sections of the analysis that remain unchanged. Considerable computer run time and cost may be saved with proper application of this capability.

4.2.6 Unsymmetrical Load-Deflection Curves

Coding has been added to KRASH to model internal beam elements which behave differently in tension and compression. Only the beam axial loads are treated in this fashion. The types of elements for which this provision is useful include seat belts and diagonal elements representing shear panels. Both of these are modeled with tension-only unsymmetrical elements in which compressive forces are not allowed. A deadband is also provided in the model

for unsymmetrical beams. In the deadband region, the beam has zero load. This can be used to represent contact between two surfaces not originally touching, but which contact each other after large deformations during a crash. An example of this is the contact between the nose wheel and the lower fuselage after impact and failure of the nose gear. This can be modeled with a beam between the nose wheel and the fuselage, using a compression-only element with deadband. Another application would be occupant to cabin structure contact.

4.2.7 Pinned-Fixed Beam End Conditions

The internal beam force/moment calculations have been extended to include all possible combinations of pinned and fixed end conditions. If both ends are pinned, both the lateral force and the moment about the pin axis are zero. This capability was previously included in KRASH. With one beam end fixed and the other pinned, only the moment at the pinned end is zero. The proper equations for this pinned-fixed situation are now included in KRASH. In the analytical model for a high-wing airplane, this type of beam can be used for the inboard wing segment, which is normally pinned at the wing junction to the fuselage and fixed to the outboard segment of the wing.

4.2.8 Additional Features

Other features that were added to KRASH during Task II include:

- Summaries of beam element rupture and yielding .
- Summary time history plot of mass accelerations, velocities, and displacements; beam forces, deflections and stresses; external spring forces and deflections; occupant DRI's; and cg translational velocities.
- The use of the capability to define failure element by a limiting force as well as a limiting deflection as originally coded.
- The incorporation of a standard material code for common materials which includes Modului of Elasticity (E), and Rigidity (G) as well as associated yield compression, tension and shear stresses.
- Low-pass filtering of acceleration data.

A complete description of KRASH Task II refinements is provided in Section 4 of Reference 2. Detailed discussions of KRASH theory, application and supporting design data is presented in References 4, 5 and 6.

4.3 TASK III MODIFICATIONS

The experience obtained during Task I and Task II efforts, as well as feedback from users, indicated additional refinements would improve model stability and/or enhance KRASH usage. The following sections describe the various Task III changes.

4.3.1 Nonlinear Damping Forces

The computation of damping forces is made consistent with the manner in which nonlinear strain forces are computed. Now the nonlinear damping forces, like the nonlinear strain forces, are a function of the respective 6 x 6 stiffness reduction (KR) matrix for each element. With this coding change the user no longer has to input a zero damping value for a load limited beam representation (NP=5, Figure 4-1) to assure that a constant total force is maintained in the nonlinear region. The coding assures that the total damping force as well as the total strain force is constant after the element yields and until such time as "bottoming" or rupture occurs. The change in coding provides the user a more desirable representation for all the beam element types. Figure 4-1 shows the various beam element types internally coded in KRASH. The user can also input any load-deflection characteristic that is representative of the behavior of the structure he is investigating.

4.3.2 Resized Program

KRASH has been resized to increase its capacity so that 150 beam elements and 180 nonlinear beam degrees of freedom can be treated. This is a 50-percent increase for both inputs. Each beam can have as many as six nonlinear degrees of freedom ($x, y, z, \phi, \theta, \psi$). Consequently 30 beams each having 6 nonlinear degrees of freedom can be modeled. In the case of a symmetrical model, however, usually 3 degrees of freedom (x, z, θ) are essential. Therefore, the user would normally be able to treat at least 60 beams nonlinearly. In the

process of resizing the program, unused variables were eliminated and a general programming cleanup was included.

4.3.3 Mass Location Plots

A plot-print routine has been incorporated into KRASH which allows the user to plot the locations of several masses simultaneously at selected intervals during the analysis. The plot-print routine is an expanded version of the routine incorporated as part of the effort described in Reference 16. The plot-print routine allows the user to specify the intervals at which plots are desired (multiple of print intervals); number of plots at each interval (maximum of 10); masses which are to be plotted (maximum of 50); planar view to be plotted (XY, XZ or YZ); and coordinate spacing. The user has the flexibility to request a different number of masses as well as different mass locations for each plot.

The user can designate the plot spacing or have the program select the spacing. When the program self-spaces, the program computes the difference between the maximum and minimum values associated with the mass points for the vertical and horizontal directions. The maximum difference is then divided by 10 equally spaced divisions in the horizontal direction and 8 equally spaced divisions in the vertical direction. By specifying the spacing for the coordinates the user can be assured that each plot will be of the same scale and therefore direct comparisons will be easier. The mass locations are presented in the form of a symbol such as an asterisk and an identifying mass location number. In the event a mass location is off the scale, an error message will signify to the user that the point was not plotted. Figure 4-2 illustrates the plot-print output. The plot routine does not connect the various points.

4.3.4 Energy Error Messages

Several error messages associated with intolerable energy deviations have been incorporated into the program. The program checks to see if the following three tolerances are exceeded:

- Total energy growth exceeds "X" percent.

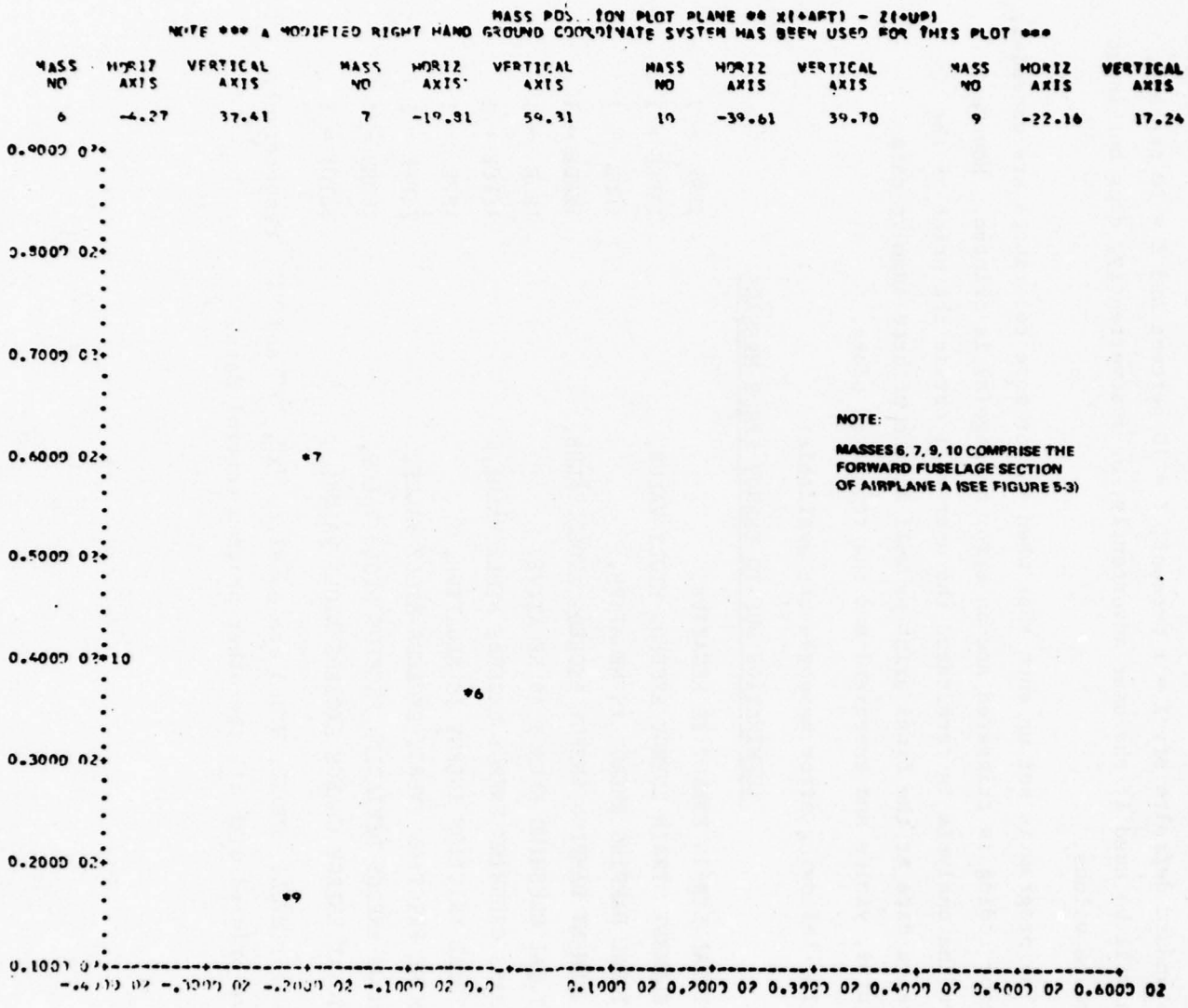

Figure 4-2. Sample Mass Location Plot

- Individual negative strain, damping, crushing, or friction energy terms exceed "Y" percent of their respective totals.

- Individual mass energy deviation exceeds "Z" percent.

The values of "X", "Y" and "Z" can be selected by the user. The program has standard defaults of; X = 1 percent, Y = 10 percent and Z = 30 percent, which will be used if the user advertently, or inadvertently, does not input tolerance values.

The program is set up such that when one or more tolerances are exceeded, an error coding is triggered and an error message(s) is printed. However, before the analysis is terminated the user will obtain the print of the requested data at the final print as well as the printed summary data (ruptures, yields and energies) and the requested plots.

The following error messages are available:

TERMINATION DUE TO ENERGY ERROR MESSAGE

TOTAL STRAIN ENERGY IS NEGATIVE,	IESE = 1
ELEMENT STRAIN ENERGY EXCEEDS NTOL2 VALUE,	IEPSE = 1
TOTAL DAMPING ENERGY IS NEGATIVE,	IEDE = 1
ELEMENT DAMPING ENERGY EXCEEDS NTOL2 VALUE,	IEPDE = 1
TOTAL CRUSHING ENERGY IS NEGATIVE,	IECE = 1
MASS CRUSHING ENERGY EXCEEDS NTOL2 VALUE,	IEPCE = 1
TOTAL FRICTION ENERGY IS NEGATIVE,	IEFE = 1
MASS FRICTION ENERGY EXCEEDS NTOL2 VALUE,	IEPFE = 1
MASS ENERGY DEVIATION EXCEEDS NTOL3 VALUE,	IEDEV = 1
TOTAL ENERGY CHANGE EXCEEDS NTOL1 VALUE,	IETOT = 1

Values for NTOL1, NTOL2, NTOL3 are equal to "X", "Y" and "Z", respectively, and are printed with all the other program control data.

SECTION 5

PARAMETER VARIATION STUDY

5.1 MATH MODEL DESCRIPTIONS

The parameter variation study was conducted using three different light fixed-wing airplane configurations. The math model identification is as follows:

A. Single-engine, high-wing, 4 occupants, maximum T.O. weight = 2300 lb

B. Single engine, low-wing, 1 occupant, maximum T.O. weight = 3900 lb

C. Single-engine, high-wing, 2 occupants, maximum T.O. weight = 1600 lb

The airplane configurations represent two different airplane categories as noted in Section 2, Table 2-2. Models A and C represent semimonocoque fuselage construction as illustrated in Figure 5-1. The Model B represents a welded tube type airframe construction as shown in Figure 5-2. The three airplane math models are presented in Figures 5-3, 5-4, and 5-5 for A, B and C, respectively. A summary of the model sizes is provided in Table 5-1. For each model and crash condition analyzed, a symmetrical model is established. Table 5-2 describes mass and node point designations for the three models. Table 5-3 shows the range of impact conditions for the parameter variation study. The initial pitch rate for the nose-down impact is 0.32 rad/sec. The initial pitch rate for the nose-up (flared) impact is 0.12 rad/sec. For the analysis of the impacts onto a flexible surface, the soil was represented as having a flexibility of 0.00036 inches per pound. The coefficient of friction (μ) value between the flexible surface and airplane structure was taken as 1.5. Both the flexibility and μ values are based on Task II (Reference 2) analytical and experimental data. For impacts onto a rigid surface (concrete) a value of 0.4 was used. All analysis results are obtained using a 70 Hz cutoff frequency which is the KRASH equivalent for the test 100 Hz low-pass filter.

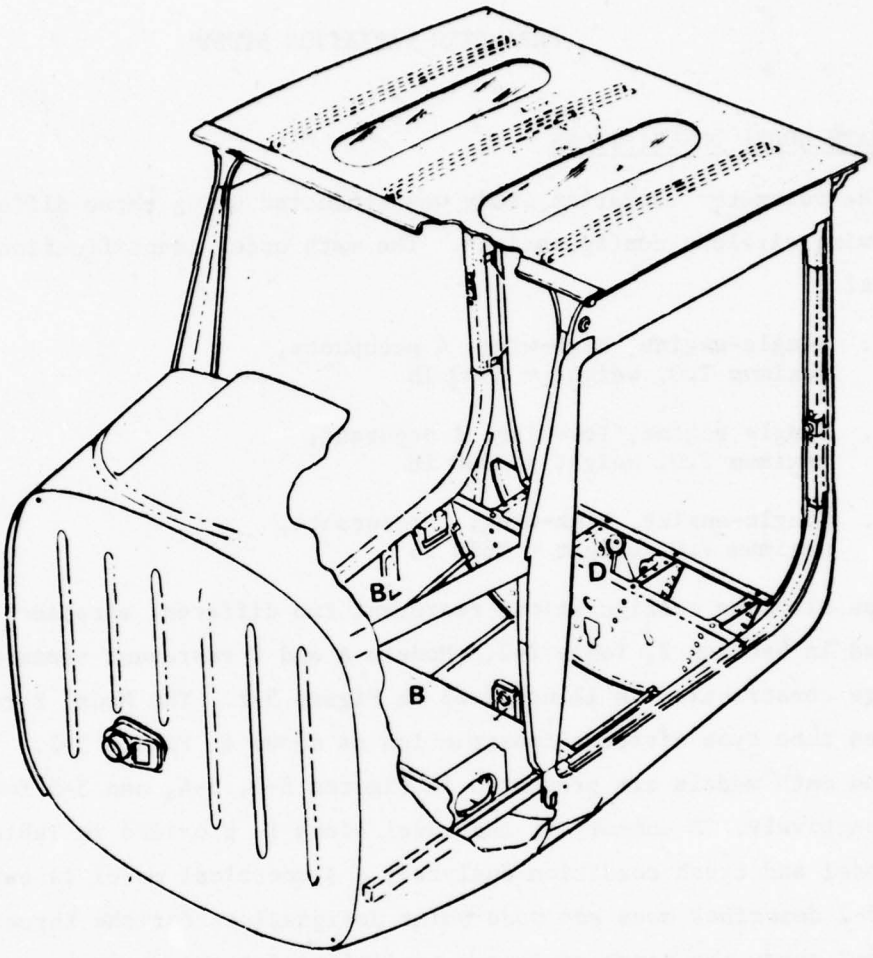

Figure 5-1. Semimonocoque Fuselage Structure

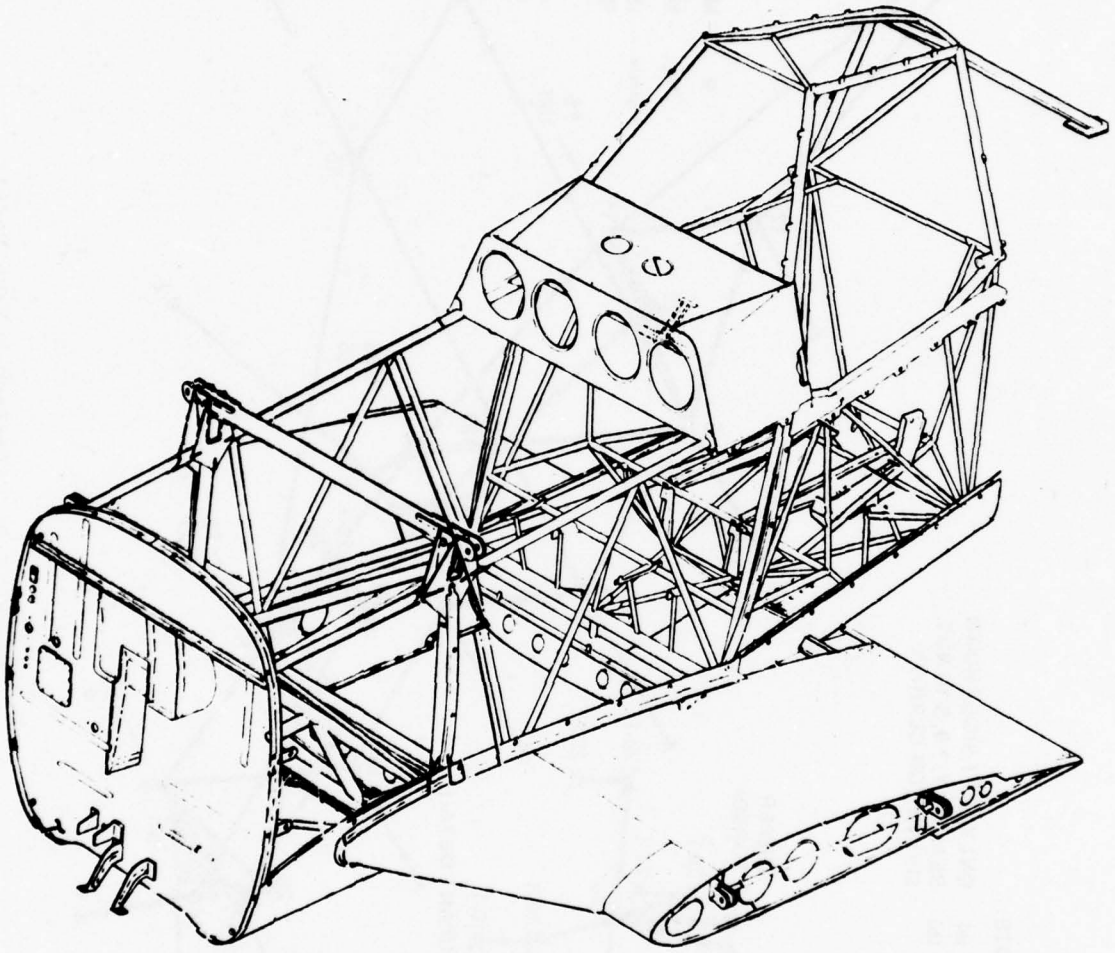

Figure 5-2. Welded Tubular Fuselage Structure

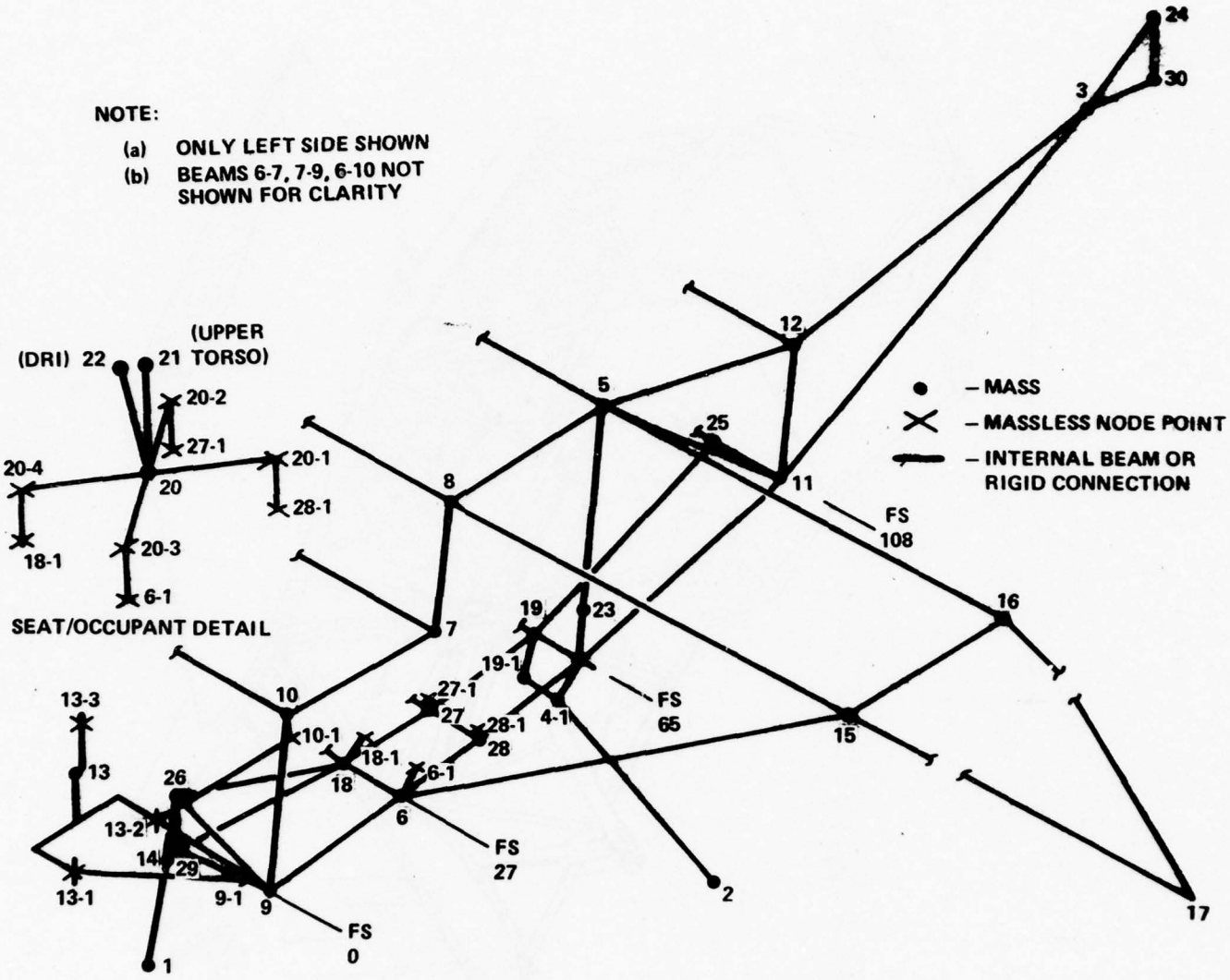

Figure 5-3. Airplane A Math Model

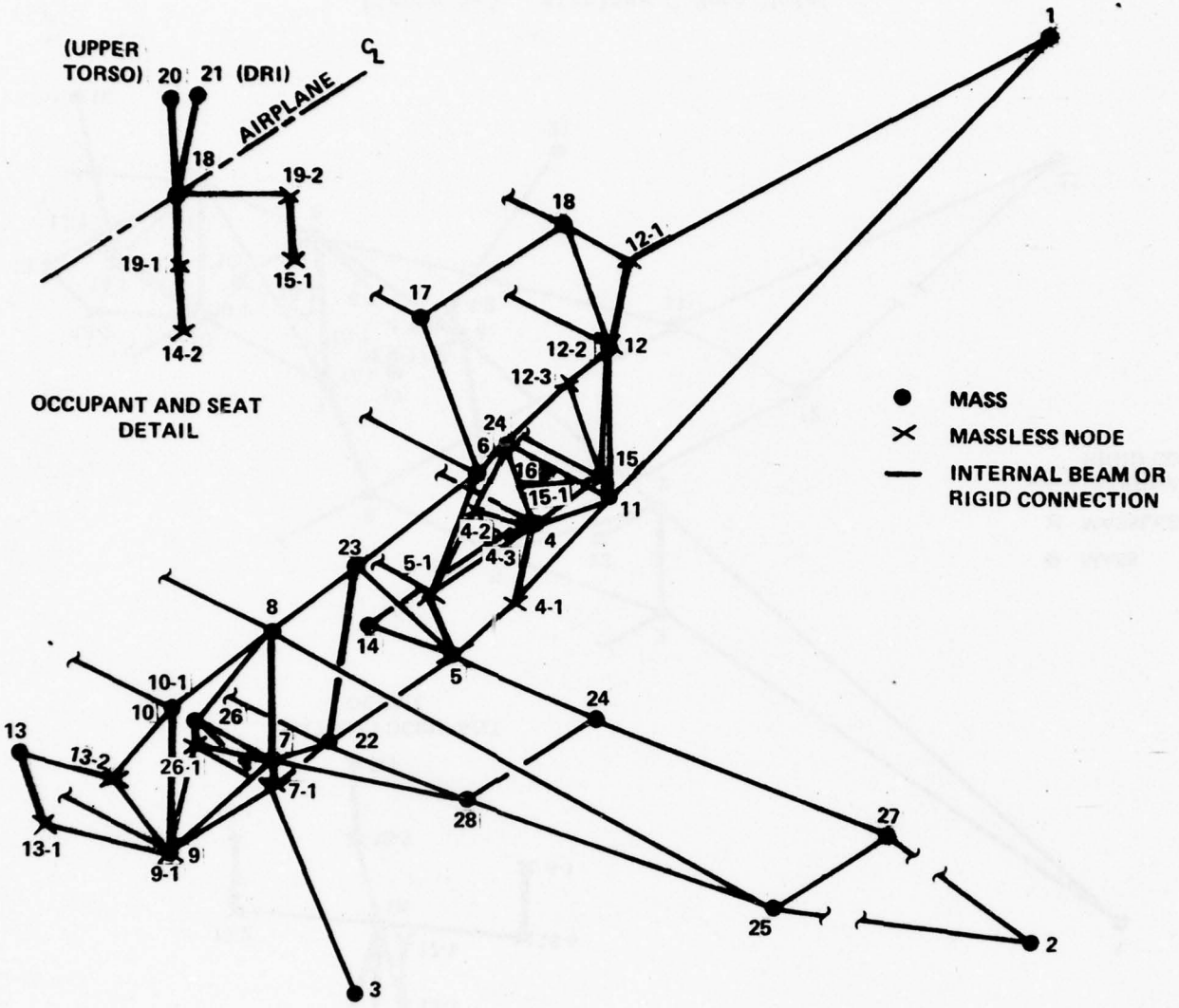

Figure 5-4. Airplane B Math Model

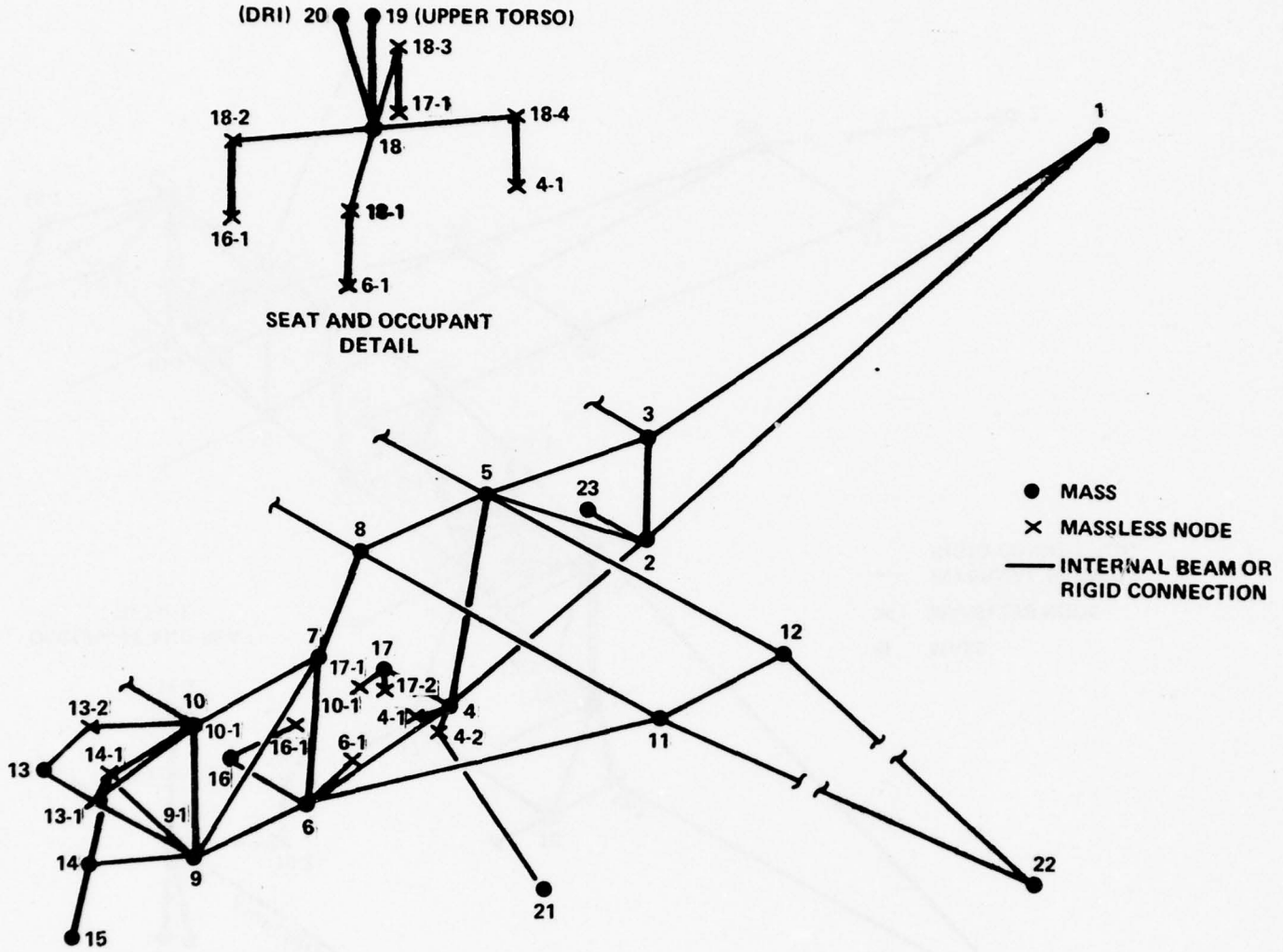

Figure 5-5. Airplane C Math Model

TABLE 5-1. MATH MODELS ELEMENT SUMMARY

	Model A	Model B	Model C
Masses	30	29	23
Massless Nodes	19	16	16
Beams	60	71	46
Nonlinear Beams	67	57	41
External Springs	22	15	17
Nonsymmetrical Beams	3	0	2
Dri Elements	1	1	1

TABLE 5-2. MATH MODELS MASS AND NODE POINTS

	Model A (a)	Model B (b)	Model C (c)
Engine c.g.	13	13	13
Engine Mounts	13-1, 13-2	13-1, 13-2	13-1, 13-2
Cabin Floor	4,6,18,19, 27,28	4,4-1,5,11, 15, 15-1	4,6,16,17
Occupiable Volume	4,5,8,6	4,6,11,12,15, 17,18,24	4,5,8,6
Seat, Occupant Lower Torso	20	19	18
Occupant Upper Torso and Dri	21,22	20,21	19,20
Nose Gear and Support Structure	1,14,26,29	Tail Skid Configuration	14,15
Main Gear and Bulkhead Attachment	2,4-1,19-1, 4,19	3,7-1,26-1	4-2,17-2,21
Wing-Airframe Attachments	5,6,8,15	5,7,8,25,28 22	5,6,8,11
Seat Leg-Floor Intersection	6-1,18-1, 28-1,27-1	14-2, 15-1	6-1,16-1, 4-1,17-1

(a) See Figure 5-3
(b) See Figure 5-4
(c) See Figure 5-5

TABLE 5-3. IMPACT CONDITION RANGE, PARAMETER VARIATION STUDY

Math Model (a)	Run	Pitch Angle (Deg.)				Flight Path Angle (Deg.)				Velocity MPH			Terrain		(b) μ		Lift Weight		Comments
		-15	-30	-45	+10 +15 +20	-15	-30	-45	-10 -15 -20	45	55	65	Conc.	Soil	0.4	1.5	0	0.65	
A	1		X				X				X		X		X		X		Base case, nose down
	2		X				X					X	X		X		X		Vary velocity
	3	X				X					X		X		X		X		Vary impact angle θ
	4			X				X			X		X		X		X		Vary impact angle θ
	5			X			X			X			X		X		X		Vary θ and velocity
	6	X				X						X		X		X	X		Vary θ and flex. ground
	7				X				X		X		X		X			X	Base case, flared impact
	8				X				X			X	X		X			X	Vary velocity
	9				X				X			X	X		X		X		Zero lift
	10				X				X			X		X		X	X		Flexible ground
B	11		X				X				X		X		X		X		Base case, nose down
	12				X				X		X		X		X			X	Base case, flared impact
C	13		X				X				X		X		X		X		Base case, nose down
	14				X				X		X		X		X			X	Base case, flared impact

(a) A - single engine, high-wing configuration, max. T.O. weight = 2300 lb, 4 occupants
B - single-engine, low-wing configuration, max. T.O. weight = 3900 lb, 1 occupant
C - single-engine, high-wing configuration, max. T.O. weight = 1600 lb, 2 occupants

(b) μ = coefficient of friction

5.2 PARAMETER VARIATION STUDY RESULTS

5.2.1 Model A, B, and C Comparisons

For the models, a comparison of occupant and mass responses, system energies, velocity changes, and structural yield, failures and loads was made for base nose-down and base nose-up (flared) impact conditions. The nose-down case comprises conditions 1, 11 and 13 for models A, B and C, respectively. The nose-up case comprises conditions 7, 12 and 14, for models A, B and C, respectively. The impact parameters for the nose-down base case are referred to as -30/-30/55.* The nose-up impact parameters are +15/-15/55.*

At the initiation of impact, kinetic energy accounts for approximately 95 percent of the total energy for all models and potential energy accounts for the remaining energy. The data presented in Table 5-4 show that the kinetic energy as a percent of the total energy is relatively close for all three models during the nose-down impact condition (40.3 to 50.5 percent) and during the nose-up impact (73.1 to 75.6 percent) at the conclusion of comparable analytical times. However, since the Model B airplane is substantially heavier it actually absorbs significantly more energy during the respective crash conditions as compared to Models A and C. At its peak, strain accounts for approximately 8.4 percent, 13.3 percent and 14.2 percent of the total energy absorbed for Models A, B and C, respectively, in the nose-down impact analysis. At its maximum, crushing accounts for approximately 10 percent, 9.8 percent and 8.6 percent of the total energy for Models A, B and C, respectively during the nose-down impact analysis. Strain and crushing energies decrease both in absolute value and percent of total as the structure unloads. Damping and friction energy, which are irreversible, increase in time and at the conclusion of the respective analyses are at their maximum values. For the nose-down impact analysis, peak friction energy varies from 27.5 percent to 35.4 percent of the total energy and damping energy varies from 2.1 percent to 7.6 percent of the total. For the nose-up impact analysis,

*$\theta/\gamma/V$ = pitch angle (degrees)/flight-path angle (degrees)/flight-path velocity (mph)

TABLE 5-4. ENERGY DISTRIBUTION SUMMARY, MODELS A, B, AND C

		Model A	Model B	Model C
Nose-Down Impact Condition	Total Energy (in-lb)	3.054×10^6	4.2545×10^6	2.154×10^6
	Initial Kinetic Energy[a]	94.1	95.0	95.3
	Maximum Value[a] - Strain	8.4	13.3	14.21
	Damping	2.12	7.55	2.40
	Crushing	9.95	9.77	8.57
	Friction	35.37	34.14	27.49
	Final Value[a] - Kinetic	44.57	40.26	50.5
	Potential	3.04	2.77	1.77
	Strain	7.85	12.36	13.11
	Damping	2.12	7.55	2.40
	Crushing	7.05	2.92	4.73
	Friction	35.37	34.14	27.49
	Percent Energy Change[b]	.09	1.10[c]	.25
	Maximum Time of Analysis	.120	.120	.120
	Integration Interval (ΔT), (d)	30	30-40	30
Nose-Up Impact Condition	Total Energy (in-lb)	3.002×10^6	4.2054×10^6	2.14×10^6
	Initial Kinetic Energy[a]	95.9	96.2	96.
	Maximum Value[a] - Strain	3.48	5.23	3.58
	Damping	.44	.33	1.70
	Crushing	1.53	.78	1.97
	Friction	17.29	14.93	16.27
	Final Value[a] - Kinetic	74.04	75.57	73.06
	Potential	3.55	3.18	3.41
	Strain	3.30	5.20	3.58
	Damping	.44	.33	1.7
	Crushing	1.38	.78	1.97
	Friction	17.29	14.93	16.27
	Percent Energy Change[b]	-.01	-.01	+.14
	Maximum Time of Analysis	.144	.150	.150
	Integration Interval (ΔT), (d)	15-30	40	15-30

(a) Percent of Current Total

(b) $\left(\frac{\text{Final Total - Initial Total}}{\text{Initial Total}}\right) \times 100$

(c) Equals 0.60% energy change with ΔT = 20 μseconds

(d) Microseconds

the amount of energy absorbed is considerably less, for the respective components, as compared to the nose-down impact results. As noted earlier the kinetic energy remaining for the nose-up cases is approximately 73 to 75 percent of the total versus 40 to 50 percent of the total for the nose-down cases.

Overall, the analyses depict stable mathematical models. The overall energy growth, which is a measure of integration error, varies from -0.01 to +1.1 percent. The integration interval ranged from 15 to 40 microseconds for the analyses.

Table 5-5 shows a summary of the airplane longitudinal and vertical cg velocities obtained from the analysis of the nose-down and nose-up impact conditions for each of the three model configurations. The vertical velocity component for the nose-down condition reaches zero in 0.087 to 0.120 seconds, while the vertical velocity component for the nose-up condition reaches zero after approximately 0.140 seconds. The longitudinal velocity component reduces to approximately 23 to 30.7 percent of the original velocity for the nose-down impact. For the nose-up impact the reduction in longitudinal velocity is 10.8 to 12.8 percent of the original longitudinal component. This small reduction in longitudinal velocity explains why the kinetic energy for the nose-up condition is a higher percentage of the total energy as compared to the nose-down condition. During the nose-up impact, the airplane slides out a longer distance. If the analysis were to continue beyound 0.150 seconds, the friction and damping energies would continue to increase as the airplane comes to rest.

Table 5-6 summarizes seat leg, wing attachment, and landing gear attachment loads for the three airplanes analyzed. For comparison the failure loads are shown in Table 5-7. The analysis indicates that the potential for seat failure due to airplane longitudinal loads is greatest for the Model B airplane during a nose-down impact followed by the Model C and Model A airplanes. During the nose-down impact, potential wing strut column buckle failures for the Model A and C airplanes exist. However, the wing strut of Model B, while receiving tensile loads of a higher magnitude than compressive loads experienced by Models A and C, has a greater strength capability and

TABLE 5-5. AIRPLANE CG VELOCITY SUMMARY, MODELS A, B, C

CG Velocity Component (a)	Nose-Down Condition (e)			Nose-Up Condition (f)		
	Model A	Model B	Model C	Model A	Model B	Model C
Initial						
Longitudinal Velocity	46.9	46.9	46.9	52.4	52.4	52.4
Vertical Velocity	27.1	27.1	27.1	14	14	14
Final						
Longitudinal Velocity	34.7	32.5	36	46.8	47.9	47.1
Vertical Velocity	0	-6.4	-.86	.728	3.9	-.28
Time, Maximum (b)	0.120	0.120	0.120	0.144	0.150	0.150
Time for Vertical Velocity to Reach Zero (b)	0.120	0.087	0.111	(c)	(c)	0.141
Percent Reduction of Longitudinal Velocity	26	30.7	23.3	10.7	8.6	9.9

(a) Velocity in MPH in ground axis

(b) Time in Seconds After Impact

(c) CG Vertical Velocity Doesn't Reach Zero

TABLE 5-6. SUMMARY OF MAXIMUM SEAT LEG-FLOOR INTERSECTION AND WING-FUSELAGE ATTACHMENT LOADS, MODELS A, B, AND C

Location[e]	Nose-Down Condition[a]			Nose-Up Condition[a]		
	Model A	Model B	Model C	Model A	Model B	Model C
Seat Leg[b]						
Forward Outboard	1986	9430[d]	3875	445	575	546
Forward Inboard	2390	9430[d]	3000	299	575	463
Rear Outboard	838	11300[d]	1014	221	1019	463
Rear Inboard	1618	11300[d]	272	135	1019	515
Wing-Fuselage Attachment[c]						
Wing Column Strut	-5800[d]	-8840	-7918[d]	-1911	-1843	-6279
Wing Rear Spar	+7200	+9000	+22590	+1617	+2007	+3107
Wing Forward Spar	-6700	-22000	-20380	-2194	-2975	-6592

(a) Loads in Pounds

(b) Shear Load in Airplane Longitudinal Direction

(c) Load in Member Axial Direction; +Tensile, -Compression

(d) Exceeds Failure Load and rupture occurs

(e) See Table 5-2 and Figures 5-3, 5-4 and 5-5 for location

TABLE 5-7. FAILURE LOADS, MODELS A, B, AND C

	Model A	Model B	Model C
Wing Column Strut (a)	-5800	+37400	-7918
Wing Rear Spar Attachment (a)	(c) 20837	22500 (c)	28474 (d)
Wing Forward Spar Attachment (a) (c)	29460	42500	29460
Seat Leg Rivet and Bolt Strength (b)			
double shear rivet	1100	1100	1100
single pin shear	3025	3025	3025
double pin shear	4538	4538	4538
Landing Gear Attachment (b)			
inboard bolt	10000	67860	8280

(a) Load (pounds) in member axial direction; + tension, - compression
(b) Load (pounds) in airplane longitudinal direction
(c) bolt shear
(d) tear out

is not expected to fail. Wing spar failures are possible for the Model B (forward) and Model C (rear) airplanes. For the nose-up impact configuration the loads for the most part appear to be well below their respective failure values.

Table 5-8 provides a summary of maximum filtered accelerations at the engine cg, the occupant lower and upper torso, and at the seat leg-floor intersection in the longitudinal and vertical directions. The time histories of the acceleration responses at the above noted locations are provided in Figures 5-6 through 5-15. From Figure 5-6 through 5-10 and Table 5-8 it can be seen that the most severe peak longitudinal responses occur for Model C, while the maximum peak vertical accelerations occur for Model B. The responses for the nose-up impact (Figures 5-10 through 5-15 and Table 5-8) show substantially lower responses than do the corresponding nose-down impacts. Table 5-9 summarizes the yields and ruptures for the three models.

TABLE 5-8. MAXIMUM FILTERED ACCELERATIONS AND TIMES TO OCCURRENCE, MODELS A, B AND C

Location	Direction	Nose-Down Condition						Nose-up Condition					
		Model A		Model B		Model C		Model A		Model B		Model C	
		(a)	(b)	(a)	(b)	(a)	(b)	(a)	(b)	(a)	(b)	(a)	(b)
Engine cg	Up	48.7	0.075	116	0.078	59.3	0.066	11.6	0.075	13.5	0.102	21.2	0.099
	Down	24.4	0.105	39	0.102	24.2	0.078	8.7	0.060	9.9	0.069	23	0.135
	Aft	63.6	0.081	57.7	0.072	73	0.060	11.	0.096	7.	0.090	27.7	0.090
	Forward	11.9	0.117	35.4	0.078	19.4	0.120	6.3	0.084	10.	0.078	19.1	0.102
Occupant Lower Torso	Up	47.2	0.078	38	0.084	64	0.078	7.6	0.132	17.6	0.051	25.6	0.138
	Down	28.	0.090	39.6	0.108	13.9	0.120	5.2	0.084	5.	0.102	11	0.111
	Aft	46.7	0.063	132	0.081	93	0.117	13.2	0.102	10.6	0.078	10.8	0.150
	Forward	31	0.120	44	0.114	10-	0.100	17.	0.093	6.7	0.063	4.7	0.102
Occupant Upper Torso	Up	19	0.081	12	0.072	30	0.090	8.7	0.138	19.3	0.063	16	0.147
	Down	2.9	0.117	-	-	13	0.120	-	-	9.2	0.117	-	-
	Aft	26.6	0.120	37.2	0.096	24	0.120	-	-	1.9	0.114	-	-
	Forward	-	-	-	-	2.6	0.093	1.6	0.141	4.1	0.075	2.	0.144
Forward Seat Leg - Floor Intersection (c)	Up	56.2	0.078	53.7	0.12	80.8	0.075	14.6	0.132	17.8	0.051	19.5	0.138
	Down	20.2	0.120	77	0.108	7	0.075	6.6	0.084	5.9	0.117	6.4	0.108
	Aft	34	0.090	151	0.078	186	0.081	7	0.087	9.6	0.075	38	0.102
	Forward	23.6	0.096	70	0.102	128	0.096	8.6	0.102	10.6	0.072	18	0.111
Rear Seat Leg-Floor Intersection (c)	Up	43.9	0.087	57.5	0.093	72.7	0.084	17.8	0.099	17.6	0.051	24.7	0.138
	Down	30	0.120	27.1	0.108	13.3	0.108	3.9	0.084	6.4	0.102	-	-
	Aft	37.9 34.3	0.072 0.087	143	0.084	68	0.096	10.8	0.102	4.1	0.117	38	0.102
	Forward	18.8	0.096	66	0.099	42.3	0.099	5.6	0.081	6.2	0.069	39	0.111

(a) G_{peak} value, 70 Hz. Low-Pass Filter

(b) Time in seconds after impact

(c) Outboard location

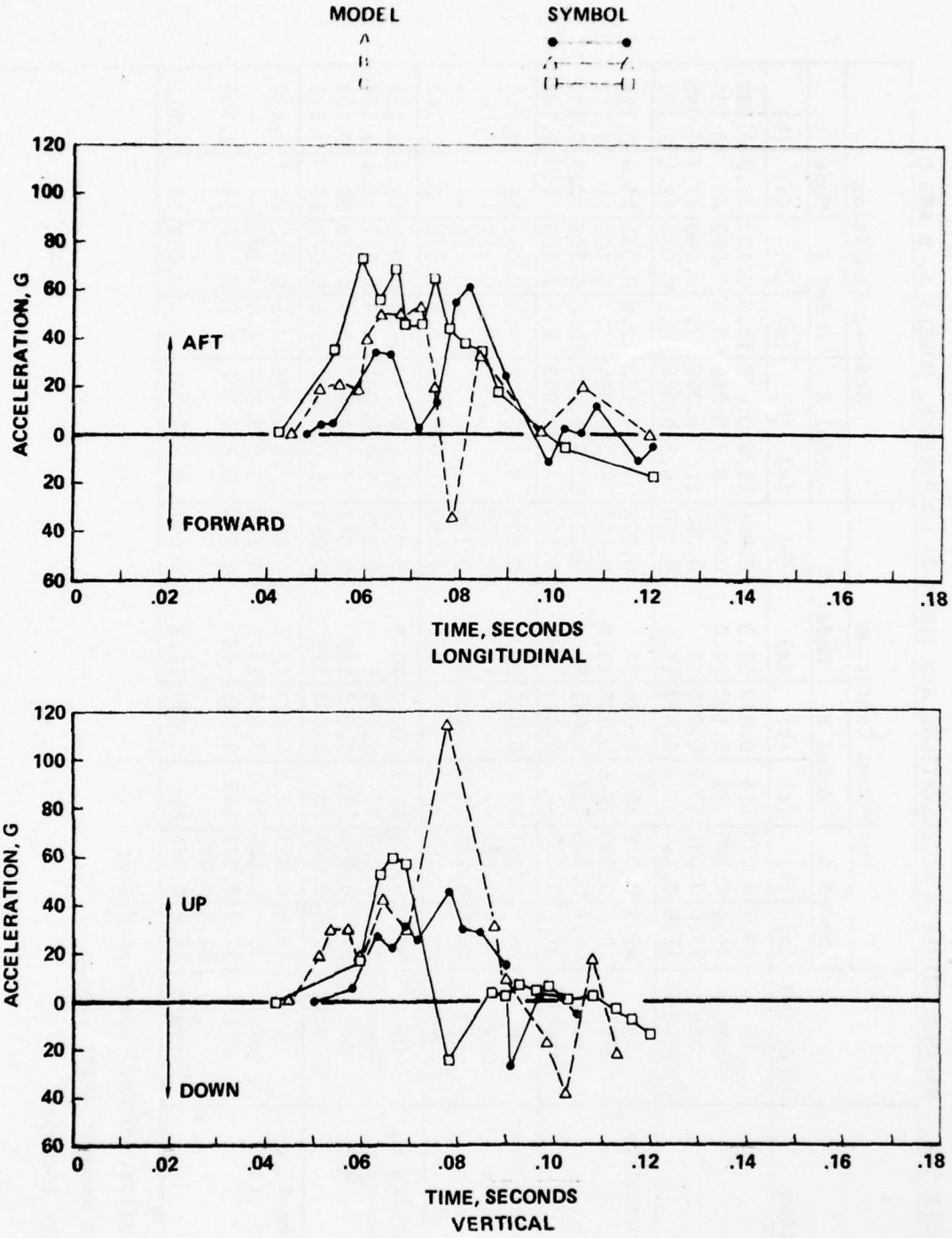

Figure 5-6. Engine CG Longitudinal and Vertical Accelerations Versus Time, Models A, B and C, Nose-Down Impact

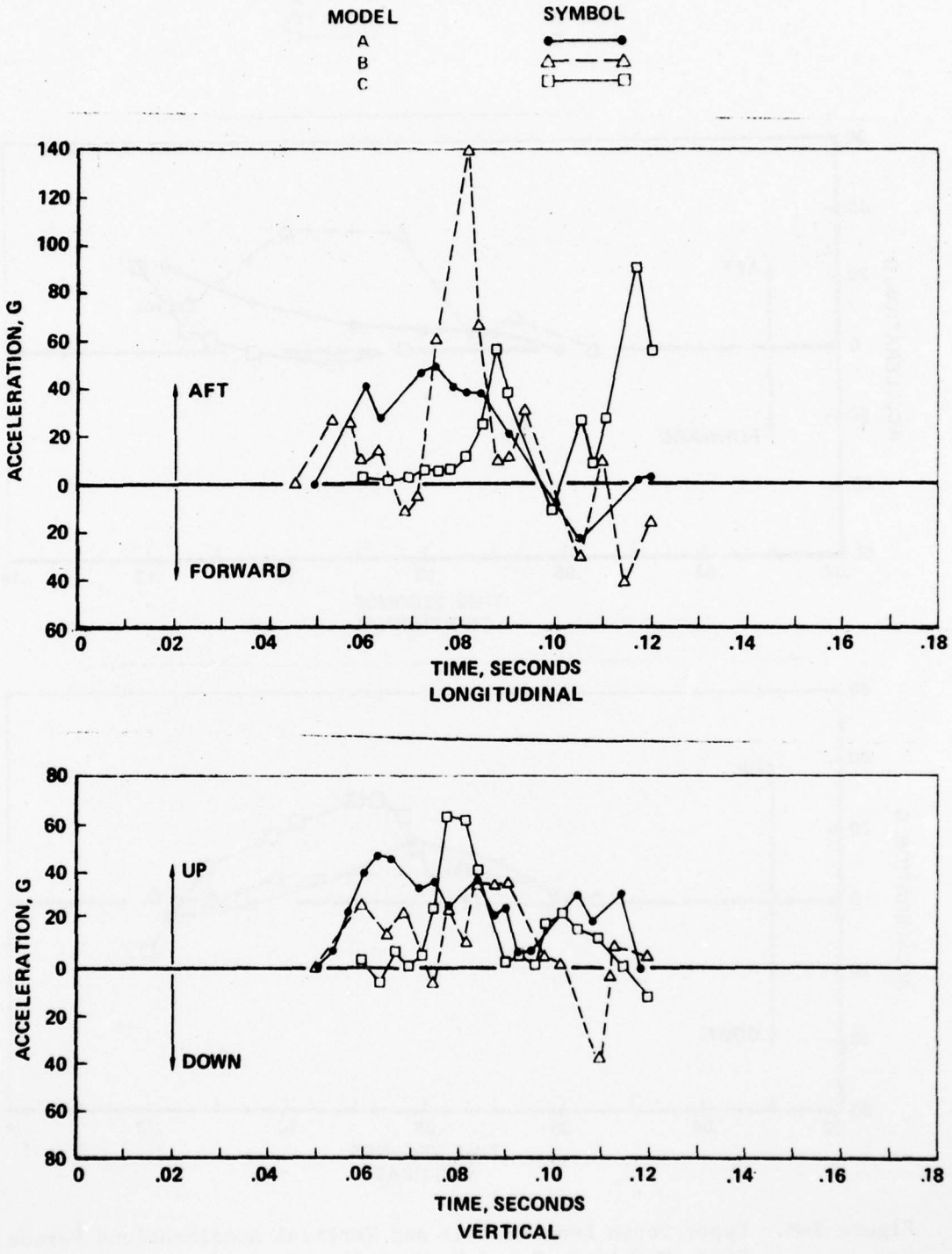

Figure 5-7. Lower Torso Longitudinal and Vertical Accelerations Versus Time, Models A, B and C, Nose-Down Impact

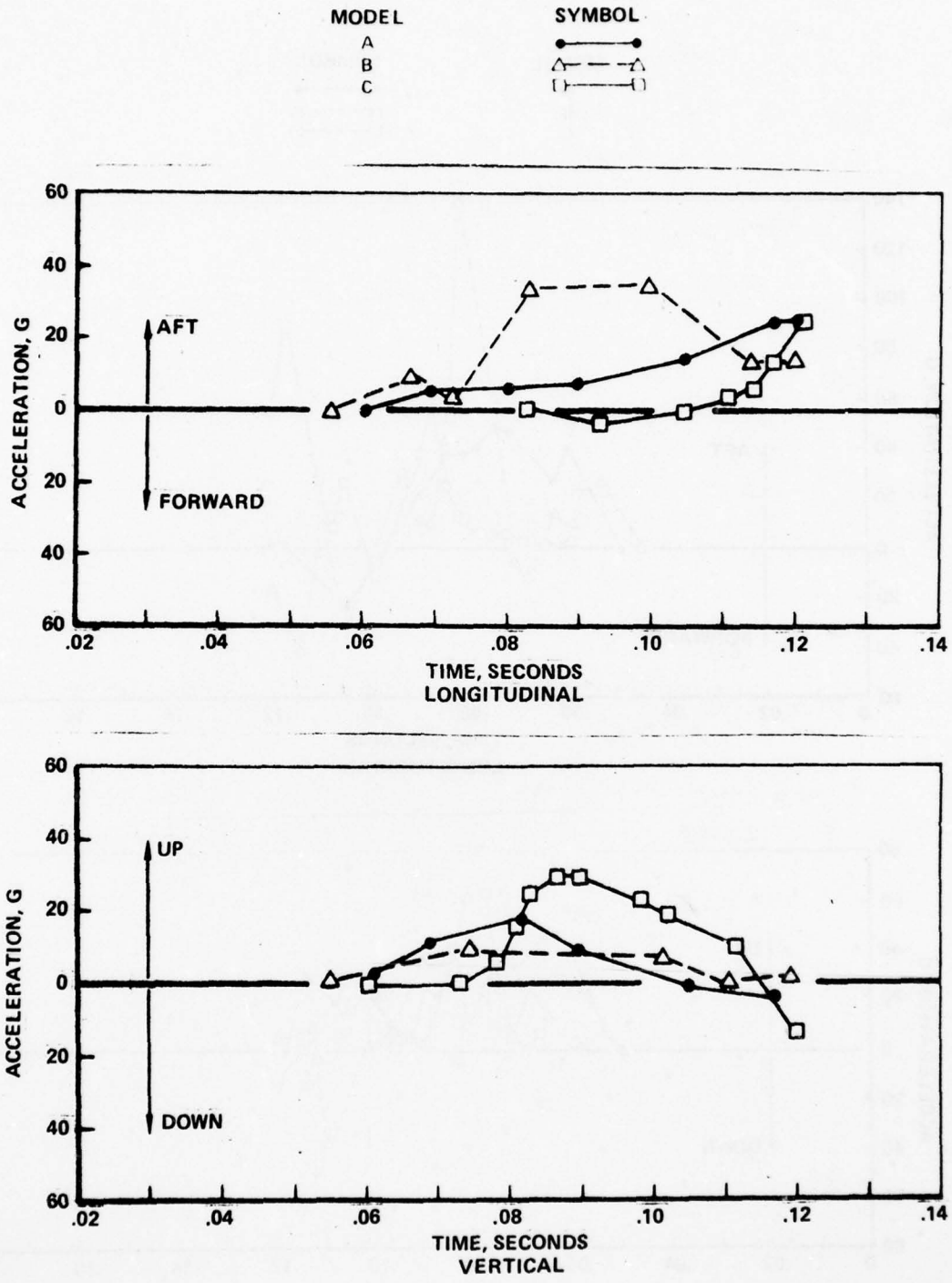

Figure 5-8. Upper Torso Longitudinal and Vertical Accelerations Versus Time, Models A, B and C, Nose-Down Impact

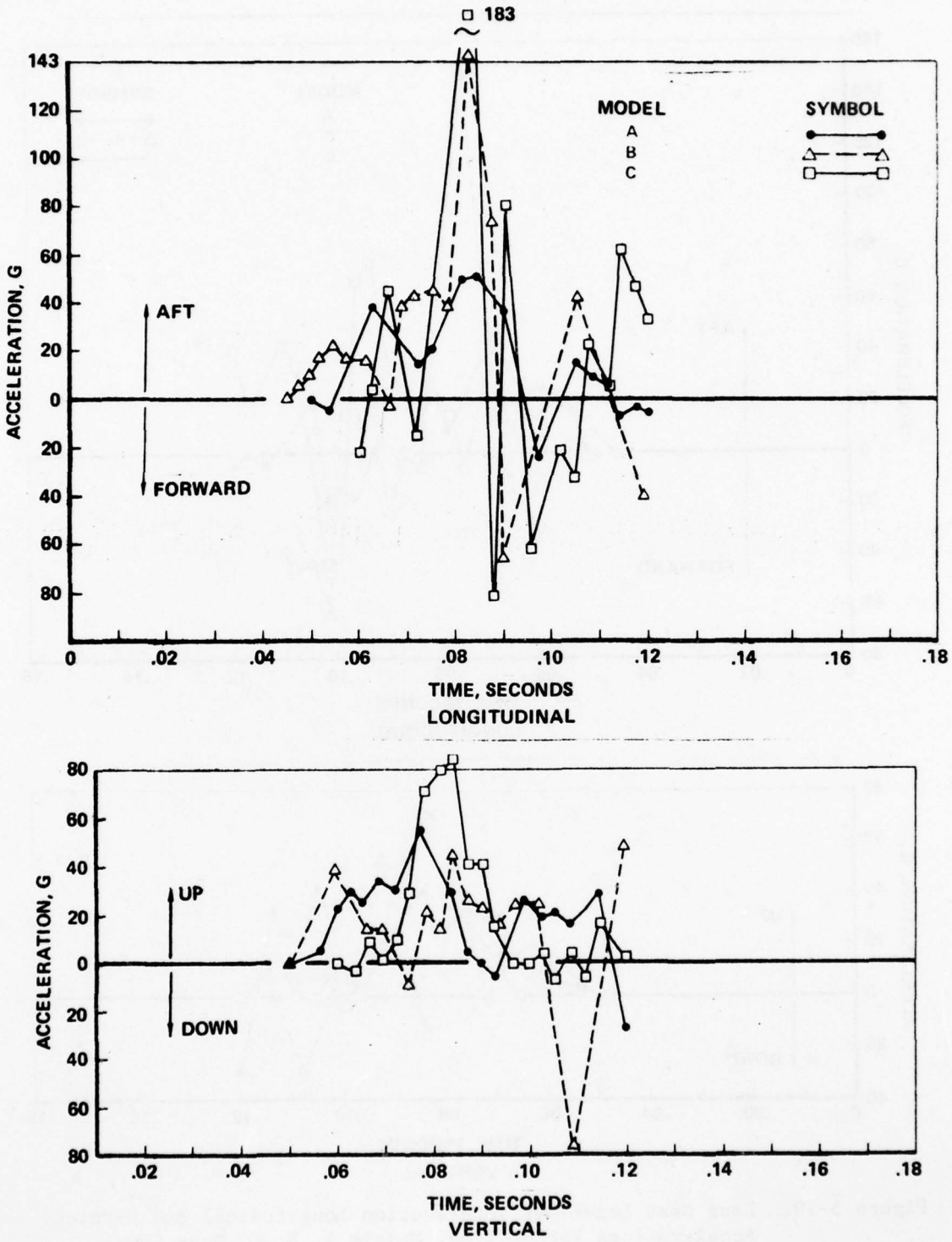

Figure 5-9. Forward Seat Leg-Floor Intersection Longitudinal and Vertical Accelerations, Models A, B and C, Nose Down Impact

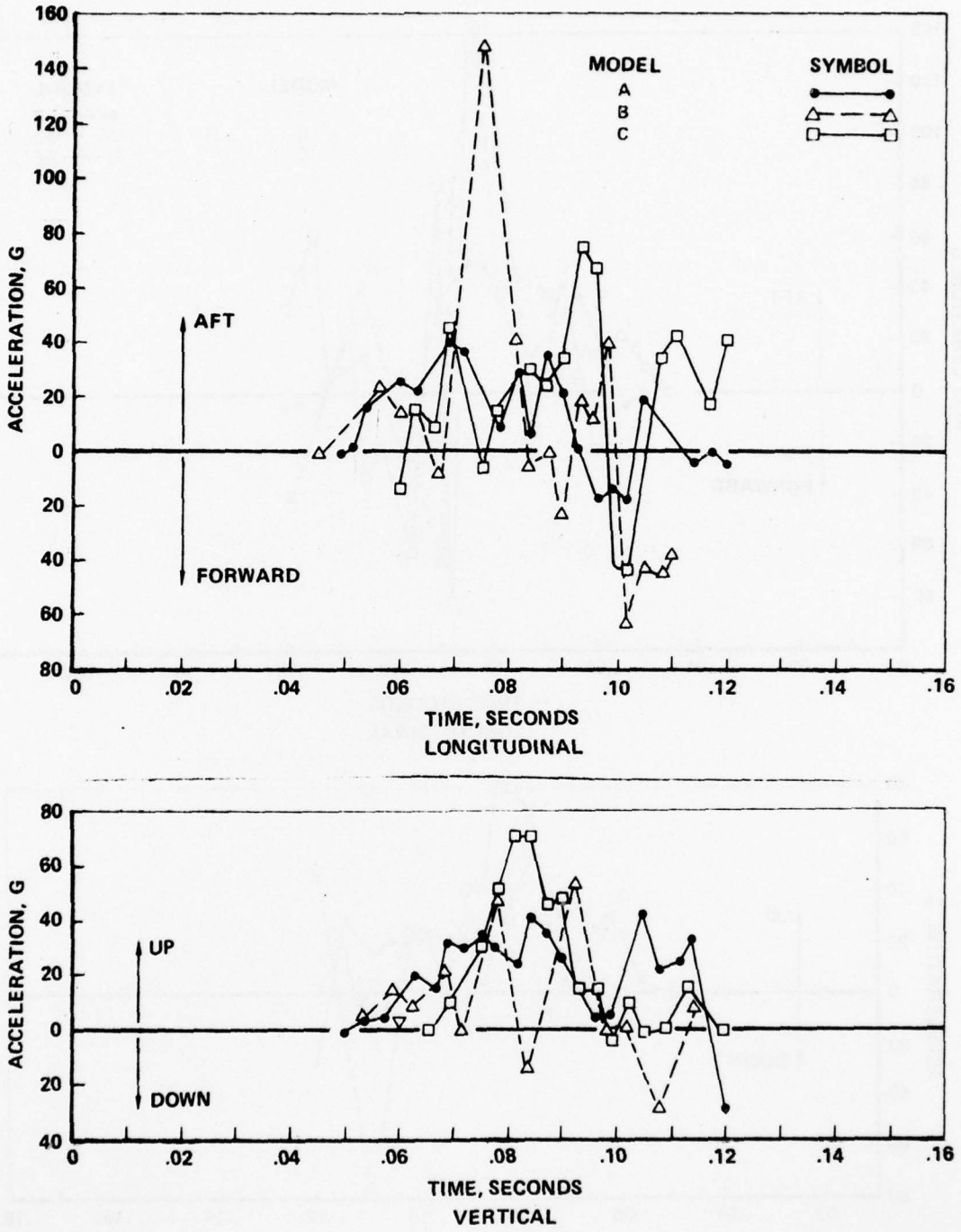

Figure 5-10. Rear Seat Leg-Floor Intersection Longitudinal and Vertical Accelerations Versus Time, Models A, B, C, Nose-Down Impact

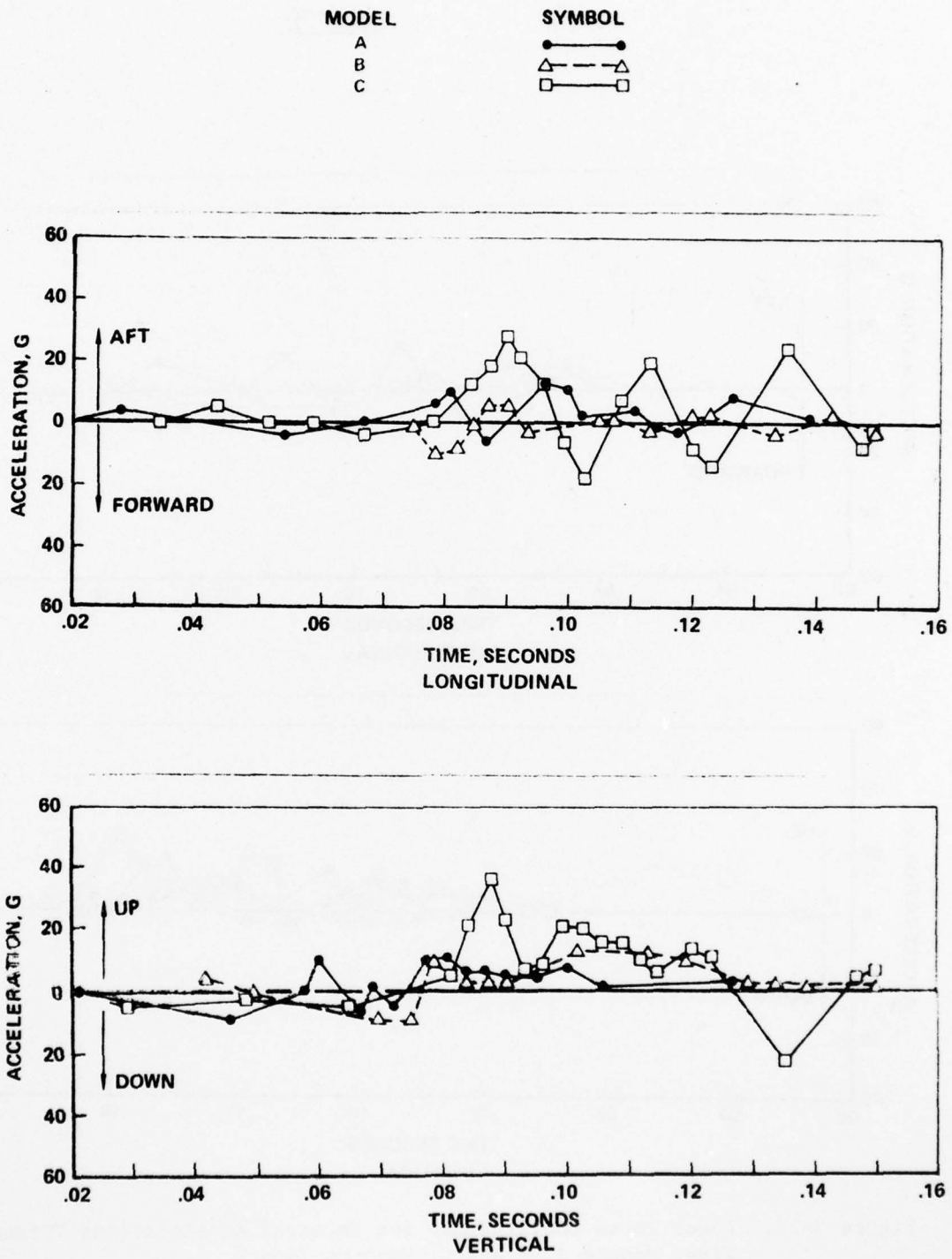

Figure 5-11. Engine CG Longitudinal and Vertical Accelerations Versus Time, Models A, B and C, Nose-up Impact

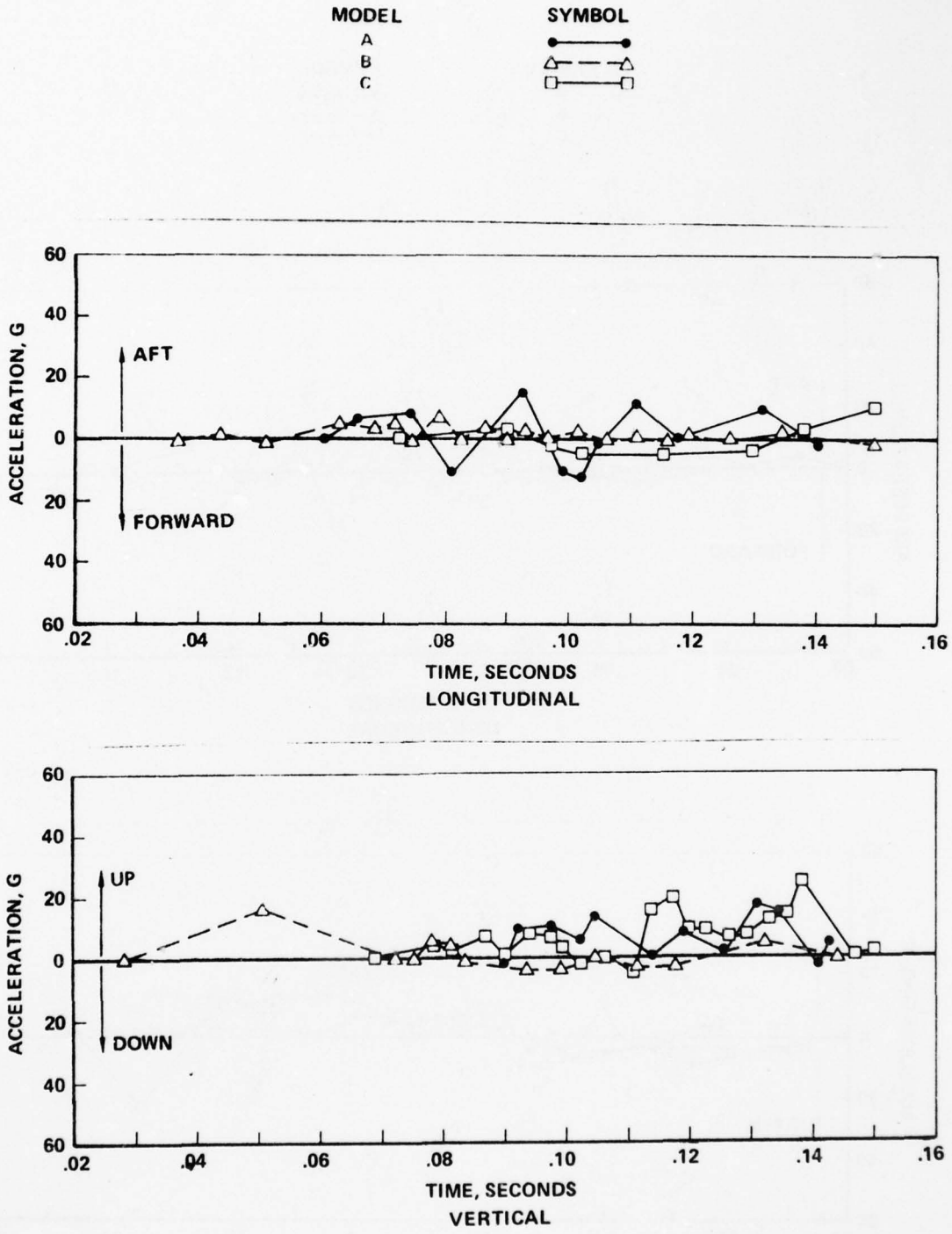

Figure 5-12. Lower Torso Longitudinal and Vertical Accelerations Versus Time, Models A, B and C, Nose-Up Impact

AD-A063 840 LOCKHEED-CALIFORNIA CO BURBANK F/G 1/2
DEVELOPMENT, EXPERIMENTAL VERIFICATION, AND APPLICATION OF PROG--ETC(U)
DEC 78 G WITTLIN DOT-FA75WA-3707
UNCLASSIFIED LR-28682 FAA-RD-78-119 NL

2 OF 2
AD A063 840

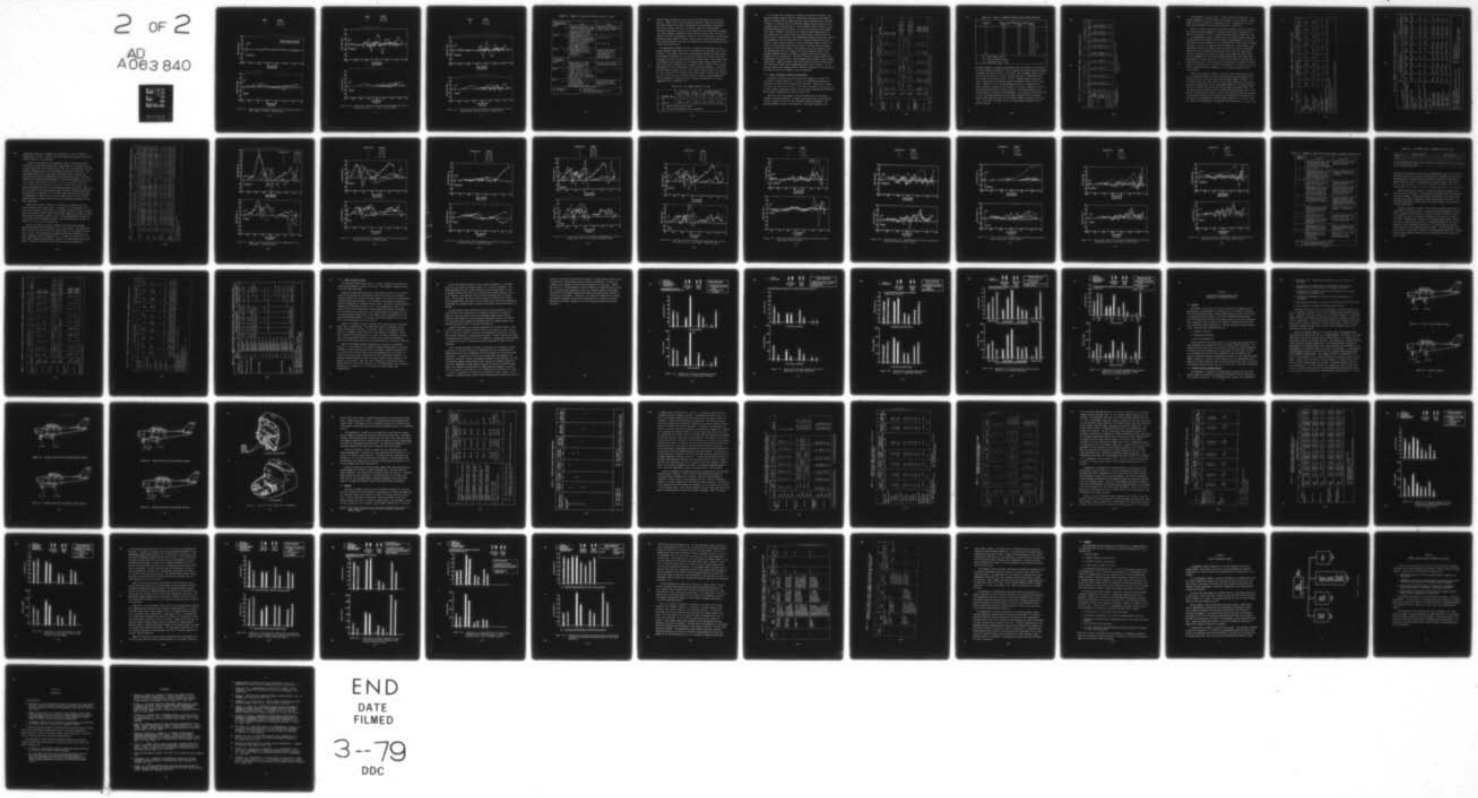

END
DATE FILMED
3--79
DDC

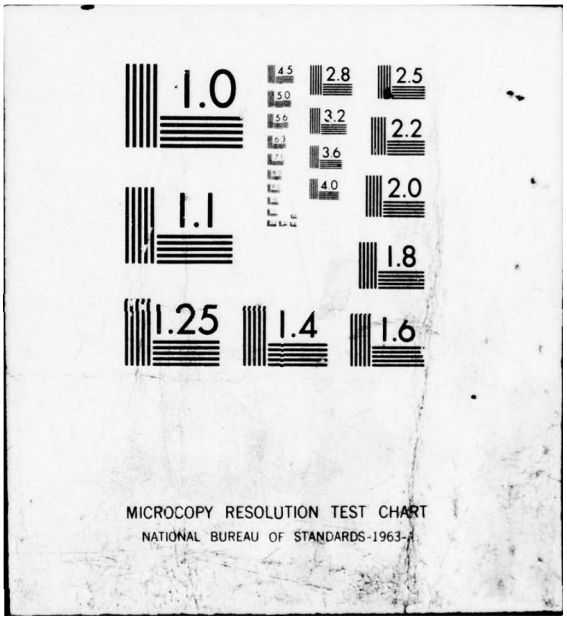
1.0
1.1
1.25
1.4
1.6
1.8
2.0
2.2
2.5
2.8
3.2
3.6
4.0
4.5
5.0
5.6
6.3
MICROCOPY RESOLUTION TEST CHART
NATIONAL BUREAU OF STANDARDS-1963-A

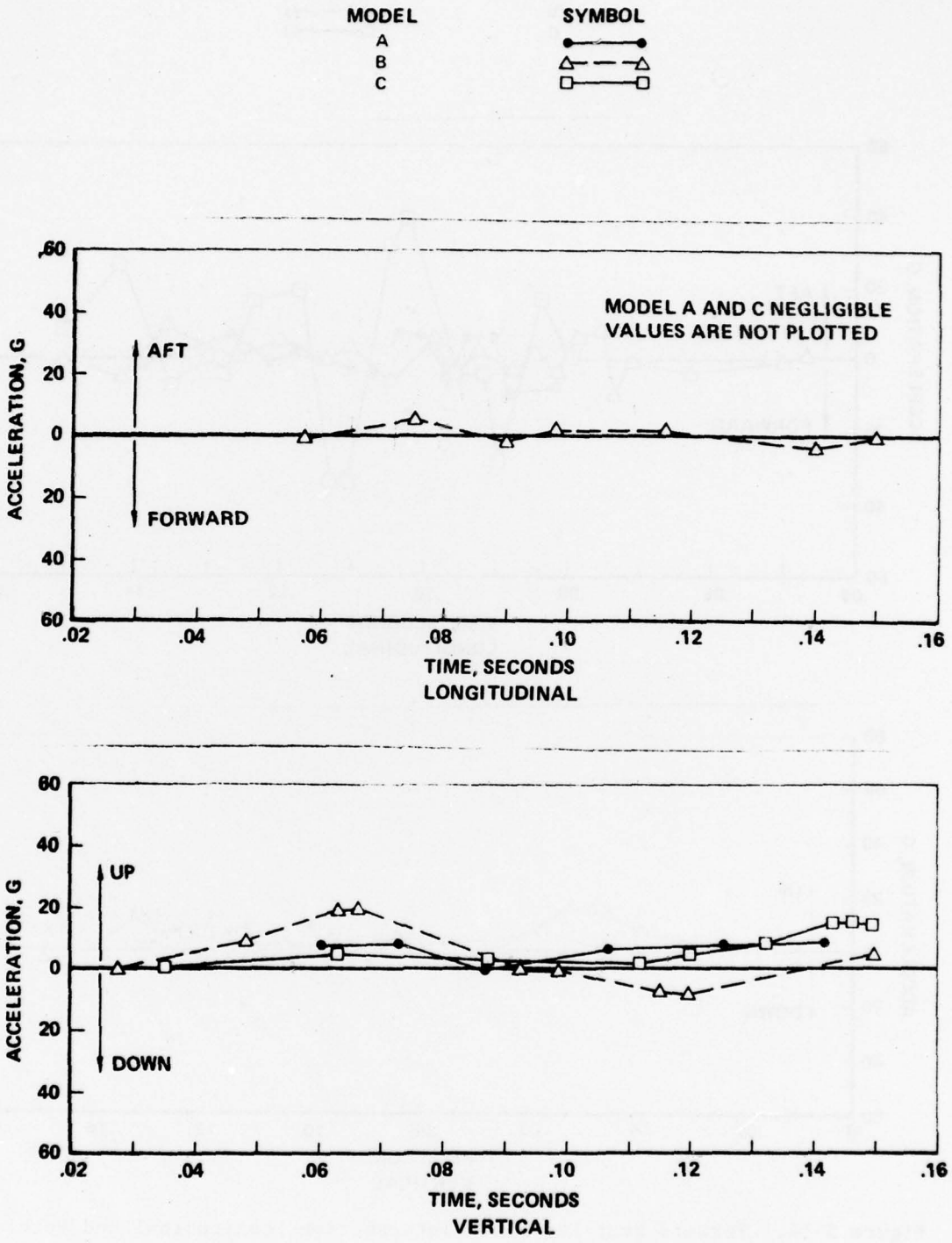

Figure 5-13. Upper Torso Longitudinal and Vertical Accelerations Versus Time, Models A, B and C, Nose-Up Impact

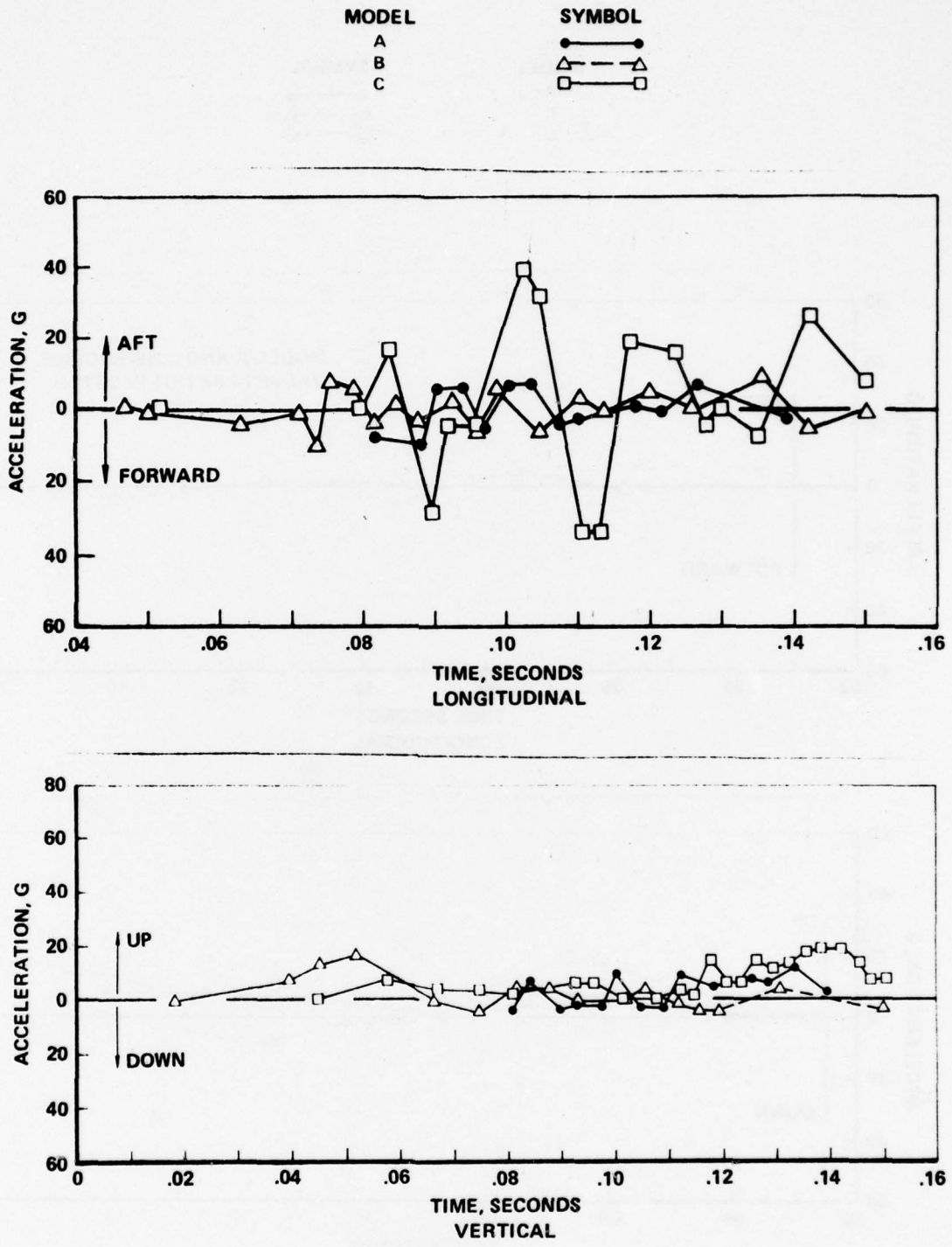

Figure 5-14. Forward Seat Leg-Floor Intersection Longitudinal and Vertical Accelerations, Models A, B and C, Nose-Up Impact

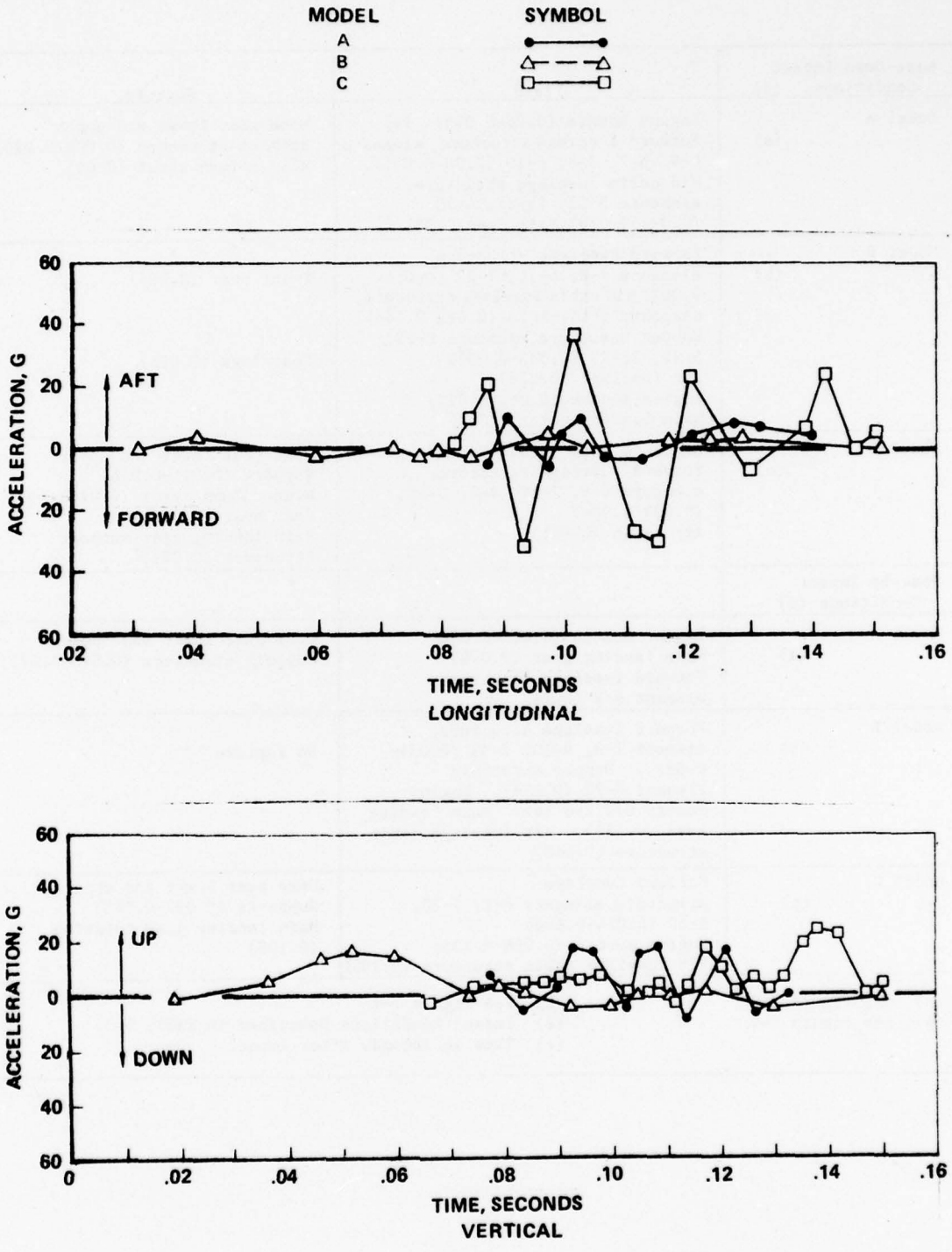

Figure 5-15. Rear Seat Leg-Floor Intersection Longitudinal and Vertical Accelerations, Models A, B and C, Nose-Up Impact

TABLE 5-9. SUMMARY OF YIELDS AND RUPTURES, MODELS A, B AND C

Nose-Down Impact Conditions (d)	Yield	Rupture
Model A (a)	Engine Mounts (0.06-0.072) (e) Forward fuselage structure, elements 6-9, 6-7, 7-8, 6-10 (0.06-0.051). Mid cabin fuselage structure, elements 5-23, 19-27, 4-28 (0.072-0.078) Tail cone 0.081	Nose gear lower and upper support structure (0.008-0.020). Wing column strut (0.06)
Model B (b)	Forward fuselage structure, elements 7-8, 9-10, 7-22 (0.018-0.062. Mid cabin fuselage structure, elements 6-24, 6-23 (0.061-0.104) Hopper structure, elements 8-22, 5-22, 22-23 (0.033-0.059) aft fuselage (0.028) engine mounts (0.062-0.077) Main landing gear (0.067)	Front spar (0.065) Seat legs (0.075)
Model C (c)	Engine mounts (0.014-0.058) Forward fuselage structure, elements 6-9, 7-10, 4-6, 9-10, (0.039-0.084) Aft cabin (0.071)	Nose gear lower and upper support (0.011-0.056) Wing column strut (0.074) Rear spar (0.011) Main landing gear support Structure (0.081)
Nose-Up Impact Conditions (d)		
Model A (a)	Engine mounts (0.079-0.086) Main landing gear (0.078) Forward fuselage structure, element 6-9 (0.147)	Nose gear lower and upper support structure (0.048-0.072)
Model B (b)	Forward fuselage structure, element 7-8, 9-10, 7-33 (0.034-0.065). Hopper structure element 8-22 (0.074). Engine mounts 0.072-0.142. Main landing gear (0.121). Aft fuselage cabin structure (0.040)	No rupture
Model C (c)	Forward fuselage structure, elements 6-9, 7-10, 9-10 (0.024-0.106) Engine mounts (0.086-0.133) Aft fuselage cabin structure (0.106)	Nose gear lower and upper Supports (0.087-0.088) Main landing gear rotation (0.105)

(a) See Figure 5-3
(b) See Figure 5-4
(c) See Figure 5-5
(d) Impact Conditions Described in Table 5-3
(e) Time in Seconds After Impact

Model B shows substantially more structural yielding but little potential failure. Model C shows the most potential failure. Model B, not having a nose gear, impacts on the main landing gear in the nose-down configuration much earlier than do the other two models. While the two nose-wheel-configured airplanes (A and C) initial failures are at the nose gear supports, very little energy is absorbed by these structures until after the nose gear supports fail and the fuselage is contacted. On the other hand, the tail wheel equipped airplane (Model B) absorbs energy through the structure immediately after impact because of the high load capability of the main landing gear which contacts the ground first.

The analytically obtained occupant responses are delineated in terms of Dynamic Response Index (DRI) values and occupant lower and upper torso accelerations. The occupant lower torso representation combines the lower mass of the occupant (44 percent of total occupant weight) and the mass of the seat attached to the floor via the stiffness of the seat legs. The occupant torso representation has 44 percent of the occupant weight spring connected to the lower torso with a stiffness which provides a 10-Hz. response. The occupant representation is not restrained by either a shoulder harness or a seat belt. The DRI values are shown in Table 5-10. Model C results exhibit the highest DRI (14.1) value for the nose-down impact while Model B results show the highest DRI (14.9) value for the nose-up impact. However, neither maximum DRI value is expected to yield more than a 2-percent probability of a spinal compression injury (Reference 17).

TABLE 5-10. DRI SUMMARY, MODELS A, B AND C

Maximum Value	Nose-Down Condition			Nose-Up Condition		
	Model A	Model B	Model C	Model A	Model B	Model C
DRI	10.2	6.9	14.1	8.4	14.9	12.1[b]
Time (a)	0.084	0.075	0.096	0.078	0.072	0.150

(a) Time in Seconds After Impact

(b) DRI value increasing at end of analysis

The occupant peak acceleration responses, acceleration durations, and maximum impulses computed from the acceleration histories are presented in Table 5-11, along with the human tolerance values (Reference 18). The data in Table 5-11 indicates that the nose-down impacts are more severe for the occupants than the nose-up impacts, while the Model B and C results for the nose-down impacts show high peak g's in the aft direction for the occupant lower torso. However, the analytically obtained peak accelerations are 17.5 percent and 41.9 percent below the severe injury tolerance level for Models B and C, respectively. When comparing acceleration level and duration, the responses in the aft direction are of a shorter duration than that required to cause a serious injury. In the up direction, Model C results are higher for the occupant lower torso but still 20 percent below the peak g required to cause severe injury. The occupant upper torso response levels are substantially below the occupant lower torso response levels. When comparing maximum impulses, the Model C occupant lower torso results are highest for the up directions. The Model C results in the up direction are approximately 63 percent and 74 percent higher than the Model B and A results respectively. Model B occupant lower torso results in the aft direction are over 100 percent higher than corresponding Model A and C results. For the occupant upper torso responses Model A results are highest in the up direction and Model B results are highest in the aft direction.

5.2.2 Model A Parameter Variation Study Results

The Model A airplane was used to evaluate responses as a function of variations in impact conditions. A total of 10 conditions including the nose-down and nose-up base conditions were analyzed. Conditions 1 through 10, Table 5-3, represent the range of the Model A parameter investigation. Two of the 10 cases (conditions 6 and 10) were performed using ground flexibility. The 10 impact conditions are listed in Table 5-12.

Table 5-13 shows the summary of energy distribution for the Model A parameter variation analyses. At impact the kinetic energy varies between 93 and 97 percent of total for the different conditions analyzed. The remaining energy at time = 0 is potential. The kinetic energy for the

TABLE 5-11. COMPARISON OF OCCUPANT RESPONSES AND HUMAN TOLERANCE DATA, MODELS A, B AND C

Location	Direction	Nose-Down Condition			Nose-Up Condition			Tolerance, Severe Injury	
		Model A	Model B	Model C	Model A	Model B	Model C		
Peak G (a)									
Lower Torso	Up	47.2	38	64	7.6	17.6	25.6	80	(a)
	Down	28	39.6	13.9	5.2	5.	11.	70	
	Aft	46.7	132	93	13.2	10.6	10.8	160	
	Fwd.	31	44	10	17	67	4.7	90	
Upper Torso	Up	20.	37.2	24	8.7	19.3	16	80	(a)
	Down	2.9	-	2.6	-	-	-	70	
	Aft	26.6	12	30	-	1.9	-	160	
	Fwd.	-	-	13	1.6	4.1	2	90	
Duration (b)									
Lower Torso	Up	40 (0.002)	30 (0.015)	60 (0.007) 42 (0.012)	10 (0.008)	10 (0.010)	10 (0.020)	42 (0.007-0.050) 50 (0.02-0.160)	(b)
	Down	-	-	-	-	-	-	75 (0.02), 44 (0.1)	
	Aft	40 (0.004)	75 (0.007) 44 (0.012)	75 (0.004) 44 (0.008)	10 (0.004)	4 (0.015)	5 (0.020) -	55 (0.02), 40 (0.1)	
	Fwd.	-	-	-	5 (0.004)	-	5 (0.030)		
Upper Torso	Up	10 (.02)	19 (.03)	20 (.02)	8 (0.015)	20 (0.004)	16 (0.010)	42 (0.007-0.050) 50 (0.02-0.160)	(b)
	Down	-	-	-	-	-	-		
	Aft	20 (.02)	30 (.02)	10 (.02)	-	-	-	75 (0.02), 44 (0.1)	
	Fwd.	-	-	-	-	-	-	55 (0.02), 40 (0.1)	
Maximum Impulse (g-msec)									
Lower Torso	Up	887	515	699	187	360	437	280-2100	
	Down	81	90	33	-	-	-	1000-8000	
	Aft	1248	1287	747	105	78	77	1500-4400	
	Fwd.	300	233	38	72	-	136	1100-4000	
Upper Torso	Up	442	401	600	280	624	485	280-2100	
	Down	-	-	-	-	180	-	1000-8000	
	Aft	875	1361	180	14	83	-	1500-4400	
	Fwd.	-	176	38	-	-	-	1100-4000	

(a) Peak in g's

(b) g's and seconds, duration in parenthesis

TABLE 5-12. MODEL A PARAMETER VARIATION STUDY IMPACT CONDITIONS

Condition No.	Impact Angle (deg.)	Flight-Path Angle (deg.)	Velocity (MPH)
1	-30	-30	55 (a)
2	-30	-30	65 (a)
3	-15	-15	55 (a)
4	-45	-45	55 (a)
5	-45	-45	45 (a)
6	-15	-15	65 (b)
7	+15	-15	55 (c) (a)
8	+15	-15	65 (c) (a)
9	+15	-15	65 (a)
10	+15	-15	65 (b)

(a) rigid impact surface
(b) flexible impact surface
(c) lift/weight ratio = 0.65

nose-down impacts, is reduced substantially with the exception of condition 3. For the -30-degree (conditions 1 and 2) impacts, the kinetic energy is reduced to between 44.6 and 49 percent of the total. The -45-degree impacts (conditions 4 and 5), result in a kinetic energy reduction to between 30.6 and 35.3 percent of the total energy. For the -15-degree impact (condition 3) onto a rigid surface, the kinetic energy is reduced to 69.5 percent of the total. However, for the -15-degree impact onto soil (condition 6), the kinetic energy is reduced to 18.2 percent of the total, primarily due to the large energy absorption via ground friction. The kinetic energy for the nose-up impacts is reduced to approximately 67 to 74 percent (conditions 7-9) of the total energy except where soil impact (condition 10) is involved. However, when impacting onto soil the kinetic energy is reduced to 20.7 percent of the total, once again due to the large energy dissipation due to ground friction.

TABLE 5-13. ENERGY DISTRIBUTION SUMMARY, MODEL A PARAMETER VARIATION STUDY

	Nose-Down Conditions						Nose-Up Conditions			
	1	2	3	4	5	6	7	8	9	10
Total Energy (in-lb)	3.03 x 10^6	4.18 x 10^6	3.04 x 10^6	3.04 x 10^6	2.51 x 10^6	4.18 x 10^6	3.02 x 10	4.14 x 10^6	4.14 x 10^6	4.14 x 10^6
Initial Kinetic Energy[a]	94.1	95.8	94.7	95.	93.	94.7	95.9	97.	97.	97.
Maximum Value[a] - Strain	8.4	10.4	3.17	33.03	34.97	10.99	3.30	3.05	4.00	6.54
Damping	2.12	1.76	1.04	7.02	6.22	1.99	0.44	0.75	0.80	1.65
Crushing	9.95	9.23	2.66	19.34	19.53	6.74	1.38	1.84	3.33	6.70
Friction	35.37	31.9	21.14	20.72	19.02	56.13	17.28	22.06	24.48	62.78
Final Value[a] - Kinetic	44.57	49.01	69.5	30.61	35.28	22.52	74.04	69.8	66.9	20.66
Potential	3.04	2.02	2.61	2.55	3.29	2.61	3.55	2.5	1.56	1.65
Strain	7.9	9.3	3.09	33.03	28.96	10.99	3.30	3.05	3.86	6.36
Damping	2.12	1.76	1.04	7.02	6.22	1.99	0.44	0.75	0.80	1.65
Crushing	7.1	6.01	2.66	6.08	7.23	6.76	1.38	1.84	2.42	6.89
Friction	35.37	31.9	21.14	20.72	19.02	56.2	17.28	22.06	24.48	62.78
Percent Energy Change[b]	+0.09	+0.18	+0.30	+1.17(c)	+0.66	+.03	-0.01	+0.04	+0.07	+0.13
Maximum Time of Analysis[d]	0.120	0.120	0.150	0.120	0.120	0.150	0.144	0.150	0.150	0.150
Integration Interval[e] (ΔT)	30	30	30	30	30	30	15-30	15-30	15-30	15-30

(a) Percent of current total

(b) $\left(\frac{\text{Final Total - Initial Total}}{\text{Initial Total}}\right)$ +100

(c) Reduced to $\approx \pm 0.58$ with ΔT reduced to 15 μ seconds

(d) Time in seconds after impact

(e) Microseconds

The integration interval used is between 15 and 30 microseconds. The overall energy growth varies between -0.01 percent to +1.17 percent. Energy growth is in part a measure of integration error. Consequently, the small energy growth present in the analyses indicates a stable model.

Table 5-14 shows the airplane cg velocity summary for the 10 conditions. The vertical velocity component is reduced to less than 10 percent of its initial value except for the -45 degree nose-down impacts (conditions 4 and 5). The longitudinal velocity component, in the nose-down impact cases onto a rigid surface, is reduced within the range of approximately 23 to 33 percent from its initial value at time = 0.120 seconds for the -30 and -45 degree conditions. For the -15 degree nose-down impact onto a rigid surface, the longitudinal velocity is reduced only 11.2 percent at time = 0.150 seconds. However, for the -15 degree nose-down impact onto soil, the longitudinal velocity is reduced 64.2 percent at time = 0.150 seconds and the vertical velocity component is -47 inches per second indicating a more abrupt stop and tendency to rotate nose over. For the nose-up impacts, the reduction in longitudinal velocity is 10.7 percent to 14.6 percent at time=0.150 seconds except for the impact onto soil where the reduction is 64.2 percent. In this case the vertical velocity component is -121 inches per second at time 0.150 seconds.

Table 5-15 provides a summary of loads for the 10 conditions analyzed. For the nose-down impacts, the loads show a trend toward increasing as the flight-path velocity and the impact and flight-path angles increase. The -15 degree impact onto soil results in the severest loads for all locations except for the seat legs in the longitudinal direction. The nose-up impact onto soil (condition 10) provides relatively high longitudinal loads. The -45 degree nose-down impact cases also provide relatively high loads as compared to the base case (condition 1) and to the nose-up impacts onto concrete. Single-pinned connection seat fasteners show a potential for failure due to the load in the longitudinal direction under conditions 4, 5, and 10. With the double-pin configuration, the potential for failure due to a load in the

TABLE 5-14. AIRPLANE CG VELOCITY SUMMARY, MODEL A PARAMETER VARIATION STUDY

CG Velocity Component (a)	Nose-Down Conditions						Nose-Up Conditions			
	1	2	3	4	5	6	7	8	9	10
Initial										
Longitudinal Velocity	46.9	55.4	52.4	38.4	34.5	52.4	52.4	61.9	61.9	61.9
Vertical Velocity	27.1	32.	14	38.4	34.5	14	14.4	16.5	16.5	16.5
Final(b)										
Longitudinal Velocity	34.7	42.7	46.4	25.8	23.9	22.6	46.7	53.5	52.9	22.2
Vertical Velocity	0	3.1	1.1	9.5	10.7	-2.7	.73	-4.1	-4.3	-6.8
Time, Maximum(b)	0.120	0.120	0.150	0.120	0.120	0.150	0.144	0.150	0.150	0.150
Time for Vertical Velocity to Reach Zero(b)	0.120	(c)	(c)	(c)	(c)	0.144	(c)	0.132	0.129	0.129
Percent Reduction in Longitudinal Velocity Component	26	23	11.2	33	30.8	56.9	10.7	13.6	14.6	64.2

(a) Velocity in Miles per hour in ground axis

(b) Time in Seconds After Impact

(c) CG Vertical Velocity doesn't reach zero at analysis maximum time.

TABLE 5-15. SUMMARY OF LOADS, MODEL A PARAMETER VARIATION STUDY[a]

Location[g]	Nose-Down Conditions						Nose-Up Conditions			
	1	2	3	4	5	6	7	8	9	10
Main Landing Gear Support[b] beams (4,19 and 4-1, 19-1)	2770	6479	3093	6694	5835	7100	613	1848	3877	6665
Wing-Fuselage Column Strut[c] [f] (beam 6,15)	5800[d]	5800[d]	5800[d]	5800[d]	5800[d]	5800[d]	1911	4632	5800[d]	5800[d]
Rear Spar Attachment[c] [e] beam (5,16)	7200	9712	3786	7320	12530	8527	1617	2645	4043	8810
Front Spar Attachment[c] [f] (beam 8,15)	6700	10770	4111	6336	11820	8460	2194	1937	4306	8837
Seat Legs[b]										
Forward Outboard (beam 6-1,20-3)	1986	2479[h]	1122	1763[h]	1957[h]	2100	445	1893	1930	3970
Forward Inboard (beam 18-1, 20-4)	2390	3047[h]	1000	2923[h]	4530[d]	2357	299	1584	1362	3605
Rear Outboard (beam 20-1, 28-1)	838	933[h]	530	1177[h]	750[h]	1540	135	637	593	1862
Rear Inboard (beam 20-2, 27-1)	1618	4530[h]	1152	1318[h]	1795[h]	890	221	1230	930	3357

(a) Load in Pounds
(b) Load in Airplane Longitudinal Direction
(c) Member Axial Load
(d) Exceeds Failure Load and Element Ruptures
(e) Tensile Loads
(f) Compressive Loads
(g) See Figure 5-3 for Element Location
(h) Element Rupture in Axial Direction

longitudinal direction is highest for conditions 2, 4 and 5 followed by conditions 6, 10 and 2. The rear spar and forward spar loads are well below failure loads for all conditions.

Table 5-16 and Figures 5-16 through 5-25 show the peak acceleration levels and the acceleration histories, respectively, for the engine cg, the occupant lower torso, the occupant upper torso, and the forward and rear seat leg-floor intersections in the longitudinal and vertical directions. The more severe impact velocity and angle conditions result in higher peak accelerations in both the longitudinal and vertical directions. The nose-up impacts onto concrete are mild compared to the nose-down impact results insofar as peak accelerations are concerned. The nose-up impact without lift onto a rigid surface (condition 8) results in substantially higher peak vertical accelerations than the corresponding condition with lift (condition 7). Both the nose-down and nose-up impact cases onto soil indicate high peak aft accelerations. In general, the acceleration histories show the pulse shape for longitudinal accelerations in the soil impact cases to be of a higher magnitude and of a longer duration than the corresponding responses for the other conditions.

Table 5-17 provides a summary of the structural elements which the analyses indicate fail and/or yield. In general, for the nose-down conditions (1-6) the events occur earlier as the impact velocity and angle increase. The nose-up impact results indicate less severe damage and a longer time after impact before yielding or failure occurs. The data summarized in Table 5-17 is consistent with the energy, velocity, and acceleration data provided in Tables 5-13, 5-14 and 5-15, respectively.

Tables 5-18 and 5-19 provide a summary of DRI values and occupant responses obtained from the analyses of the 10 conditions. The maximum DRI value is 19, which occurs toward the latter stages of the analyses of conditions 3 and 9. This represents approximately 10-percent probability of a spinal compression injury (Reference 18). All other DRI values are 12.1 or less, which represents practically no chance of a spinal compression type of injury. The data in Table 5-19 shows that the lower and upper torso

TABLE 5-16. MAXIMUM FILTERED ACCELERATIONS AND TIME TO OCCURRENCE, MODEL A PARAMETER VARIATION STUDY

Location	Direction	Nose-Down Impact Conditions												Nose-Up Impact Conditions							
		1		2		3		4		5		6		7		8		9		10	
		(a)	(b)	(a)	(b)	(a)	(b)	(a)	(b)	(a)	(b)	(a)	(b)	(a)	(b)	(a)	(b)	(a)	(b)	(a)	(b)
Engine c.g.	Up	48.7	0.075	65.4	0.069	26	0.135	80	0.063	50.3	0.048	10	0.147	11.6	0.075	30.6	0.150	50.9	0.123	36.1	0.144
	Down	24.4	0.105	52.3	0.090	5	0.036	54	0.066	25.2	0.069	86	0.132	8.7	0.060	13.5	0.054	24.8	0.150	85.2	0.135
	Aft	63.6	0.081	92.9	0.069	38	0.144	154	0.045	127	0.048	71	0.132	11	0.096	28.8	0.135	55.8	0.150	117.6	0.135
	Forward	11.9	0.117	30.3	0.096	10	0.123	70	0.090	16.6	0.069	-	-	6.3	0.084	21.6	0.147	28.1	0.144	2.2	0.048
Occupant Lower Torso	Up	47.2	0.078	41.3	0.075	34	0.138	34	0.042	40.3	0.048	42	0.141	17.6	0.132	29.2	0.126	47.4	0.126	44.7	0.126
	Down	28	0.090	5.4	0.087	2.3	0.036	20	0.084	18.4	0.069	6.9	0.147	5.2	0.084	2.8	0.081	12	0.093	3.4	0.105
	Aft	46.7	0.063	54.4	0.057	17.6	0.132	61	0.042	68.2	0.060	69.1	0.120	13.2	0.102	15.8	0.096	18.2	0.096	46.8	0.126
	Forward	31	0.120	26.7	0.090	1.8	0.075	40	0.057	23	0.096	-	-	17	0.093	44.2	0.15	17.8	0.120	20.4	0.138
Occupant Upper Torso	Up	19	0.081	16.2	0.075	27	0.144	12	0.057	9.9	0.054	4.1	0.111	8.7	0.138	16.3	0.132	27.8	0.132	7	0.051
	Down	2.9	0.117	2.3	0.102	0.5	0.021	2	0.090	14.1	0.081	20.8	0.138	-	-	-	-	1.6	0.096	6.8	0.132
	Aft	26.6	0.120	15.2	0.102	2	0.129	7.5	0.080	31.8	0.090	68	0.150	-	-	1.1	0.090	1.5	0.093	53	0.138
	Forward	-	-	-	-	2.3	0.102	-	-	-	-	-	-	1.6	0.141	3.8	0.132	6.6	0.138	-	-
Forward Seat Leg - Floor Intersection (c)	Up	56.2	0.078	61.3	0.072	33	0.138	40	0.066	59.6	0.060	32.2	0.135	14.6	0.132	30.5	0.15	46.8	0.123	38	0.126
	Down	20.2	0.120	19.1 21.0	0.087 0.105	2.9	0.036	48	0.087	22.7	0.114	8	0.144	6.6	0.084	4.4	0.078	6.1	0.093	1.6	0.078
	Aft	33 34	0.069 0.090	88.9	0.081	17.5	0.132	61.5	0.042	62.7	0.054	78.5	0.123	7	0.087	14.9	0.135	18.5	0.141	52.6	0.129
	Forward	23.6	0.096	32.4	0.087	6.6	0.027	15	0.051	4.5	0.120	11.4	0.138	8.6	0.102	74.5	0.147	37.8	0.144	15.9	0.138
Rear Seat Leg - Floor Intersection (c)	Up	43.9	0.087	83.8	0.078	30	0.138	45	0.063	40.8	0.075	56	0.141	17.8	0.099	25.3	0.126	40	0.126	46.6	0.126
	Down	30	0.120	43.8	0.108	2.8	0.063	18	0.081	24.2	0.111	10.3	0.150	3.9	0.084	4.8	0.138	18.7	0.084	6.4	0.135
	Aft	37.9 34.3	0.072 0.087	73.2	0.081	22.8	0.132	56	0.051	61	0.051	80	0.123	10.8	0.102	45.6	0.147	27.9	0.144	58	0.147
	Forward	18.8	0.096	34.2	0.087	4.8	0.027	28	0.072	5.5	0.120	-	-	5.6	0.081	11.5	0.135	20.6	0.150	20.6	0.138

(a) G peak value, 70 Hz, Low Pass Filter
(b) Time in seconds after impact
(c) Outboard location

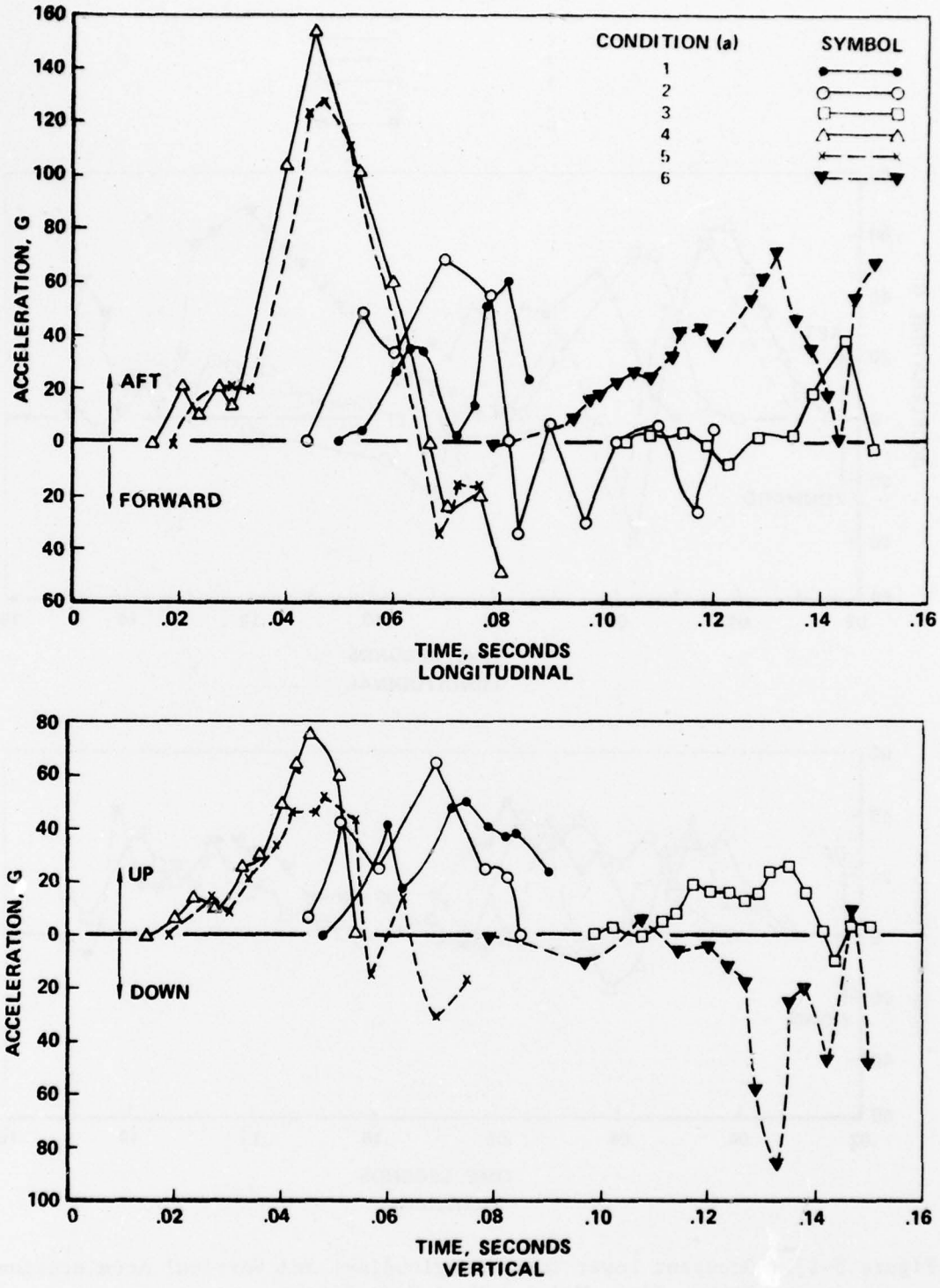

Figure 5-16. Engine CG Longitudinal and Vertical Accelerations Versus Time, Model A Nose-Down Impact

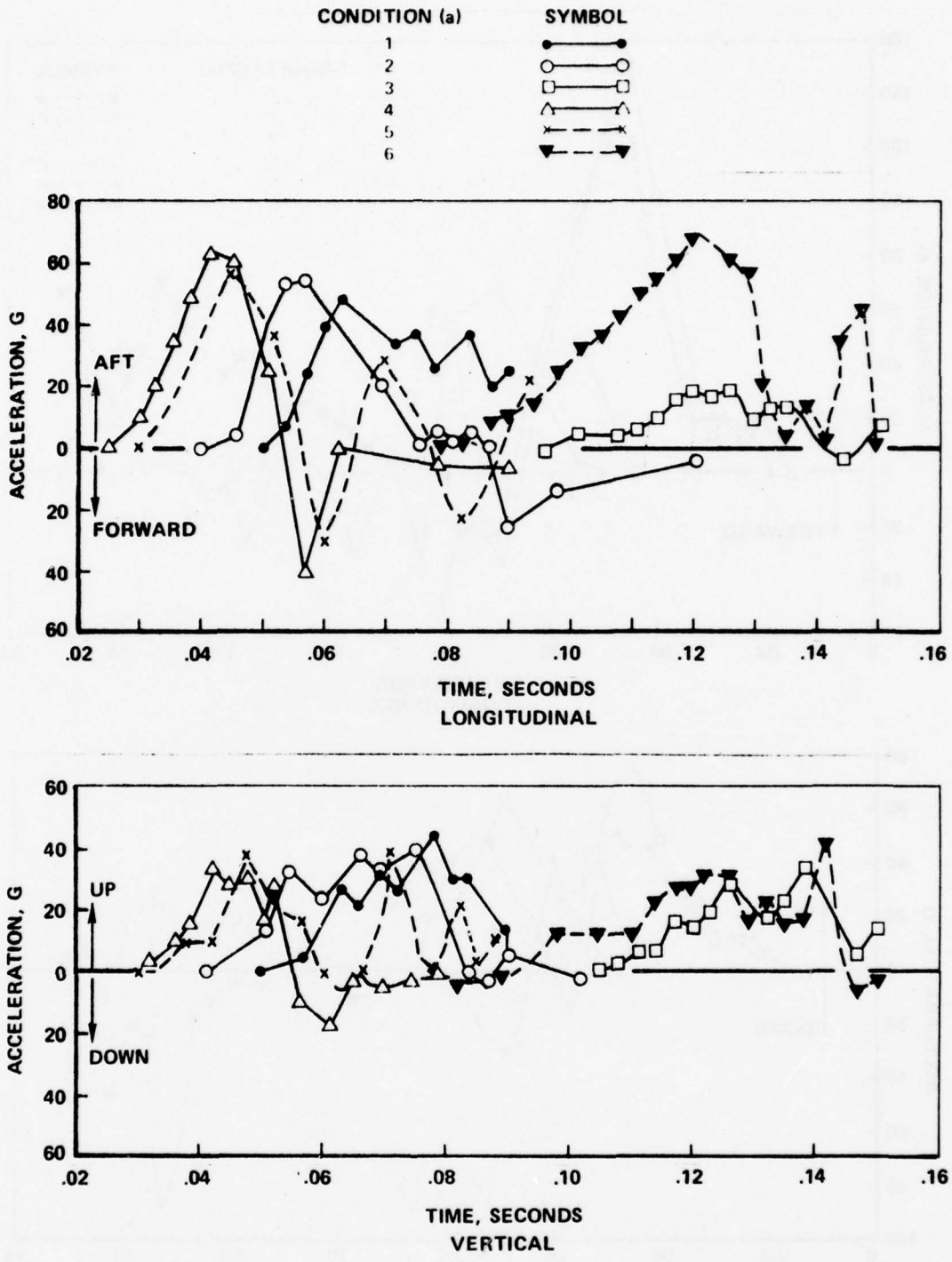

Figure 5-17. Occupant Lower Torso Longitudinal and Vertical Accelerations Versus Time, Model A Nose-Down Impact

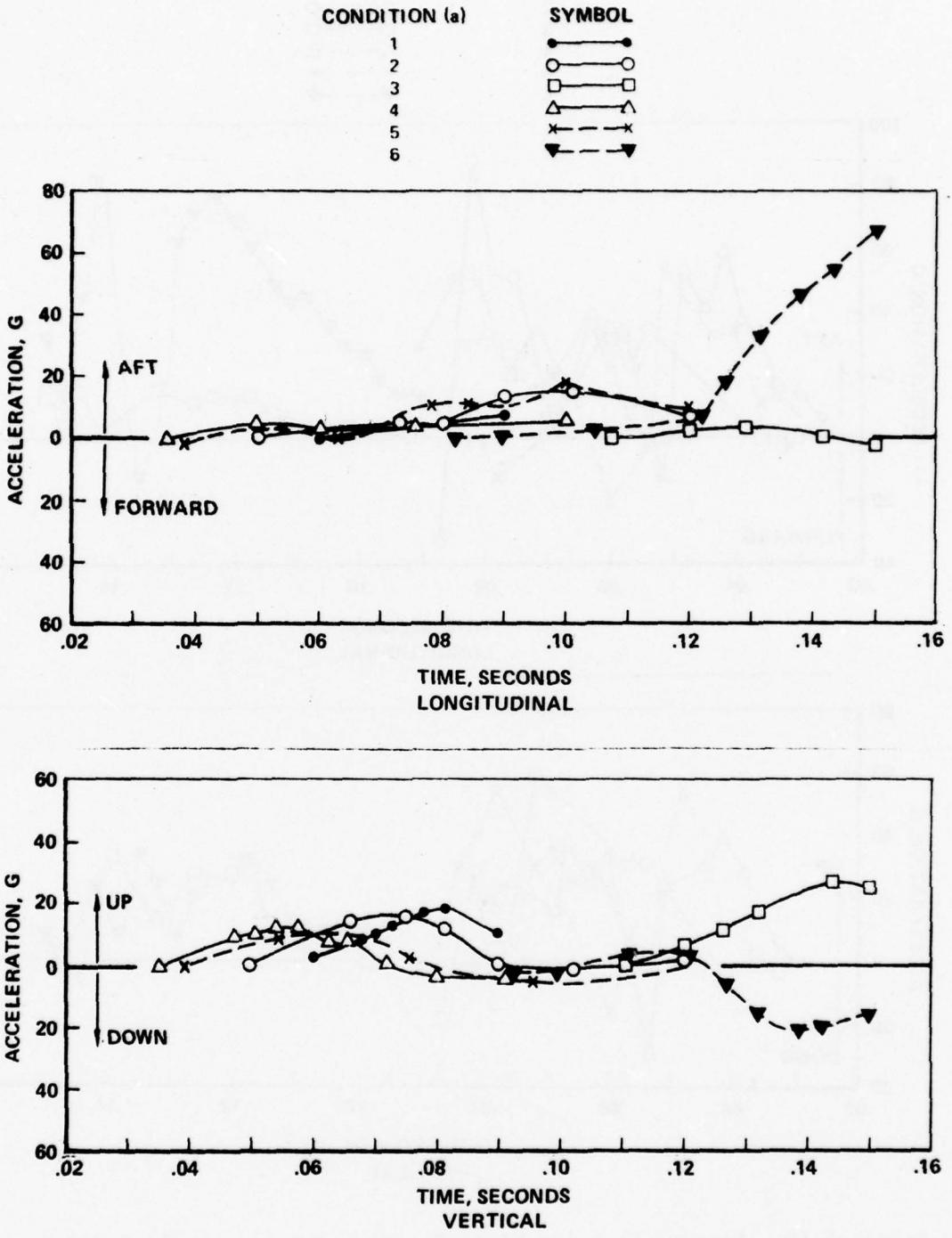

Figure 5-18. Occupant Upper Torso Longitudinal and Vertical Accelerations Versus Time, Model A Nose-Down Impact

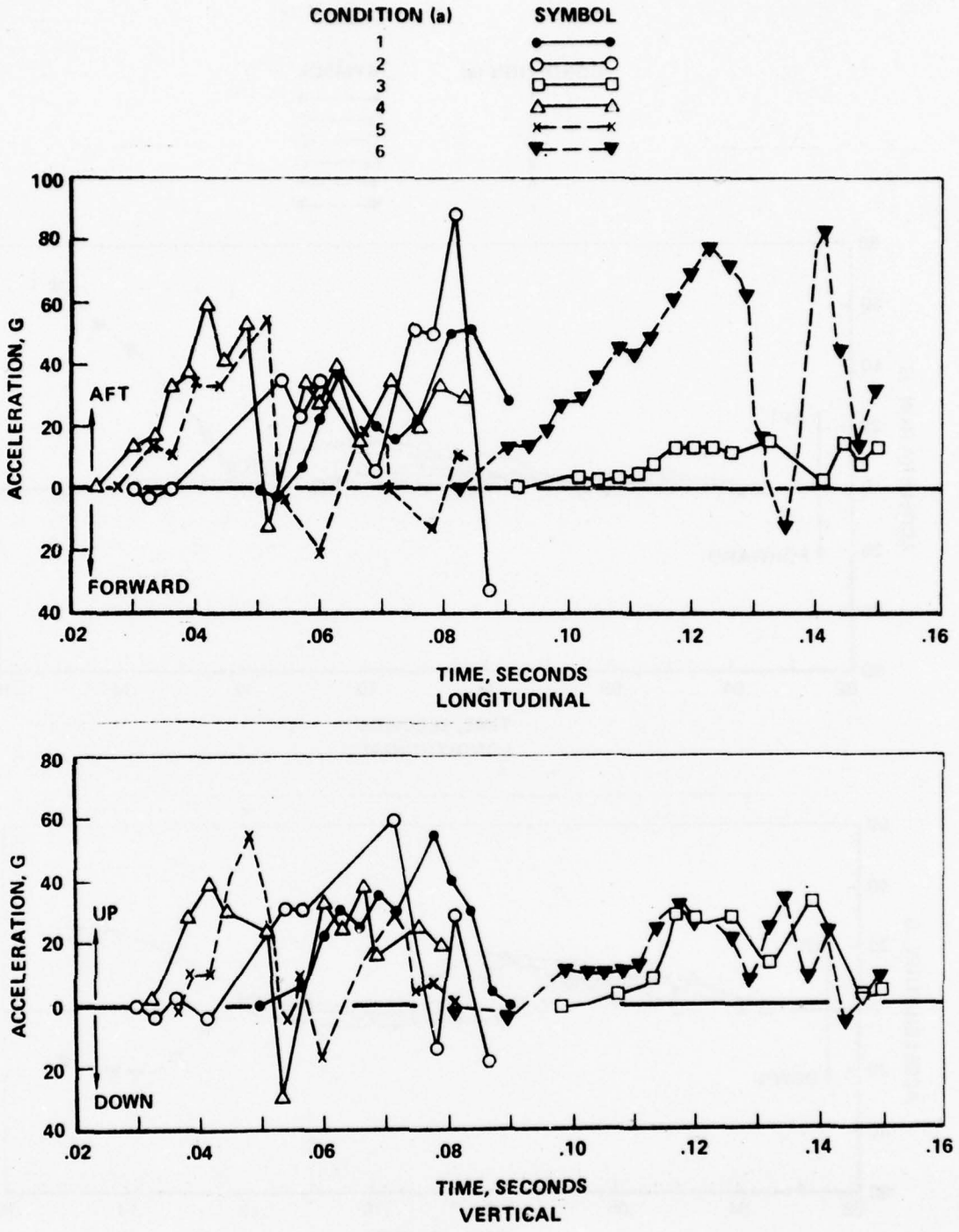

Figure 5-19. Forward Seat Leg-Floor Intersection Longitudinal and Vertical Accelerations Versus Time, Model A Nose-Down Impact

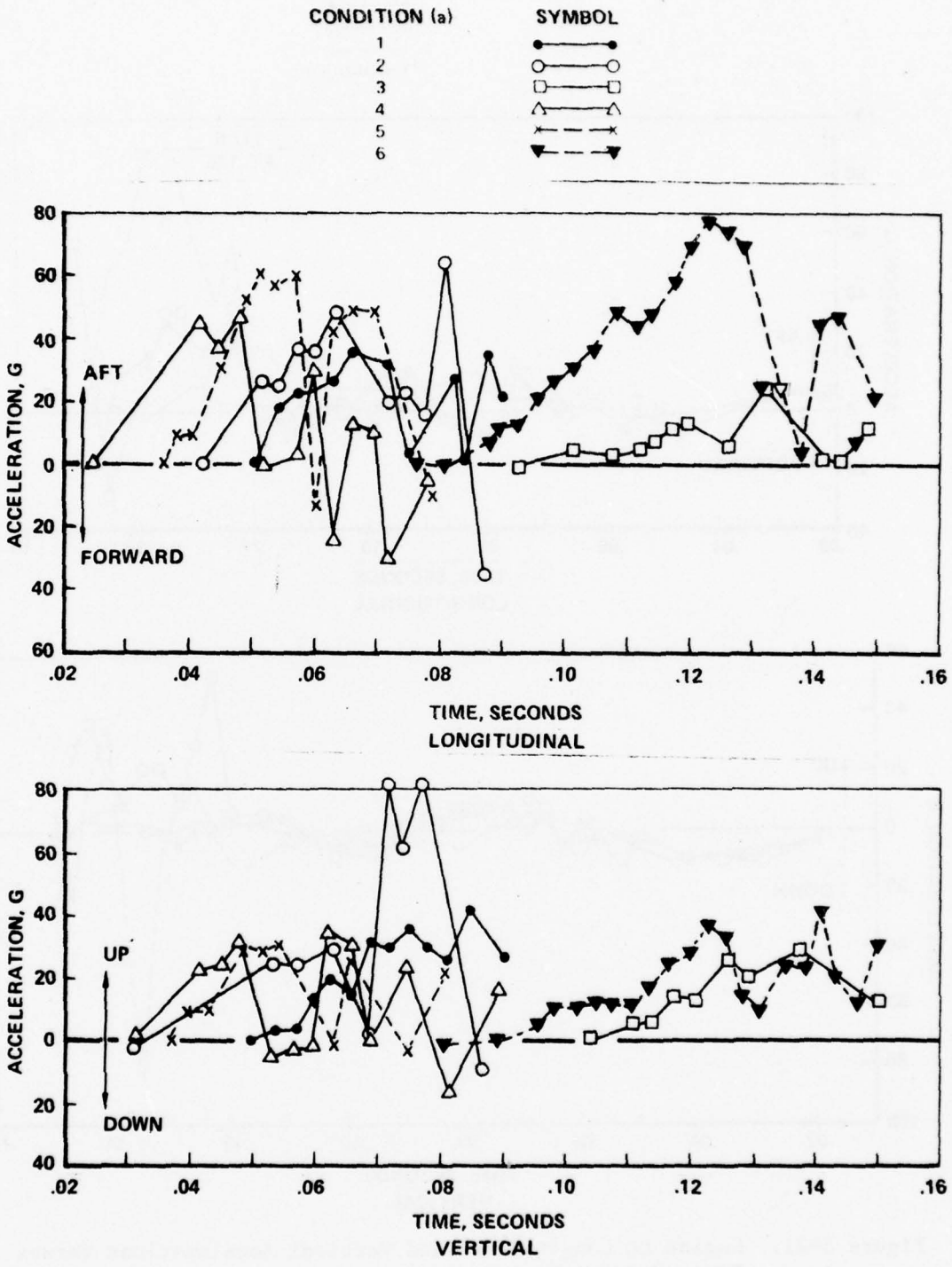

Figure 5-20. Rear Seat Leg-Floor Intersection Longitudinal and Vertical Accelerations Versus Time, Model A Nose-Down Impact

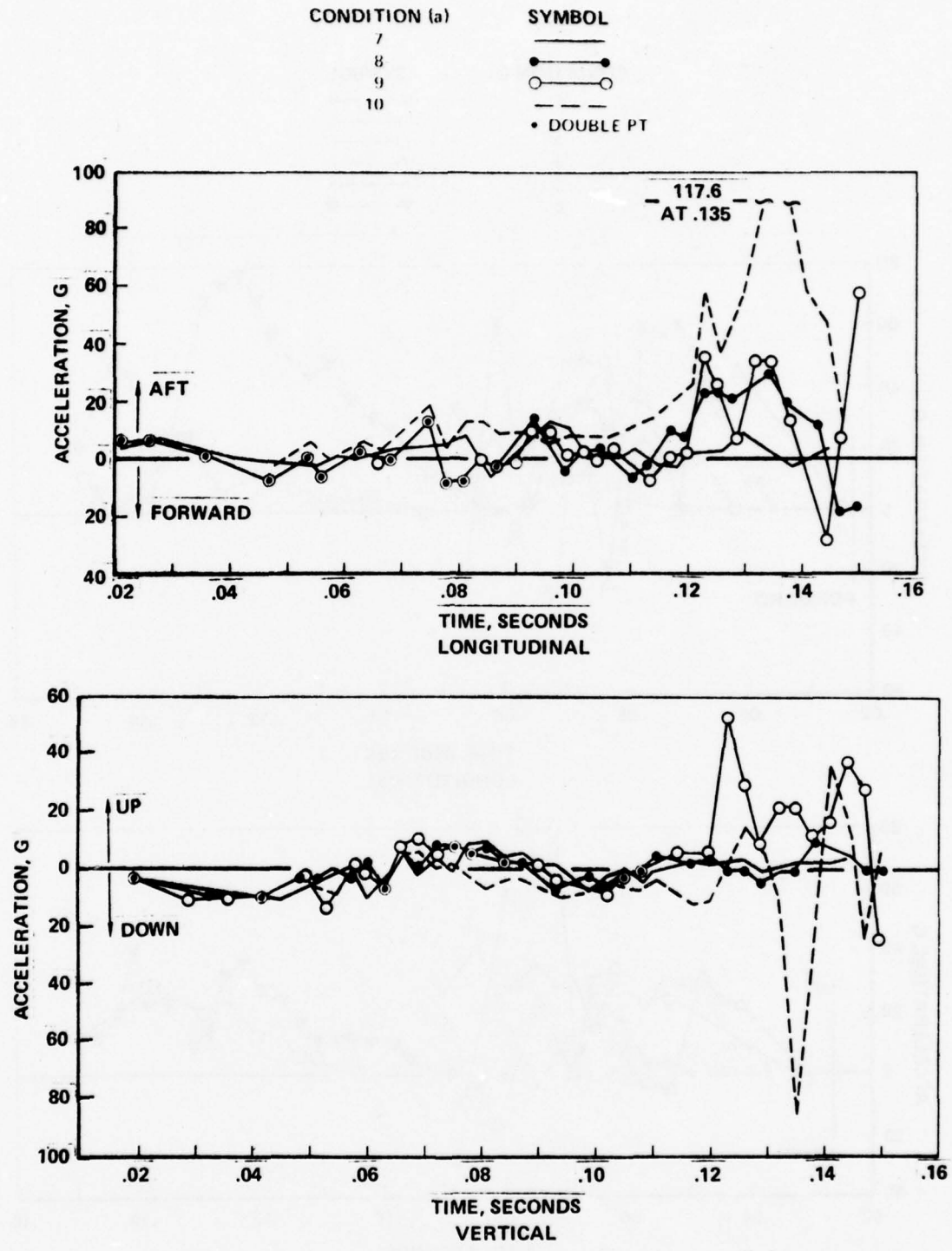

Figure 5-21. Engine CG Longitudinal and Vertical Accelerations Versus Time, Model A Nose-Up Impact

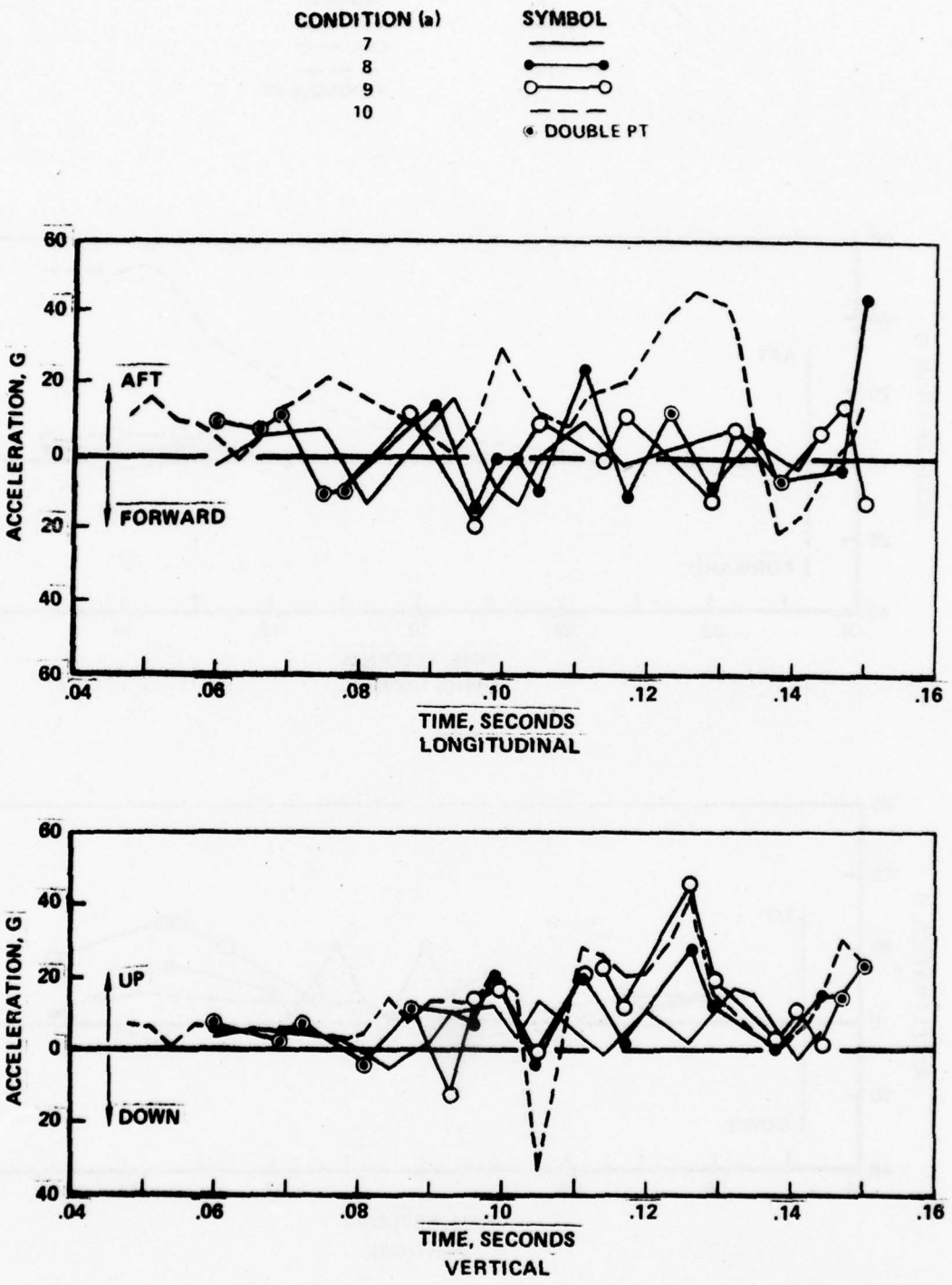

Figure 5-22. Occupant Lower Torso Longitudinal and Vertical Accelerations Versus Time, Model A Nose-Up Impact

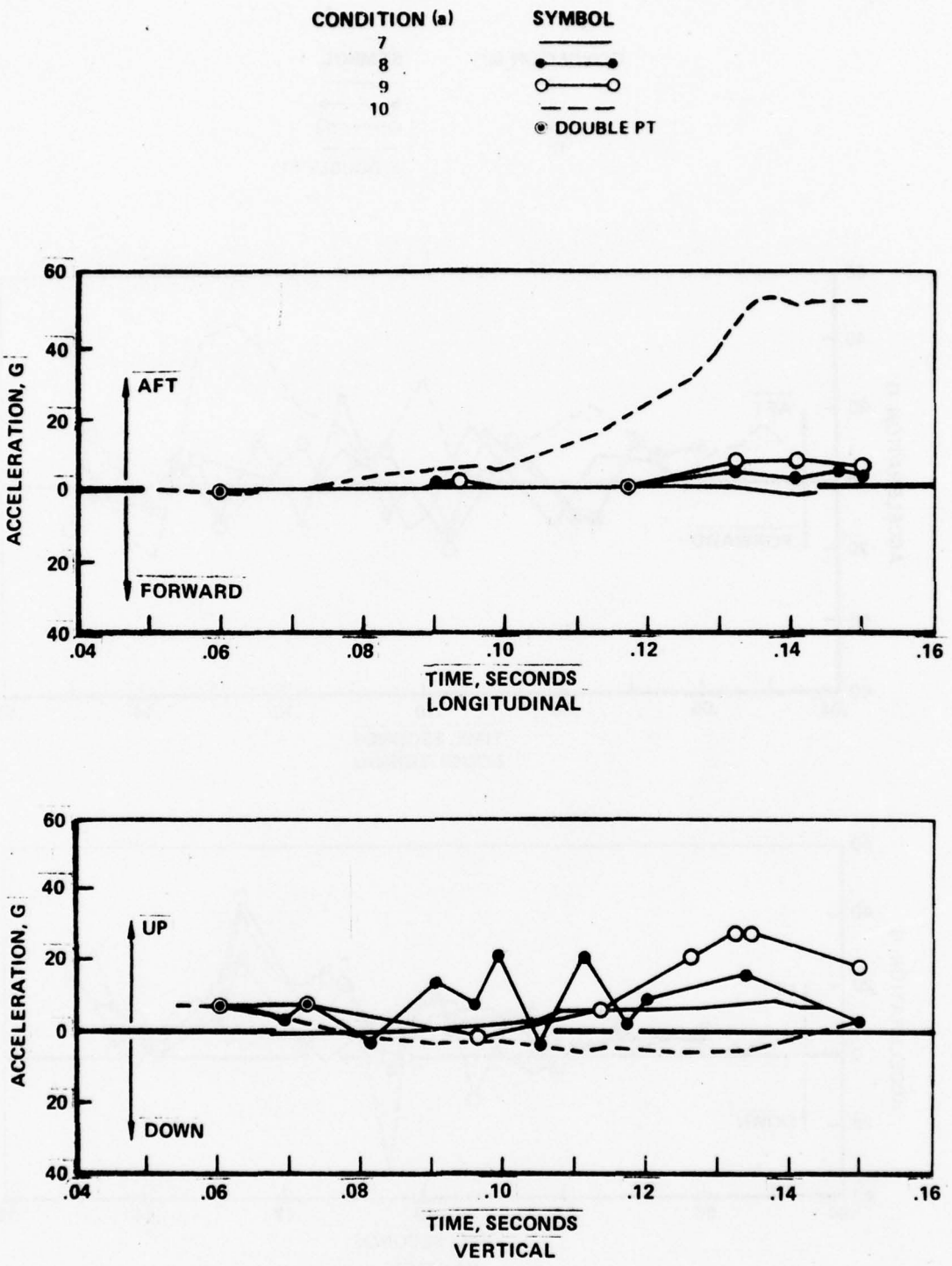

Figure 5-23. Occupant Upper Torso Longitudinal and Vertical Accelerations Versus Time, Model A Nose-Up Impact

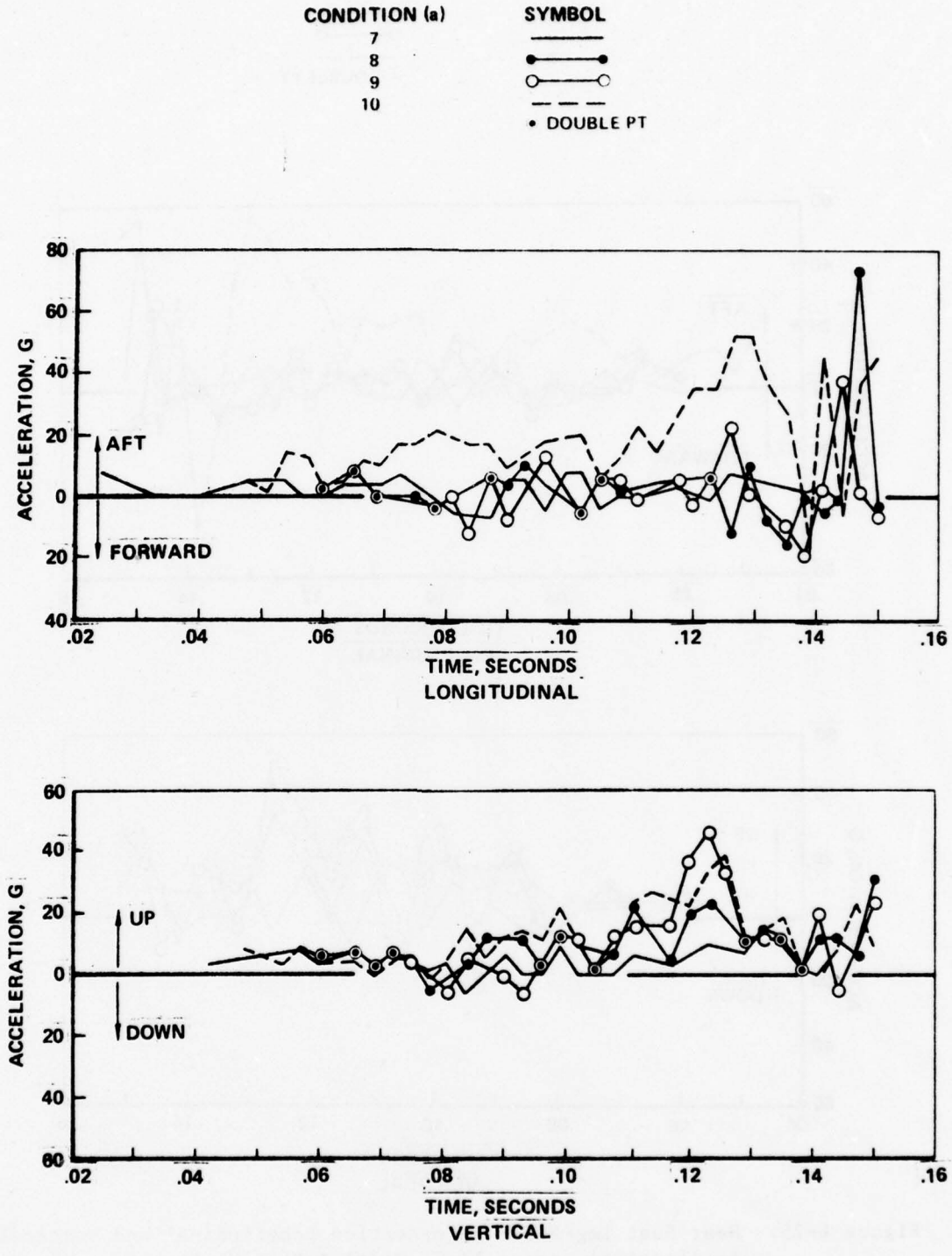

Figure 5-24. Forward Seat Leg-Floor Intersection Longitudinal and Vertical Accelerations Versus Time, Model A Nose-Up Impact

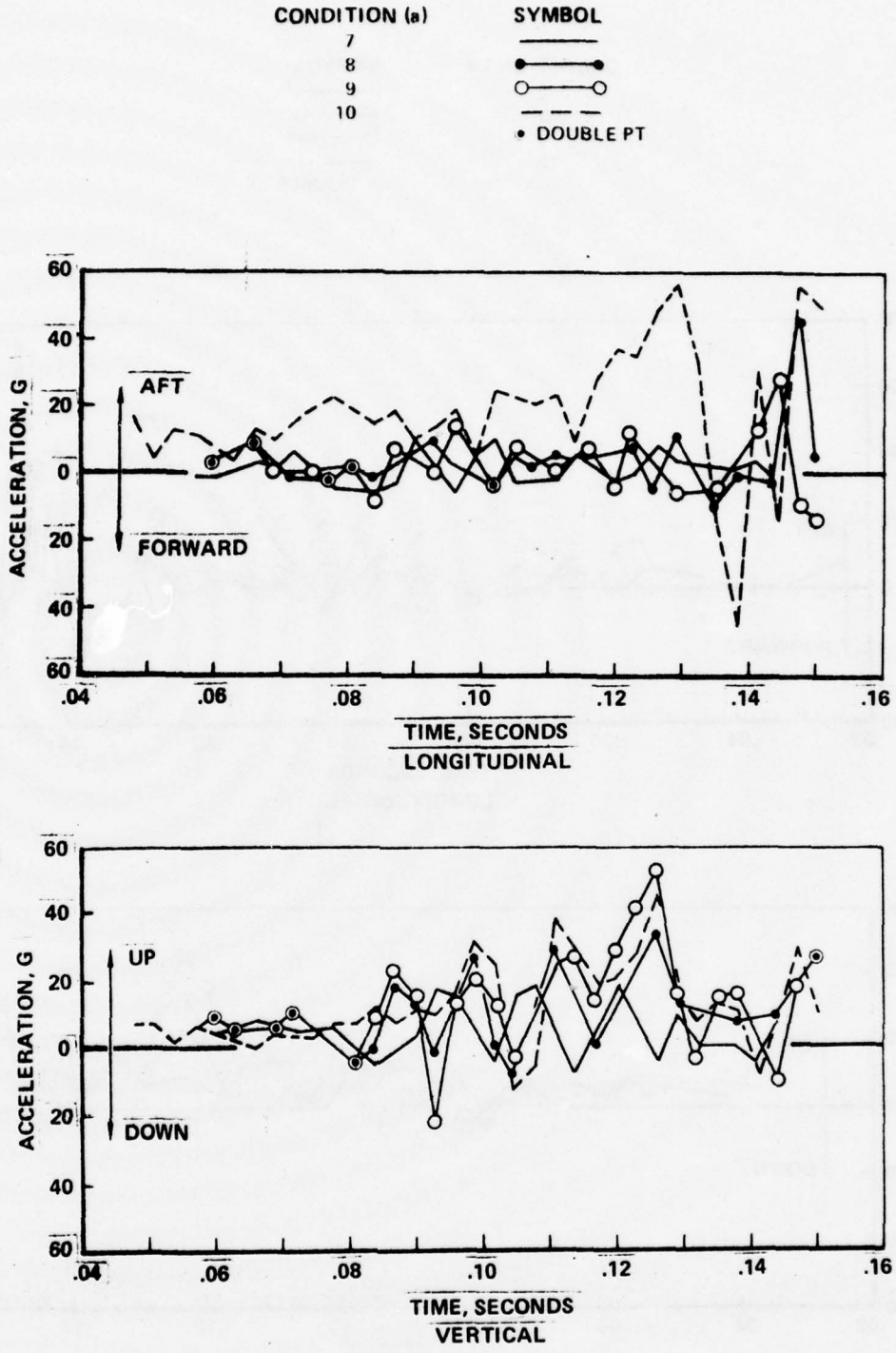

Figure 5-25. Rear Seat Leg-Floor Intersection Longitudinal and Vertical Acceleration Versus Time, Model A Nose-Up Impact

TABLE 5-17. SUMMARY OF YIELDS AND RUPTURES, MODEL A PARAMETER VARIATION STUDY

Impact (c) Condition	Yield (a) (b)	Rupture (a) (b)
1	Engine mounts (0.06-0.072). Forward fuselage structure, elements, 6-9, 6-7, 7-8, 6-10 (0.06-0.067). Mid cabin fuselage structure, elements 5-23, 19-27, 4-23, 4-28 (0.072-0.108). Tail cone (0.081).	Nose gear lower and upper support structure (0.008-0.020). Wing column strut (0.061).
2	Engine mounts (0.052-0.062). Forward fuselage structure, elements 6-9, 18-29, 26-29, 9-29, 9-10, 6-10, 6-7, 7-8, 18-26, 18-27 (0.05-0.064). Midcabin fuselage structure elements 19-27, 4-28, 19-25, 4-23 (0.961-0.099). Tail cone (0.069).	Nose gear lower and upper support structure (0.008-0.017). Wing column strut. (0.053) Seat legs (0.07-0.091).
3	Engine mounts (0.117-0.141). Forward fuselage structure, elements 6-10, 9-10, (0.128-0.136).	Nose gear lower and upper support structure (0.008-0.022). Wing column strut (0.122).
4	Engine mounts (0.024-0.047). Forward fuselage structure elements 18-29, 6-9, 6-10, 7-8, 18-26, 9-10, 6-7, 26-29, 7-10, 9-29 (0.036-0.054). Mid cabin fuselage structure elements 6-28, 19-25, 4-23, 5-23 (0.081-0.085).	Nose gear lower and upper support structure (0.006-0.010). Wing column strut (0.038). Forward fuselage structure elements 18-29, 18-28, 6-9 (0.049-0.051). Seat legs (0.054-0.061).
5	Engine mounts (0.027-0.055). Forward fuselage structure elements 6-9, 18-29, 6-10, 18-26, 7-8, 9-10, 18-29, 26-29, (0.028-0.071).	Nose gear lower and upper support structure (0.006-0.010). Wing column strut (0.043). Forward fuselage structure members (18-26, 18-29, 6-9 (0.054-0.056) seat legs (0.057-0.117).
6	Engine mounts (0.102-0.141) forward fuselage structure elements 18-29, 6-9, 6-10, 18-26, 7-8, 9-10 (0.104-0.130) aft cabin 19-25 (0.145).	Nose gear lower and upper support 0.007-0.13. Wing column strut (0.112).
7	Engine mounts (0.079-0.086). Main landing gear (0.102).	Nose gear lower and upper support structure (0.055-0.069).
8	Engine mounts (0.074-0.124) main landing gear (0.078). Forward fuselage structure elements 6-9 (0.147).	Nose gear lower and upper support structure (0.048-0.072).
9	Engine mounts (0.074-0.082). Main landing gear, 2-4 (0.070). Forward fuselage structure elements, 6-9, 9-10 (0.141-0.144).	Nose gear lower and upper support structure (0.048-0.073). Main landing gear (0.083). Wing column strut (0.119).
10	Engine mounts (0.074-0.125). Forward fuselage structure elements 18-29, 6-9, 9-10, 6-10, (0.124-0.135). Tail cone (0.132) Aft cabin (0.148)	Engine and upper support structure (0.047-0.121) Wing column strut (0.093) Main landing gear (0.098)

NOTES: (a) Time in parenthesis in seconds after impact.
(b) Elements identified in Figure 5-3.
(c) Impact conditions described in Table 5-3.

TABLE 5-18. DRI SUMMARY, MODEL A PARAMETER VARIATION STUDY

Maximum Value	Nose-Down Conditions						Nose-Up Conditions			
	1	2	3	4	5	6	7	8	9	10
DRI and	10.2	9.2	19	6.4	5.3	2.2	8.4	12.1	19.	6.3
Time (a)	0.084	0.078	0.150	0.057	0.060	0.114	0.078	0.150	0.144	0.066

(a) Time in seconds after impact

accelerations obtained from analysis are substantially lower than the levels required to cause severe injury to human beings as compiled from Reference 18. The compilation of maximum impulses presented in Table 5-19 shows that the impacts onto soil result in the maximum aft impulse values. Lower torso vertical impulse values in the vertical direction are highest for the -30 degree impact onto a rigid surface and -15 degree impact onto soil conditions.

Table 5-20 provides a summary of element deflections obtained by analysis for the 10 conditions. The deflections increase as the impact velocity and angle increase. The -45-degree impact conditions (4 and 5) are severe insofar as the forward fuselage and engine mount damage is concerned. The -30-degree high-speed (65 mph) impact and the soil impacts are also severe for the engine mounts.

Table 5-21 presents a summary of the external structure deflections as represented by external springs. The springs represent deformation of tires and/or crushing of structure which contacts the rigid or flexible terrain. Once again the trend of increased deformation as the velocity at impact is increased is demonstrated. However, for the higher impact angles, contact can occur at different locations and in different directions. The soil is computed to have a maximum deformation of 14 inches during the nose-down inpact and 16.2 inches during the nose-up impact. The nose-up impact onto soil results in appreciable crushing in the longitudinal direction at several locations which normally experience little deformation when the impact surface is rigid.

TABLE 5-19. COMPARISON OF OCCUPANT RESPONSES AND HUMAN TOLERANCE DATA, MODEL A PARAMETER VARIATION STUDY

Location	Direction	Nose-Down Conditions						Nose-Up Conditions				Tolerance Severe Injury
		1	2	3	4	5	6	7	8	9	10	
Peak G[a]												
Lower Torso	Up	47.2	41.3	34	34	40.3	42	17.6	29.2	47.4	44.7	80 (a)
	Down	28	5.4	2.3	20	18.4	6.9	5.2	2.8	12	3.4	70 (a)
	Aft	46.7	54.4	17.6	61	68.2	60.1	13.2	15.6	18.2	46.8	160 (a)
	Forward	31	26.7	1.8	40	23	-	17	44.2	17.8	20.4	90 (a)
Upper Torso	Up	19	16.2	27	12	9.9	4.1	8.7	16.3	27.8	7	80 (a)
	Down	2.9	2.3	0.5	2	14.1	20.8	-	-	1.6	6.8	70 (a)
	Aft	26.6	15.2	2.	7.5	31.8	68	-	1.1	1.5	53	160 (a)
	Forward	-	-	2.3	-	-	-	1.6	3.8	6.6	-	90 (a)
Duration[b]												
Lower Torso	Up	40(0.02)	35(0.01)	30(0.003)	30(0.01)	30(0.05)	30(0.005)	14(0.005)	10(0.012)	40(0.003)	40(0.002)	42 (0.007-0.050) (b)
	Down	-	-	-	16(0.02)	-	-	-	-	10(0.001)	20(0.002)	50 (0.02-0.160) (b)
	Aft	40(0.008)	50(0.005)	16(0.01)	60(0.005)	50(0.005)	60(0.01)	8(0.010	10(0.005)	10(0.003)	40(0.010)	75 (0.02), 44(0.1) (b)
	Forward	-	20(0.005)		-	20(0.005)	-	10(0.004)	5(0.010)	10(0.003)	20(0.001)	55 (0.02), 40 (0.1) (b)
Upper Torso	Up	18(0.007)	16(0.015)	25(0.01)	10(0.01)	10(0.01)	-	6(0.03)	10(0.02)	20(0.02)	-	42 (0.007-0.050) (b)
	Down	-	-	-	-	-	20(0.03)	-	-	-	6(0.020)	50 (0.02-0.160) (b)
	Aft	20(0.02)	14(0.01)	2(0.02)	4(0.04)	10(0.04)	50(0.02)	-	4(0.01)	8(0.01)	50(0.02)	75 (0.02), 44(0.1) (b)
	Forward	-	-	-	-	-	-	-	-	-	-	55 (0.02), 40(0.1) (b)
Maximum Impulse (g-msec)												
Lower Torso	Up	887	874	733	396	358	922	187	282	690	591	280-2100
	Down	81	-	-	120	152	-	-	-	-	83	1000-8000
	Aft	1248	865	399	896	828	1970	105	130	63	900	1500-4400
	Forward	300	398	-	180	168	-	72	-	117	-	1100-4000
Upper Torso	Up	442	351	580	244	203	53	280	306	841	-	280-2100
	Down	-	-	-	118	110	401	-	-	-	180	1000-8000
	Aft	875	546	50	254	510	1172	14	-	231	1782	1500-4400
	Forward	-	-	-	-	-	-	-	-	-	-	1100-4000

(a) Peak in g's
(b) g's and seconds (duration in parentheses)

TABLE 5-20. SUMMARY OF STRUCTURAL ELEMENT DEFLECTIONS, MODEL A PARAMETER VARIATION STUDY

Location[b]	Nose-Down Impact Conditions[a]						Nose-Up Impact Conditions[a]			
	1	2	3	4	5	6	7	8	9	10
Engine Mounts[c]										
9-1, 13-1[i]	1.12	4.10[f]	0.89	4.12[f]	2.1	4.07[f]	0.017	4.2[f]	4.3[f]	4.23[f]
9-1, 13-2	1.07	4.14[f]	0.68	4.14[f]	0.61	4.14[f]	0.68	2.5	3.1	4.17[f]
10-1, 13-2	3.0	2.84	2.86	4.15[f]	4.1[f]	0.76	3.85	4.2[f]	4.3[f]	4.2[f]
Forward Fuselage[c]										
18, 26	0.64	0.31	0.03	5[e]	5[e]	2.8	0.003	0.01	0.025	0.46
18, 29	0.64	0.86	0.67	5[e]	5[e]	3.8	0.008	0.021	0.025	0.4
6, 9	0.98	1.6	0.43	5[e]	5[e]	3.9	0.06	0.098	0.4	0.47
7, 9	2.34	3.7	1.05	30.0[e]	30.0[e]	3.6	0.06	.173	0.42	1.1
Landing Gear[d]										
2, 4-1	1.13	1.4	2.2	0.55	0.87	2.04	7.4	8.8	(g)	(g)
Firewall[c],[d]										
9, 10	0.1/1.9	0.04/3.2	0.07/96	0.28/22.4	0.01/13.0	0.1/2.8	0.08/0.08	0.08/0.21	0.23/0.95	0.19/0.45
Mid Cabin[c],[d]										
4, 23	2.2/0.09	3.6/0.15	0.025/0.045	0.26/0.07	0.04/0.10	0.025/0.14	0.008/0.08	0.033/0.065	0.011/0.042	0.02/0.08
5, 23	2.2/0.41	4.5/0.44	0.061/0.16	0.67/0.66	0.09/0.66	0.07/0.25	0.06/0.135	0.076/0.22	0.07/0.2	0.08/0.44
6, 7	0.24/1.02	0.02/1.9	0.021/0.031	0.022/0.58	0.02/0.44	0.02/0.1	0.005/0.15	0.009/0.005	0.023/0.095	0.004/0.08
7, 8	0.02/4.3	0.03/6	0.03/0.91	0.05/5.5	0.03/3.1	0.03/1.8	0.006/0.22	0.01/0.54	0.03/0.54	0.04/0.52
5, 8	0.01/0.3	0.02/0.37	0.01/0.16	0.026/0.25	0.014/0.23	0.012/0.18	0.005/0.047	0.011/0.073	0.011/0.09	0.006/0.15

(a) Deflection in inches
(b) See Figure 5-3 and Table 5-2 for member location and description
(c) Member axial direction
(d) Member bending
(e) Exceed failure deflection value
(f) Exceeds bottoming deflection value
(g) Exceeds failure rotation
(h) a, b denotes member connecting mass a to mass b
(i) a-i denotes mass a and node i

TABLE 5-21. SUMMARY OF MAXIMUM STRUCTURE CRUSHING, MODEL A PARAMETER VARIATION STUDY

Location	Mass No.(b)	Direction	Nose-Down Conditions(a)						Nose-Up Conditions(a)			
			1	2	3	4	5	6	7	8	9	10
Nose Gear Tire	1	Longitudinal	1.8	2.2		4.2	4.0	0.83				2.5
		Vertical	3.6	3.7	3.2	3.9	3.8	2.27	3.7	4.0	4.1	3.5
Main Gear Tire	2	Longitudinal		2.1								
		Vertical	3.5	5.1	5.5	0.47		3.52	5.7	5.9	5.9	5.3
Forward Fuselage	9	Longitudinal	10.0	11.2	6.4	9.7	9.53	8.7				13.4
		Vertical	3.1	3.6	2.3	2.8	2.5	3.5			1.25	3.2
	29	Longitudinal	11.6	12.7	11.0	11.5	11.1	9.9(c)				25.7(d)
		Vertical	5.9	6.5	5.2	6.6	6.2	4.5		3.6	4.7	4.1
Mid-Fuselage	4	Longitudinal										
		Vertical										
	6	Longitudinal										
		Vertical				2.1		0.18		1.3	3.3	2.3
	18	Longitudinal										
		Vertical		0.07	3.2	6.3	3.7	3.5	1.6	5.3	7.3	5.7
	19	Longitudinal										
		Vertical										
	27	Longitudinal										
		Vertical									1.9	0.18
	28	Longitudinal										
		Vertical									1.8	0.19
Rear Fuselage	3	Longitudinal										
		Vertical								0.34	0.4	0.11
	30	Longitudinal										
		Vertical							2.1	2.7	2.7	1.3
Engine	13	Longitudinal	13.6	16.4		19.0	16.8	12.6				12.4
		Vertical	9.4	10.5	1.4	12.2	10.4	3.2		0.33	0.73	2.5

(a) Deflection in Inches
(b) See Figure 5-3 For Mass Locations
(c) Maximum Ground Deflection = 14.0 inches
(d) Maximum Ground Deflection = 16.2 inches

5.2.3 Model A Analysis Trends

The following figures show trends of occupant responses and impulses associated with changes in surface flexibility, impact angle, flight-path velocity and flight-path angle.

Figure 5-26 compares the analytical model lower and upper torso accelerations in the vertical and longitudinal directions as well as the computed impulses (g-msec) for the base nose-down impact (-15/-15/55) for a rigid versus flexible ground impact surface. The increase in longitudinal response as a result of impacting on a flexible terrain versus a concrete or rigid surface is dramatically illustrated in Figure 5-26. The increase can be seen to be several fold for the 0.00036 lb/in ground flexibility used in the analysis. While the results are sensitive to the properties used to represent the soil, the analysis clearly shows that for the impact condition analyzed there is a greatly increased potential for occupant injury when crashes occur on a flexible surface as opposed to a rigid surface.

Figure 5-27 compares occupant responses for a nose-up versus a nose-down impact onto a rigid surface. The flight-path angle (-15 degrees) and the flight-path velocity (55 mph) are the same. However, the nose-down pitch angle is -15 degrees, while the nose-up pitch angle is +15 degrees. While both conditions are relatively mild in terms of occupant responses, the nose-down condition generally results in occupant peak acceleration responses which are several times more severe than experienced for the nose-up condition.

Figure 5-28 presents occupant responses as a function of flight-path velocity. It can be seen for the impact attitude analyzed that an 18-percent increase in flight patch velocity results in dynamic response increases of 11 to 16 percent for the seat-lower torson representation and a 71-percent increase for the upper torso occupant mass in the longitudinal direction. The occupant exposure measured in terms of g-msec impulses, shows changes of -10 percent to +24 percent. Data (not shown) comparing a flight-path velocity change from 45 to 55 mph (22.2 percent) for a 45-degree impact angle indicates increases in the range of 5.5 to 9.3 percent for the occupant peak accelerations.

Figure 5-29 shows the trend for the occupant responses for a nose-down impact for three pitch and flight angles; -15, -30, and -45 degrees. The trend indicates that the occupant responses increase significantly in the longitudinal direction as the pitch and flight path angles increase from -15 to -45 degrees. The responses in the vertical direction show a different trend. The occupant lower mass vertical response increases as the impact angle increases while the trend for the occupant upper torso peak responses is to decrease as the impact angle increases and actually reverse direction at -45 degrees.

The data used for the -30/-30/65 and the -45/-45/55 conditions in Figures 5-28 and 5-29, respectively, are obtained from Table 6-3 column (b) wherein no seat-leg rupture and forward fuselage element rupture occurs. Using this data makes for a more meaningful comparison since the occurrence of a seat-leg failure changes the responses that the occupant exhibits and poses an additional threat to occupant survivability.

Figure 5-30 compares the occupant responses for the nose-up impact condition for variation in impact terrain as well for the effect of lift. The effect of lift is to reduce the vertical peak responses by as much as 41 percent while hardly affecting the longitudinal responses. The most significant effect of impacting onto a flexible soil is to increase the longitudinal peak responses by as much as a factor of three while actually resulting in lower vertical responses.

While the data provided in Figures 5-26 through 5-30 is limited in scope it serves to illustrate the type of information that can be developed from KRASH analysis for use in evaluating structural designs in a survivable crash environment. In addition to the occupant accelerations and impulses, the trends as a function of impact and design parameters can be developed for floor acceleration, member loads and deflections, spatial and temporal energy distribution, compartment volume change, structural failures, and vehicle motion. Some of the limitations associated with KRASH usage are related to the fact that the program is considered to be of a HYBRID nature (Reference 19), since it relies on a combination of analytical and empirical data as input. The development of KRASH has been oriented toward obtaining gross vehicle behavior for

analysis of aircraft during the early stages of a design wherein detailed data is limited and various design concepts are being considered. As such, the program is not intended to perform detailed analysis of structure. However, the quality of the data needed as input to KRASH can be improved upon with the use of detailed crash simulation currently in various stages of development (Reference 19) and familiarization with KRASH requirements gained through application of the program. Furthermore, the output from KRASH can be combined with special programs, such as SOM-LA (Reference 20) to perform a detailed evaluation of occupant potential for injury during survivable crash impact situations.

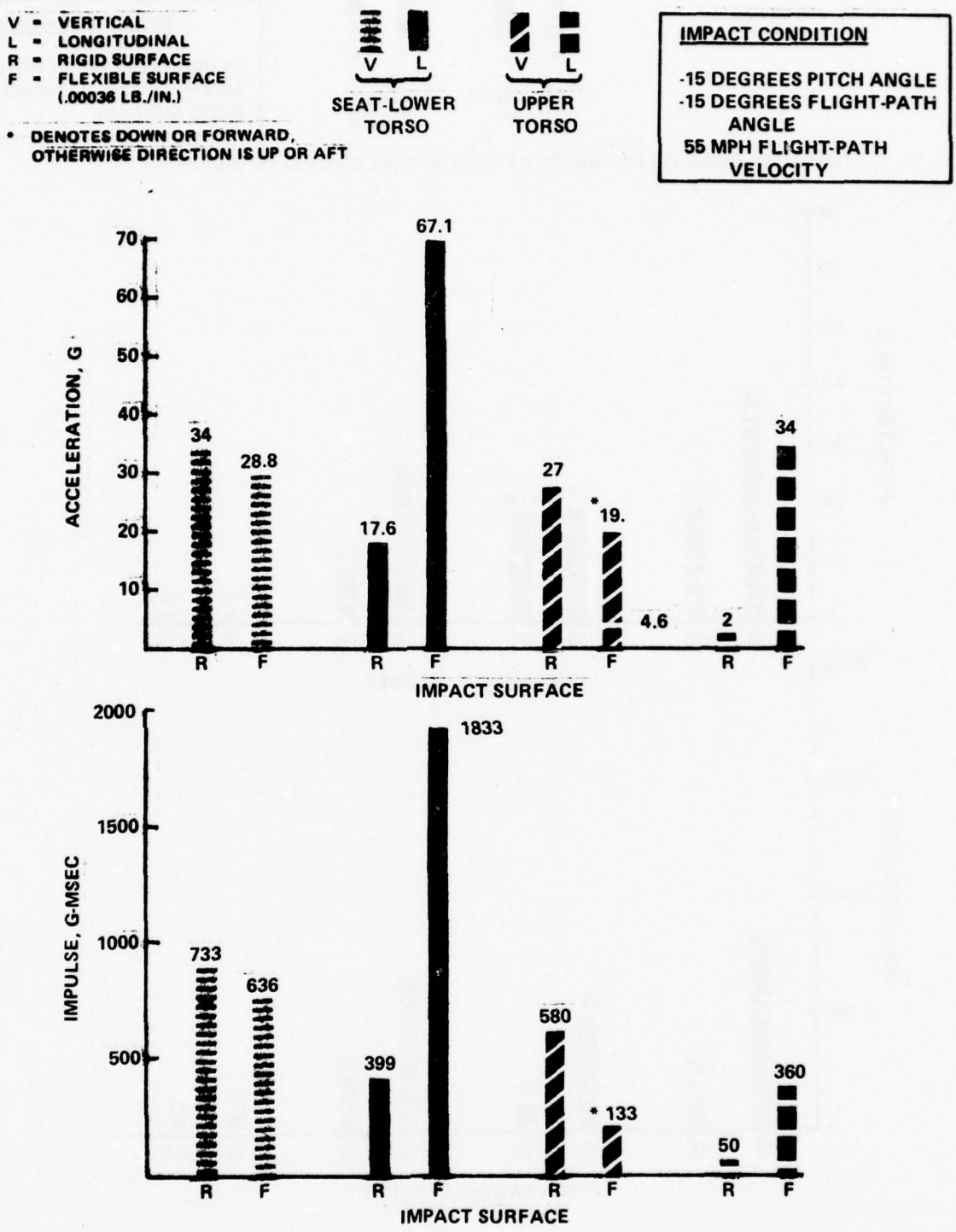

Figure 5-26. Comparison of Occupant Responses For Rigid Versus Flexible Ground Impact Surfaces

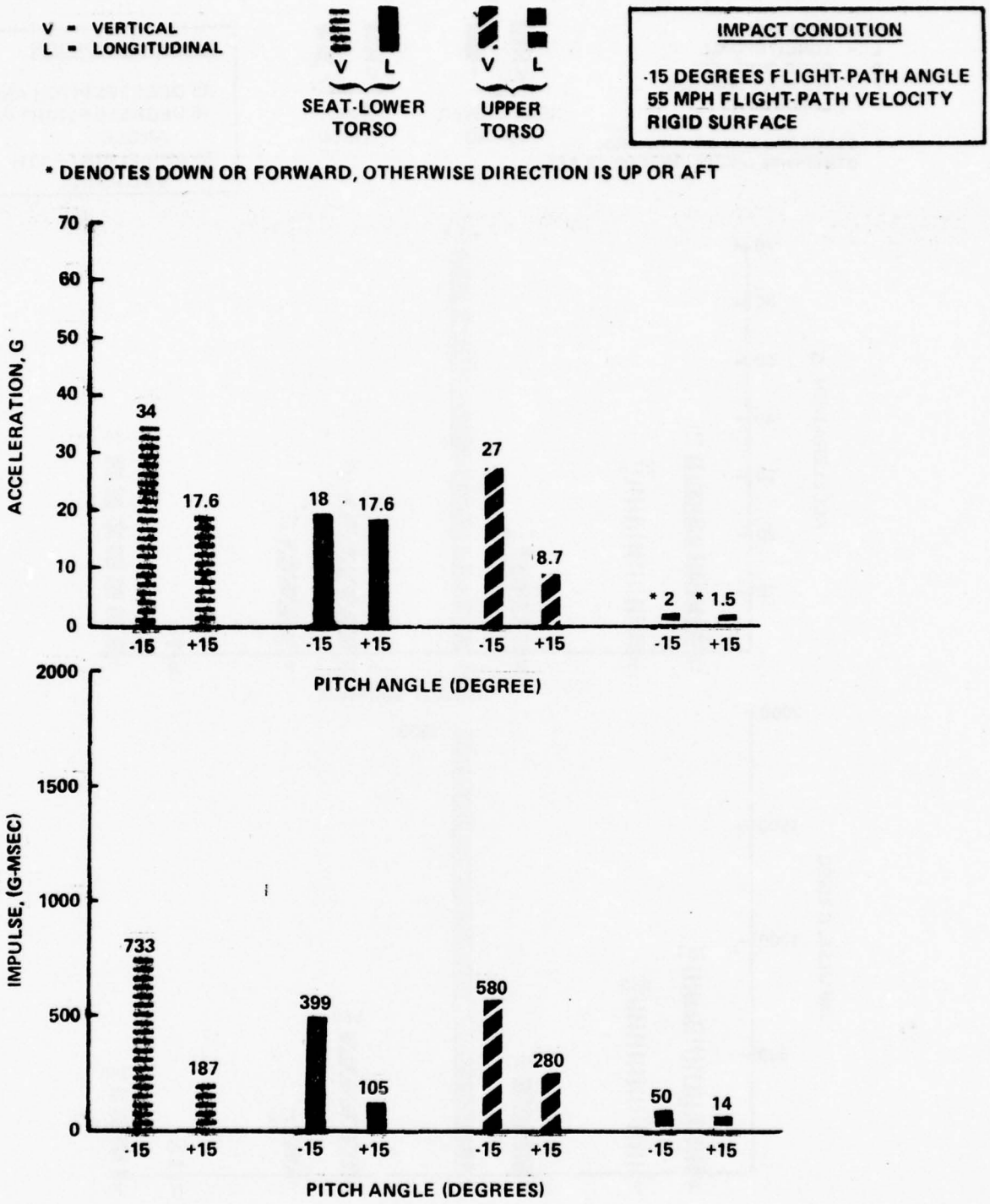

Figure 5-27. Comparison of Occupant Responses For Nose-Up Versus Nose-Down Impact Conditions

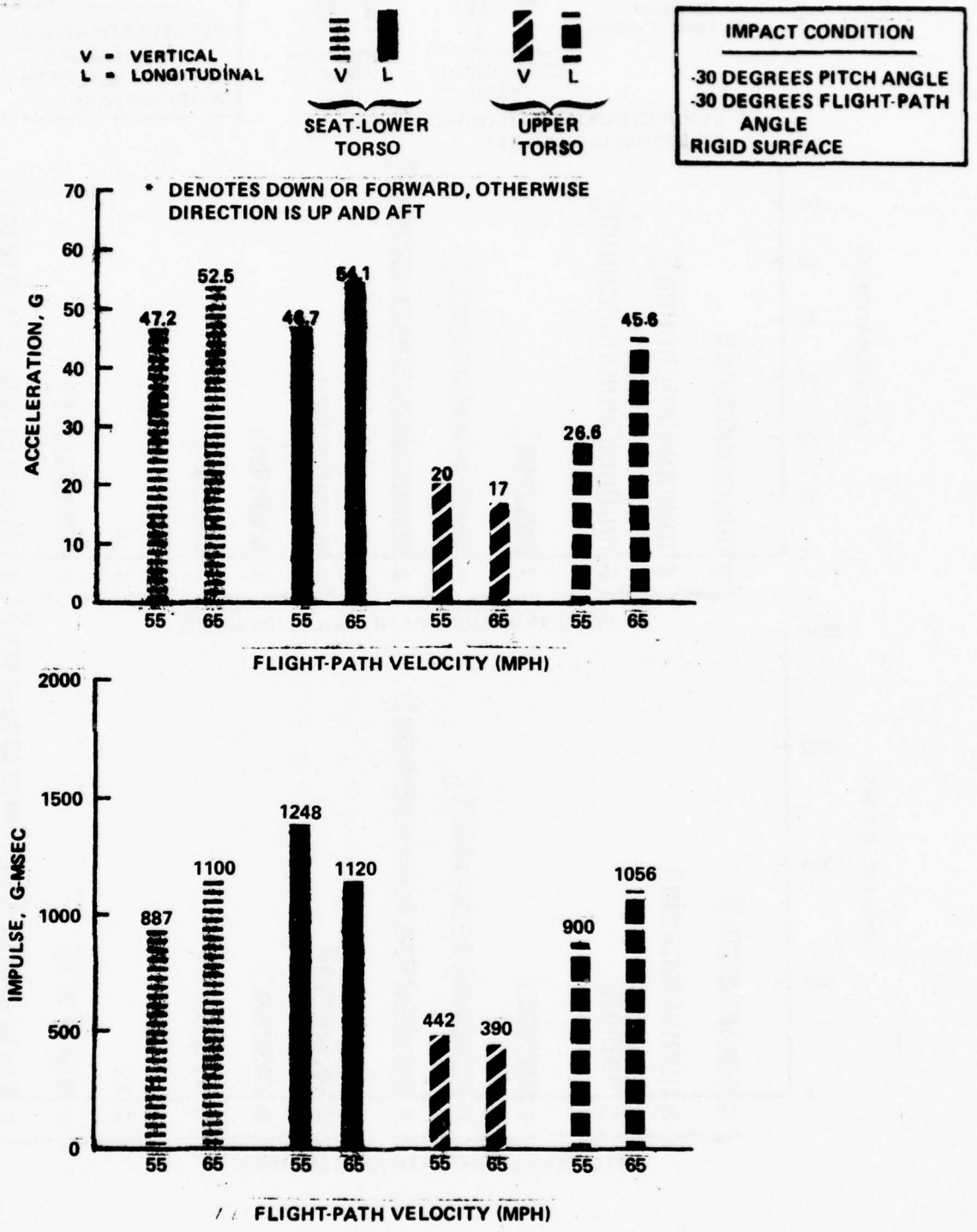

Figure 5-28. Comparison of Occupant Responses As A Function of Flight-Path Velocity

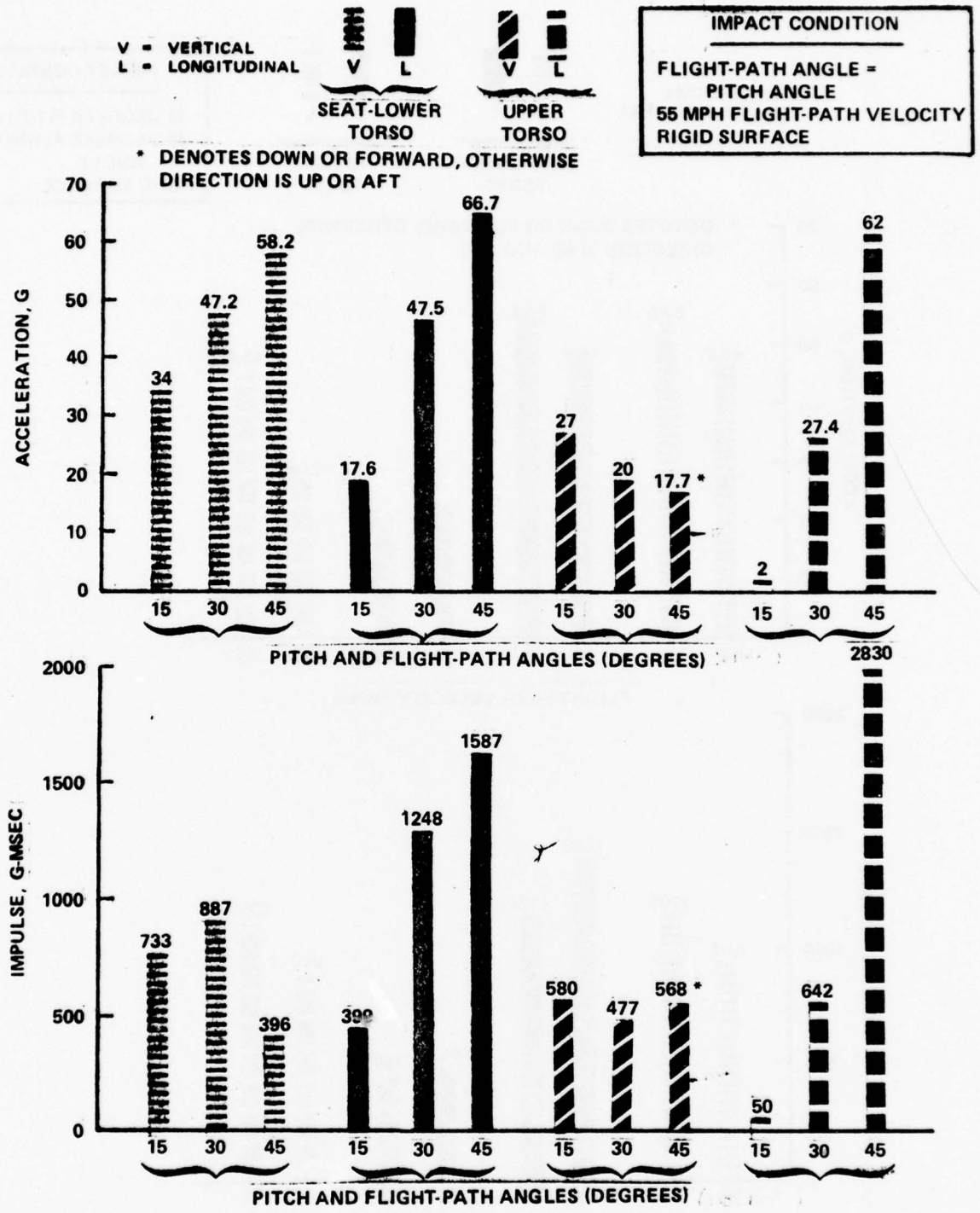

Figure 5-29. Comparison of Occupant Responses During Nose-Down Impacts for Pitch Angle Variations

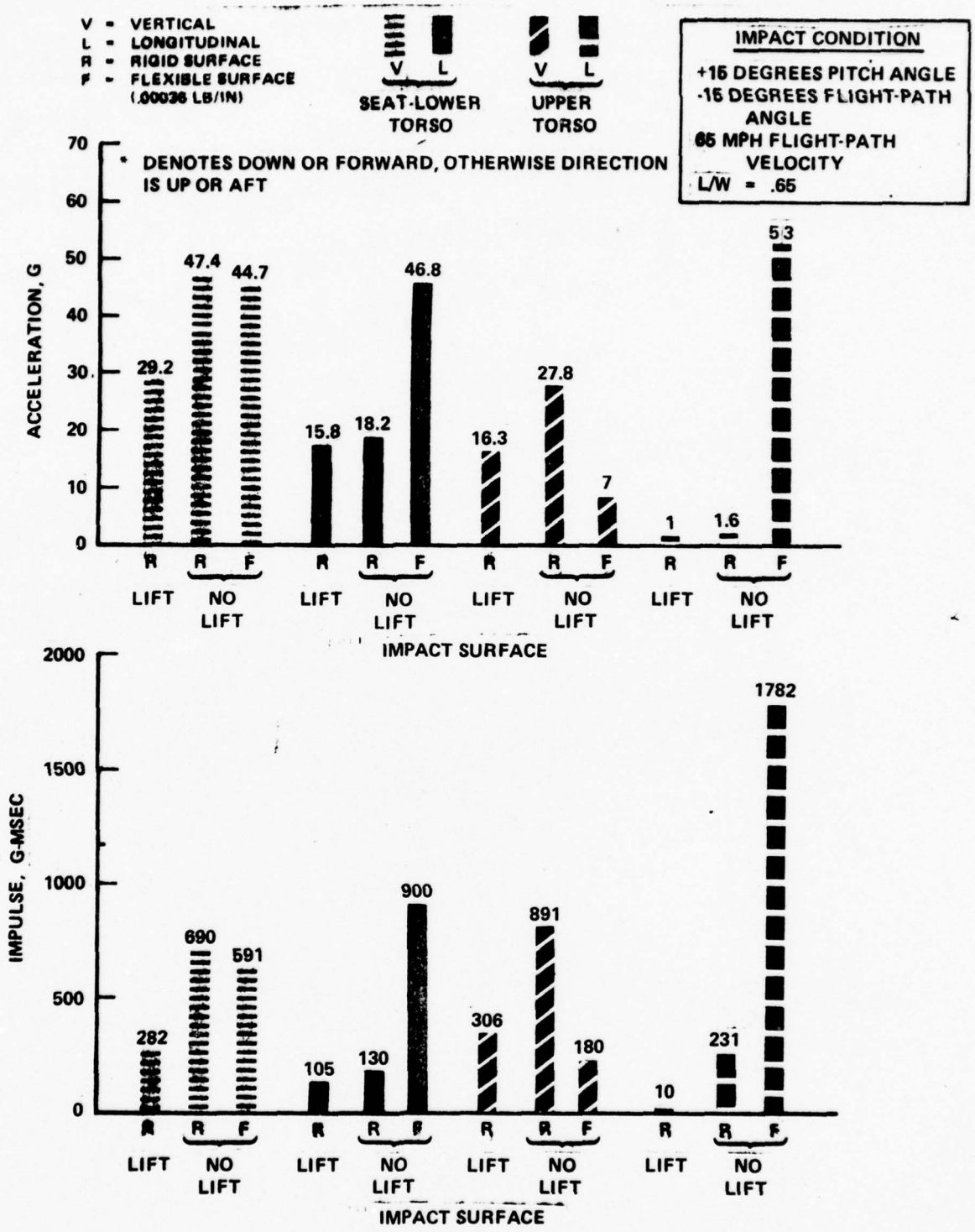

Figure 5-30. Comparison of Occupant Responses During Nose-Up Impacts for Flexible Ground Versus Rigid Ground and Lift Versus No Lift

SECTION 6

APPLICATION OF PROGRAM KRASH IN THE EVALUATION OF STRUCTURAL DESIGNS

6.1 PURPOSE

The purpose of the structural design evaluation is to demonstrate the application of program KRASH as an analytical tool to assist in assessing both the potential structural crashworthiness benefits as well as the effect of changing structural designs on structural crashworthiness capability. While it is desirable to achieve the highest level of structural crashworthiness attainable, there are many other practical considerations which must be included when evaluating new and/or improved structural design configurations. Among the major considerations are:

- Customer acceptance
- Operational performance
- Cost of implementation

Program KRASH has been shown capable of predicting vehicle gross behavior with reasonable and acceptable accuracy for several impact conditions. The program has also shown that it can be used to provide an accurate assessment of trends that can be expected for varying levels of crash impact severity. The correlation with the test data (Reference 1) and the results of the Task III parameter variation investigation (Section 5.0) have verified program KRASH's capability. Results to date, however, have not substantiated that KRASH or any other analytical tool can provide quantitative crash design loads for regions wherein interface loads are critical (i.e., seat-floor attachment).

6.2 DESIGNS CONCEPTS, WEIGHT AND COST

The assessment of potential crash improvement concepts and structural design changes was undertaken recognizing both KRASH's proven capabilities and potential limitations. The following design concepts were investigated:

- Extension of the forward fuselage region aft of the firewall by 18 inches
- The addition of a cargo pack on the underside of the fuselage extending from the aft bulkhead to the engine cowl region
- The addition of crushable material in the regions of the extended fuselage and in the cargo pack
- Provisions for breakaway of the wing at the fuselage-wing spar attachments
- Keel engine mount support in place of the current tubular mount design
- The restraint of occupants with harness and lap belts

The Model A airplane was used in the evaluation. Figure 6-1 shows a profile of the Model A airplane in its current standard length fuselage configuration. Figure 6-2 shows the airplane with an extended fuselage. The standard-length airplane with standard and extended cargo packs is shown in Figures 6-3 and 6-4, respectively. The extended-length airplane with standard and extended cargo packs is shown in Figures 6-5 and 6-6, respectively. Figure 6-7 shows the Model A airplane current tubular engine mount arrangement and the keel engine mount design concept.

Some of the design changes are for purposes other than crashworthiness improvements but may have an effect on crashworthiness. For example, the cargo pack without structural bulkheads and crushable material is a concept that is considered an option for current airplanes. The inclusion of crushable material would reduce the available cargo space. The extended forward fuselage has been added to an existing design (along with an extended aft fuselage) in the development of a stretched version of a Model A type airplane. A comprehensive crashworthiness analysis would include the aft fuselage change necessitated by performance considerations. The concepts allow for an assessment of the effect of the changes on the airplane's structure and occupant responses using KRASH. Along with the analytical results, estimates of weight and cost associated with the design changes are provided. The weight estimates are on a per airplane basis. The cost estimates per airplane are based on past experience and include nonrecurring and recurring engineering and production costs on the basis of a production run of 2000 airplanes (1000 per year for 2 years).

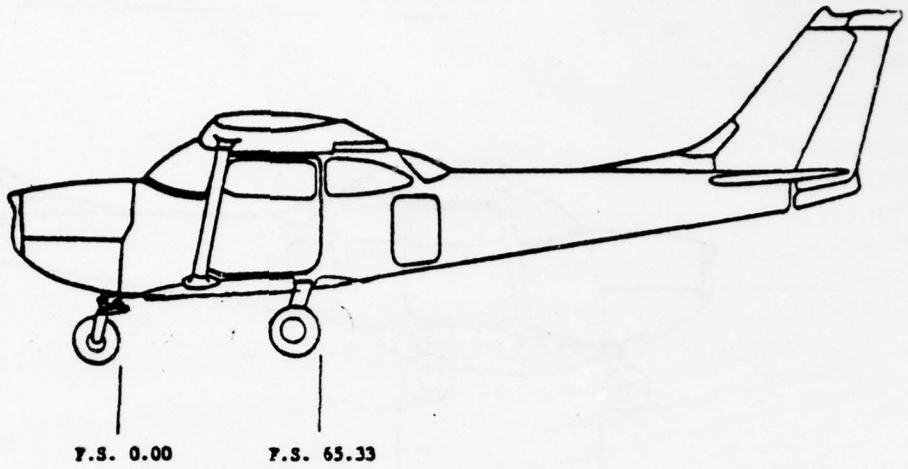

Figure 6-1. Current Standard Length Fuselage

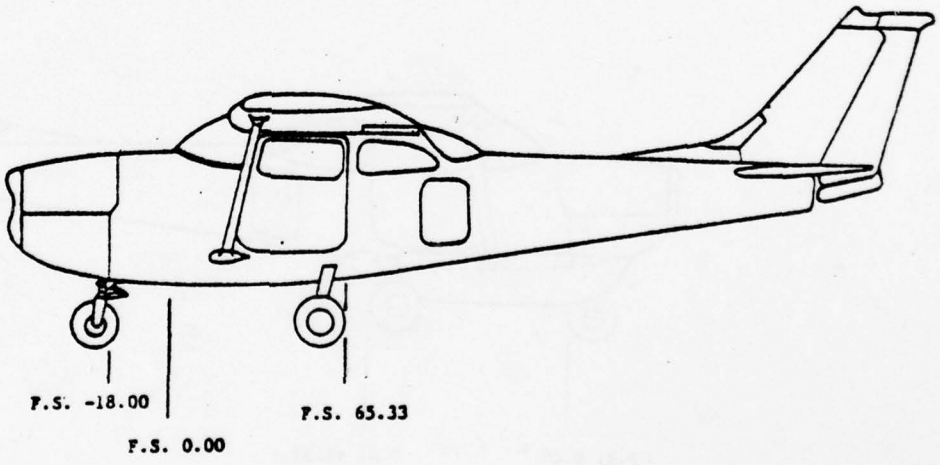

Figure 6-2. Extended Fuselage

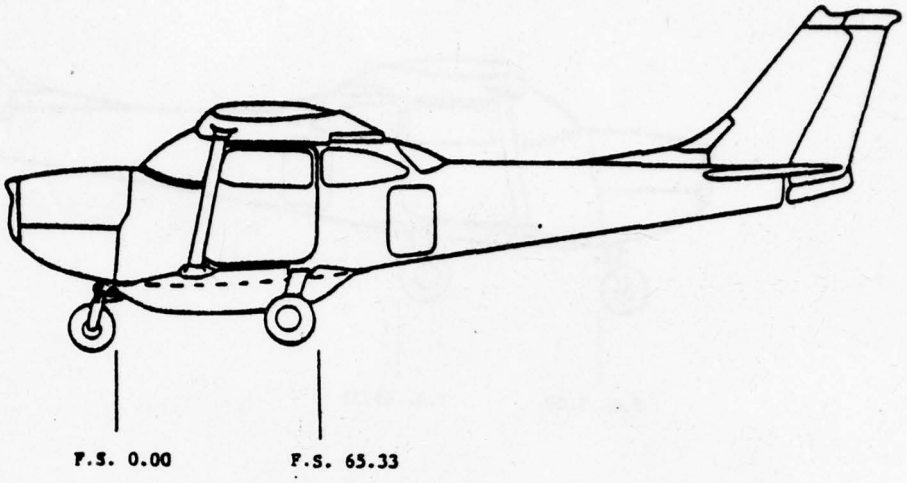

Figure 6-3. Standard Cargo Pack and Standard Length Fuselage

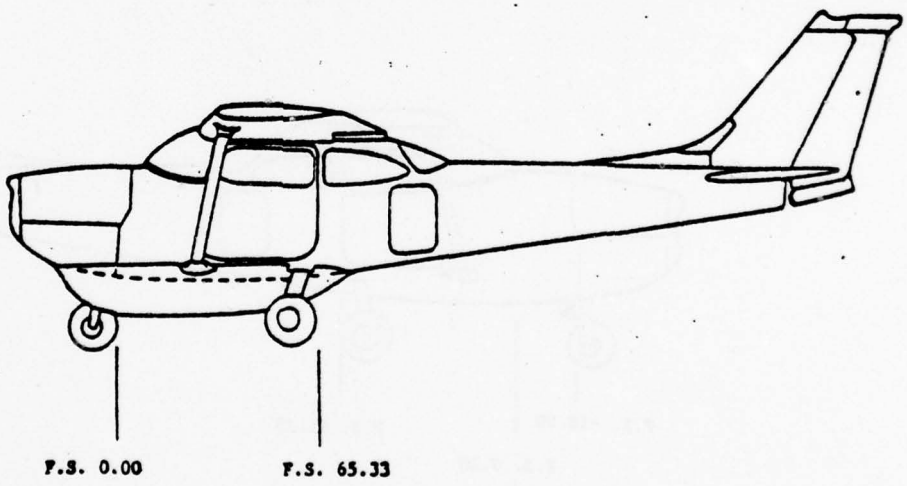

Figure 6-4. Extended Cargo Pack and Standard Length Fuselage

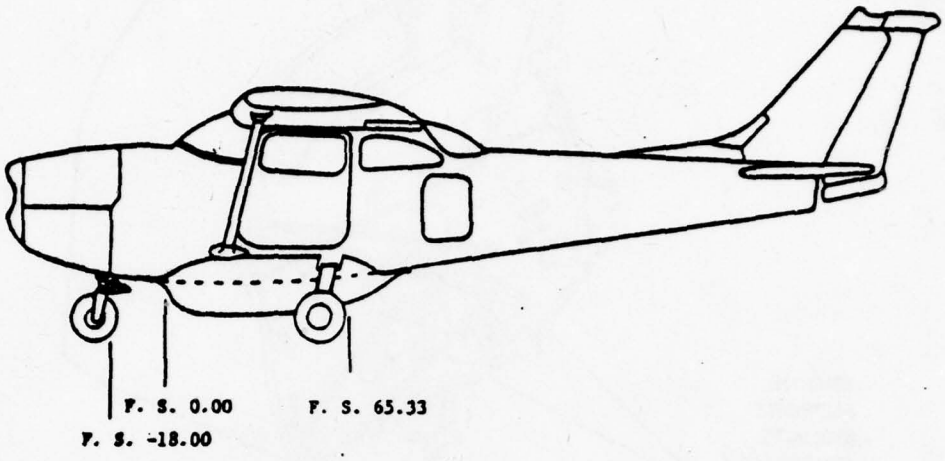

Figure 6-5. Standard Cargo Pack and Extended Fuselage

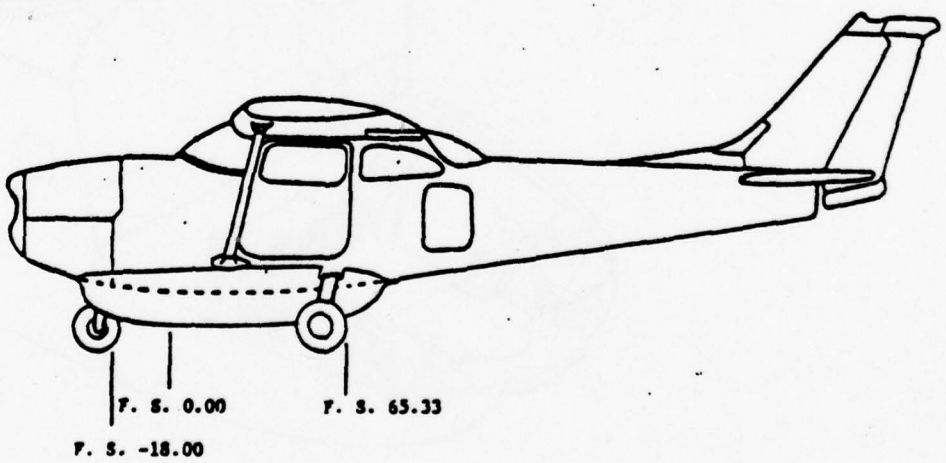

Figure 6-6. Extended Cargo Pack and Extended Fuselage

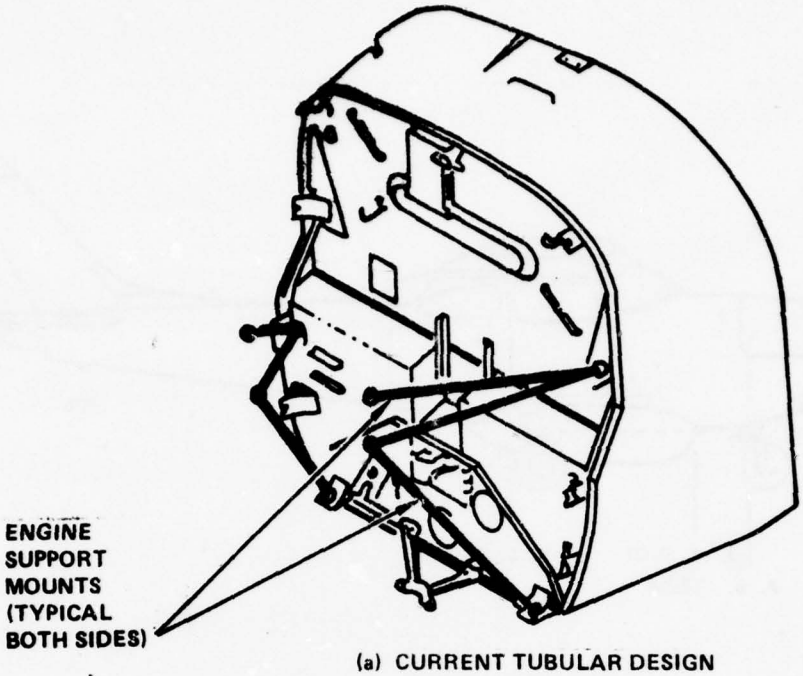

(a) CURRENT TUBULAR DESIGN

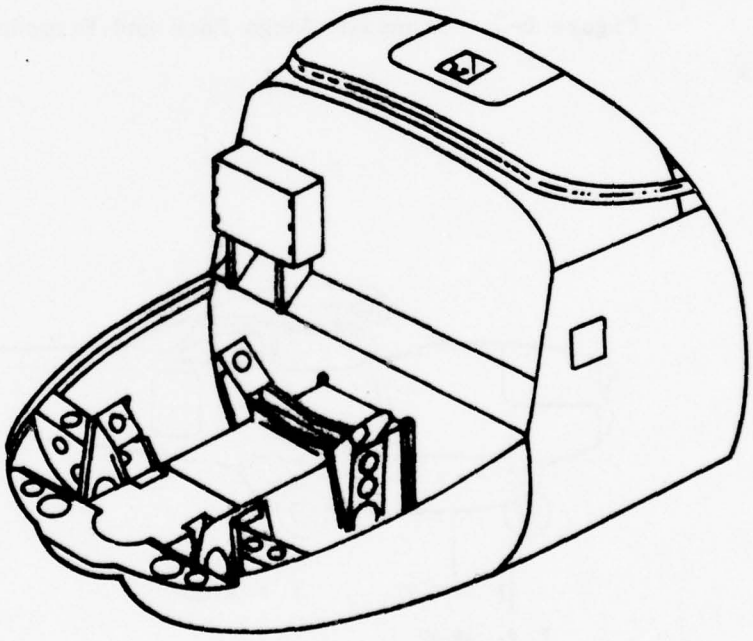

(b) KEEL DESIGN

Figure 6-7. Tubular and Keel Engine Mount Arrangements

Nonrecurring costs consist of engineering development and production tooling costs. Nonrecurring costs consist of continuing production and engineering support costs. The weight and cost estimates are based on all design changes being separate and distinctive decisions and incrementally added to an existing concept.

The combination of weight and cost penalties for more than one concept can be achieved by adding the respective penalties for each item. The design changes, while having potential application, are used in the crash evaluation investigative phase solely for demonstrating the manner in which program KRASH can assist in the design decision process. The results from KRASH have to be evaluated along with the other major considerations stated earlier.

Table 6-1 provides a summary of weight and cost associated with each design configuration. The weight and costs associated with concepts 1, 2, 7, 8 and 9 are based on historical data. The weight and costs associated with concepts 3, 4, 5 and 6 are extrapolated from concept 2 cost and weight data. The estimates are conservative in that some savings might be realized if two or more concepts were used simultaneously.

Table 6-2 shows the structural design changes that were evaluated using program KRASH and the Model A airplane configuration. The base nose-down impact condition (-30/-30/55)* onto a concrete surface was used as a reference base condition for the evaluation. With the exception of the impact onto soil terrain, the nose-down impact conditions represent a much more severe threat to occupant survivability than do the nose-up impact conditions.

6.3 RESULTS

During the parameter variation study (described in Section 5), the seat leg-floor intersection loads obtained by analysis were of sufficient magnitude to potentially cause a seat failure or result in the legs leaving the floor track. Either condition is undesirable, in that any failure of the seat-restraint system can result in severe to fatal injury to the occupants. These failures occured for the -30-degree, 65 mph impact condition (No. 2) and the

*$\theta/\gamma/V$ = impact angle (degrees)/flight-path angle (degrees)/flight-path velocity (mph)

TABLE 6-1. WEIGHT AND COST ESTIMATES FOR STRUCTURAL DESIGN CONCEPTS

Concept	Nonrecurring Cost (Dollars)	Recurring Cost (a) (Dollars)	Total Cost Per Airplane (a) (Dollars)	Additional Weight Per Airplane (Pounds)
1. Extended Forward fuselage	2,270,000	832,000	1551.00	33
2. Standard underside cargo pack fiberglass shell	409,613	2,774,387	1592.00	31.2
3. Standard underside cargo pack with reinforced bulkheads and standard airplane length	696,342	4,716,458	2706.00	53
4. Extended underside cargo pack with reinforced bulkheads and standard airplane length	854,000	5,782,377	3317.00	65
5. Standard underside cargo pack with reinforced bulkheads extended fuselage length	788,242	5,337,134	3061.00	60 (b)
6. Extended underside cargo pack with reinforced bulkheads and extended fuselage length	930,125	6,297,818	3612.00	71 (b)
7. Wing rear spar change	308,000	554,000	431.00	Negligible
8. Seat belt and harness	Negligible	224,000	224.00	2 per seat
9. Engine keel support structure	2,111,450	2,200,550	2156.00	18.7

(a) Based on 2000 airplane production run

(b) Incremental cost and weight of extended forward fuselage must be added to obtain total additional weight and cost.

TABLE 6-2. STRUCTURAL DESIGN EVALUATION CONDITIONS

Impact Condition Identification	Standard Airframe (a)	Extended Airframe (b)	Standard Cargo Pack (c)	Extended Cargo Pack (d)	Revised Rear Spar Attachment	Seat Belt and Harness	Keel Type Engine Mount
NOSE-DOWN(e)							
I-A	•		•				
-B	•			•			
-C		•					
-D		•		•			
-E	•				•		
-F	•					•	
-G	•						•

(a) See Figure 6-1
(b) See Figure 6-2
(c) See Figure 6-3
(d) See Figure 6-4
(e) -30/-30/55 Impact Condition unless otherwise stated
(f) Tubular engine mount support unless otherwise stated

-45-degree impact conditions (No. 4 and 5). In addition, several forward fuselage structural elements ruptured. To ascertain the effect on the occupant if no forward structure and seat system failures occurred, additional analyses for these three conditions were performed. The forward fuselage structural elements which previously ruptured were allowed to extend an additional 1.25 inches (≈25 percent increase). In addition, the strength capability of the seat leg-floor intersection connection was changed from a single-pin to double-pin strength insofar as airplane longitudinal direction loads are concerned, and no force cutoff in the seat leg axial direction was imposed on the seat leg-floor intersection representation. The removal of the latter restriction allows the seat leg to remain attached to the floor for evaluation purposes only, since, in reality, there is a possibility the seat rails could deform and the seat legs would become derailed, as observed in the full-scale crash tests. Comprehensive modeling of the seat leg-floor intersection is difficult without including additional extensive details. The results of revised analysis to determine the effect that seat leg-floor failures have on occupant responses is shown in Table 6-3. Without the seat-leg failures, the occupant loads generally increase since the seat system is still in contact with the floor structure and thus is excited by the floor response. However, none of the occupant responses, durations, or associated impulses appear to be of sufficient magnitude to result in serious injury to the occupant.

Table 6-4 compares the energy distribution associated with the different design concepts evaluated. While there are some differences insofar as individual energy components are concerned, total energy dissipation at comparable analysis times is approximately the same. Table 6-5 presents a summary of occupant responses for the different design concepts. The addition of the standard cargo pack changes the response for the occupants very little. In the nose-down impact, the forward fuselage structure impact with the terrain does not significantly influence the occupant responses. Table 5-21 shows

TABLE 6-3. COMPARISON OF OCCUPANT RESPONSES AND HUMAN TOLERANCE DATA WITH AND WITHOUT SEAT LEG FAILURES, NOSE-DOWN IMPACTS

Location	Direction	-30/-30/55[c] Base Condition	-45/-45/55[c] (a)	-45/-45/55[c] (b)	-45/-45/45[c] (a)	-45/-45/45[c] (b)	-30/-30/65[c] (a)	-30/-30/65[c] (b)	Tolerance Severe Injury
G peak									
Lower Torso	Up	47.2	34	58.2	40.3	34.5	41.3	52.5	80
	Down	28.	20	28.1	18.4	11.5	5.4	19.0	70
	Aft	46.7	61	66.7	56	61.3	54.4	541.	160
	Forward	31	40	12.1	23	5.8	26.7	38.6	90
Upper Torso	Up	20	12	10	9.9	10	16.2	17	80
	Down	2.9	2	17.7	16.1	17.5	2.3	6	70
	Aft	26.6	7.5	6.2	18	56.7	15.2	45.5	160
	Forward	-	-	-	-	-	-	-	90
Duration (d)									
Lower Torso	Up	40(0.02)	30(0.01)	30(0.005)	30(0.05)	20(0.026)	35(0.01)	40(0.01)	42(0.007 - 0.050)
	Down	-	16(0.02)	20(0.005)	-	10(0.004)	-	-	50(0.02 - 0.16)
	Aft	40(0.008)	60(0.005)	60(0.003)	50(0.005)	60(0.001	50(0.005)	40(0.012)	75(0.02, 44(0.1)
	Forward	-	-	-	20(0.005)	-	20(0.005)	20(0.005)	55(0.02), 40(0.1)
Upper Torso	Up	18(0.007)	10(0.01)	10(0.01)	10(0.01)	10(0.01)	16(0.015)	10(0.02)	42(0.007 - 0.050)
	Down	-	-	12(0.025)	-	10(0.020)	-	-	50(0.02 - 0.16)
	Aft	5(0.020)	4(0.04)	44(0.035)	10(0.04)	44(0.030)	14(0.01)	40(0.01)	75(0.02), 44(0.1)
	Forward	-	-	-	-	-	-	-	55(0.02), 40(0.1)
Maximum Impulse (g-msec)									
Lower Torso	Up	887	396	735	358	1064	874	1100	280 - 2100
	Down	81	120	143	152	62	-	168	1000 - 8000
	Aft	1248	896	1587	828	1736	865	1120	1500 - 4400
	Forward	300	180	24	168	-	398	300	1100 - 4000
Upper Torso	Up	442	244	164	203	167	351	390	280 - 2100
	Down	-	118	568	110	590	-	38	1000 - 8000
	Aft	900	254	2830	510	2358	546	1056	1500 - 4400
	Forward	-	-	-	-	-	-	-	1100 - 4000

(a) Occurrence of seat leg failure or pull-out from track
(b) No occurrence of seat leg failure or pull-out from track
(c) Impact angle/flight path angle/velocity
(d) G's and duration (seconds in parenthesis)

TABLE 6-4. COMPARISON OF SNERGY DISTRIBUTION AS A FUNCTION OF DESIGN CHANGES, NOSE-DOWN IMPACTS

	Base[d] Condition	Standard Cargo Pack (e)	Extended Cargo Pack (e)	Extended Forward Fuselage	Extended Forward Fuselage and Extended Cargo Pack	Restrained Occupant	Keel Type Engine Mount
Total Energy (in-lb)	3.05×10^6	3.12×10^6	3.14×10^6	3.13×10^6	3.215×10^6	3.05×10^6	3.1×10^6
Maximum Value[a]							
-Strain	8.4	8.6	11.33	9.18	10.55	9.9	10.48
-Damping	2.12	2.0	2.69	1.31	1.88	1.23	1.95
-Crushing	9.95	10.05	7.63	6.54	5.64	10.02	8.7
-Friction	35.37	35.55	35.84	29.28	32.78	35.85	35.56
Final Value[a]							
-Kinetic	44.57	44.84	46.34	52.02	48.98	45.06	45.83
-Potential	3.04	3.02	3.11	2.98	3.3	3.03	2.89
-Strain	7.9	7.7	10.15	8.55	9.94	7.6	9.38
-Damping	2.12	2.0	2.69	1.31	1.88	1.23	1.95
-Crushing	7.1	6.9	1.87	5.8	3.11	7.2	4.4
-Friction	35.37	35.55	35.87	29.28	32.78	35.85	35.56
Percent Energy Change[b]	+0.09	+0.08	+0.19	+0.13	0.20	+0.07	-0.02
Maximum Time of Analysis	0.120	0.120	0.120	0.120	0.120	0.120	0.120
Integration Interval (ΔT)(c)	30	30	30	30	30	30	30

(a) Percent of Current Total

(b) $\frac{\text{Final Total - Initial Total}}{\text{Initial Total}} \times 100$

(c) Microseconds

(d) All impact conditions are -30/-30/55

(e) Standard Fuselage Length

TABLE 6-5. COMPARISON OF OCCUPANT RESPONSES AND HUMAN TOLERANCE DATA FOR DESIGN CHANGES

Location	Direction	Base Condition (c)	Standard Cargo Pack	Extended Cargo Pack	Extended Fuselage	Extended Fus. and Cargo Pack	Restrained Occupant	Keel Type Engine Mount	Tolerance Severe Injury
G peak (a)									
Lower Torso	Up	47.2	47	47.7	30.5	33.8	47	53	80
	Down	28	10	18	4.3	18	10	23.3	70
	Aft	46.7	47	55.5	41.7	55	47	42.7	160
	Forward	31	31	48.6	44.5	36.3	31	31.5	90
Upper Torso	Up	20	20	19.5	14	14	35	15.4	80
	Down	2.9	2.9	3.9	-	5	-	2.4	70
	Aft	26.6	31	27.4	12.6	22.6	39	23.7	160
	Forward	-	-	-	-	-	-	-	90
Duration (b)									
Lower Torso	Up	40(0.02)	40(0.02)	46(0.007)	20(0.010)	20(0.018)	40(0.02)	42(0.012)	42(0.007-0.050)
	Down	-	-	-	-	-	-	-	50(0.02-0.16)
	Aft	40(0.008)	40(0.008)	55(0.004)	30(0.004)	40(0.007)	40(0.008)	25(0.027)	75(0.02), 44(0.1)
	Forward	-	-	-	40(0.002)	20(0.003)	-	-	55(0.02), 40(0.1)
Upper Torso	Up	18(0.007)	18(0.007)	18(0.005)	10(0.030)	10(0.020)	30(0.017)	14(0.006)	42(0.007-0.050)
	Down	-	-	-	-	-	-	-	50(0.02-0.16)
	Aft	20(0.020)	30(0.005)	24(0.010)	10(0.005)	20(0.005)	35(0.017)	20(0.010)	75(0.02), 44(0.1)
	Forward	-	-	-	-	-	-	-	55(0.02), 40(0.1)
Maximum Impulse (g-msec)									
Lower Torso	Up	887	887	960	620	720	887	752	280-2100
	Down	81	81	-	-	-	81	24	1000-8000
	Aft	1248	1248	1060	960	960	1248	1070	1500-4400
	Forward	300	300	400	400	280	300	160	1100-4000
Upper Torso	Up	400	442	550	450	700	1170	363	280-2100
	Down	-	-	-	-	-	-	-	1000-8000
	Aft	875	900	710	280	475	1400	540	1500-4400
	Forward	-	-	-	-	-	-	-	1100-4000

NOTES

(a) Peak in g's
(b) G's and duration (seconds in parenthesis)
(c) Analysis performed for -30/-30/55 impact conditions for all design configurations

that the forward fuselage springs do not contact the ground for the standard-length configuration base case. For the standard-length fuselage with the addition of the standard cargo pack, the forward fuselage crushes less than 0.5 inch. The extended cargo pack, however, extends into the cowl region and for the nose-down impact results in the firewall region contacting the ground surface earlier than the basic configuration without the cargo pack. The ground contact results in combined ground vertical and longitudinal loads acting on the vehicle. The aft acting ground load apparently causes the airplane to nose over as evidenced by a deeper penetration (larger compression) of the engine longitudinal ground contact spring and a lesser compression of the engine vertical ground contact spring. As a result, the occupant responses in the aft direction are higher than for the configuration without the cargo pack or with the standard cargo pack. However, none of the occupant responses are severe enough to be potentially hazardous to the occupants. While the seat leg-floor intersection loads increase with the use of the cargo pack (Table 6-6), double-pin attachments appear satisfactory. The analysis does not model seat leg derailment and cannot predict the occurrence or the consequence of this possible event. The use of the keel engine mount in place of a tubular mount results in lower impulses experienced by the occupant.

A comparison of maximum filtered accelerations for various design configurations is shown in Table 6-7. The use of either the standard or the extended cargo pack (configurations IA and IB) results in equal or greater peak responses at nearly all the locations shown. The use of the extended forward fuselage (configuration IC) generally results in lower peak responses at all the locations shown. The use of the extended fuselage and extended cargo pack (configuration ID) results in lower responses except for the engine cg and the occupant lower torso longitudinal responses. The use of the keel engine mount (configuration IG) has a mixed effect on the peak responses, some increasing, while others decrease.

Figures 6-8 and 6-9 present occupant response trend curves for the base nosedown condition versus the extended forward fuselage and engine keel support mount design concepts, respectively. From Figure 6-8 it can be seen that the occupant lower and upper torso responses are reduced from 26.3 to 35.4 percent

TABLE 6-6. COMPARISON OF SEAT LEG-FLOOR INTERSECTION LOADS AND DRI VALUES FOR DESIGN CHANGES, NOSE-DOWN IMPACT

Location	Base Condition	Standard Cargo Pack (d)	Extended Cargo Pack (d)	Extended Forward Fuselage	Extended Forward Fuselage and Cargo Pack	Restrained Occupant	Keel Type Engine Mount
		IA	IB	IC	ID	IF	IG
Seat Leg Floor Intersection(b)							
Forward Outboard	1986	1920	3675	2209	2535	1755	2270
Forward Inboard	2390	2544	2820	2033	2218	2349	2110
Rear Outboard	838	908	1470	1160	1236	1243	1206
Rear Inboard	1618	1591	3075	2181	1943	2211	2403
DRI							
Maximum Value	10.2	10.7	10.0	7.7	8.1	10.5	7.5
Time(c)	0.084	0.084	0.081	0.099	0.084	0.084	0.087

(a) Load in Pounds

(b) Load in Airplane Longitudinal Direction

(c) Time in Seconds after Impact

(d) Standard Fuselage Length

TABLE 6-7. MAXIMUM FILTERED ACCELERATIONS AND TIME TO OCCURRENCES, DESIGN CHANGE COMPARISON

Location	Direction	Design Configuration (d)											
		Base		IA		IB		IC		ID		IG	
		(a)	(b)	(a)	(b)	(a)	(b)	(a)	(b)	(a)	(b)	(a)	(b)
Engine cg	Up	48.7	0.075	44.8	0.081	56.4	0.075	56.3	0.078	85.1	0.072	42	0.066
	Down	24.4	0.105	32.2	0.120	58	0.102	15.1	0.108	28.5	0.108	18.8	0.114
	Aft	63.6	0.081	55.9	0.084	87	0.075	52.8	0.066	93.4	0.081	44	0.078
	Forward	11.9	0.117	6.5	0.120	24	0.108	14.4	0.117	14.4	0.069	-	-
Lower Torso	Up	47.2	0.078	47.4	0.078	49.7	0.069	30.5	0.087	33.8	0.069	53	0.114
	Down	28	0.090	35	0.120	18	0.117	15.8	0.141	18	0.120	23.3	0.120
	Aft	46.7	0.063	46	0.066	55.5	0.060	41.7	0.084	55	0.069	42.7	0.084
	Forward	31	0.120	26.7	0.117	48.6	0.114	44.5	0.093	36.3	0.093	31.5	0.093
Upper Torso	Up	19	0.081	20	0.081	19.5	0.075	14	0.081	14	0.081	15.4	0.084
	Down	2.9	0.117	3.7	0.114	3.9	0.111	6.1	0.135	5	0.120	2.4	0.117
	Aft	26.6	0.120	30.2	0.117	27.4	0.111	20.5	0.135	22.6	0.120	23.7	0.117
	Forward	-	-	-	-	-	-	-	-	-	-	-	-
Forward Seat Leg-Floor Intersection (c)	Up	56.2	0.078	57.5	0.078	65.9	0.072	34.4	0.078	48.2	0.081	61.4	0.078
	Down	20.2	0.120	27.6	0.120	17.5	0.117	10.3	0.096	3.7	0.093	15.4	0.093
	Aft	34	0.090	39.5	0.087	48.1	0.078	32.5	0.060	40.7	0.063	42.2	0.066
	Forward	23.6	0.096	22.2	0.099	8.9	0.108	30.7	0.072	12.7	0.102	25.2	0.117
Rear Seat Leg-Floor Intersection (c)	Up	43.9	0.087	45	0.084	45.2	0.081	26.3	0.135	30	0.075	41.1	0.114
	Down	30	0.120	33	0.120	15	0.117	22.7	0.147	14.5	0.120	23.5	0.120
	Aft	37.9	0.072	39.8	0.072	49.7	0.060	29.1	0.081	37.2	0.063	46.9	0.066
	Forward	34.3 18.8	0.087 0.096	21.6	0.099	23.9	0.090	12	0.090	23.7	0.057	22	0.117

(a) G peak value, 70Hz. Low Pass Filter
(b) Time in seconds after impact
(c) Outboard Location
(d) See Table 6-2 for design configuration identification

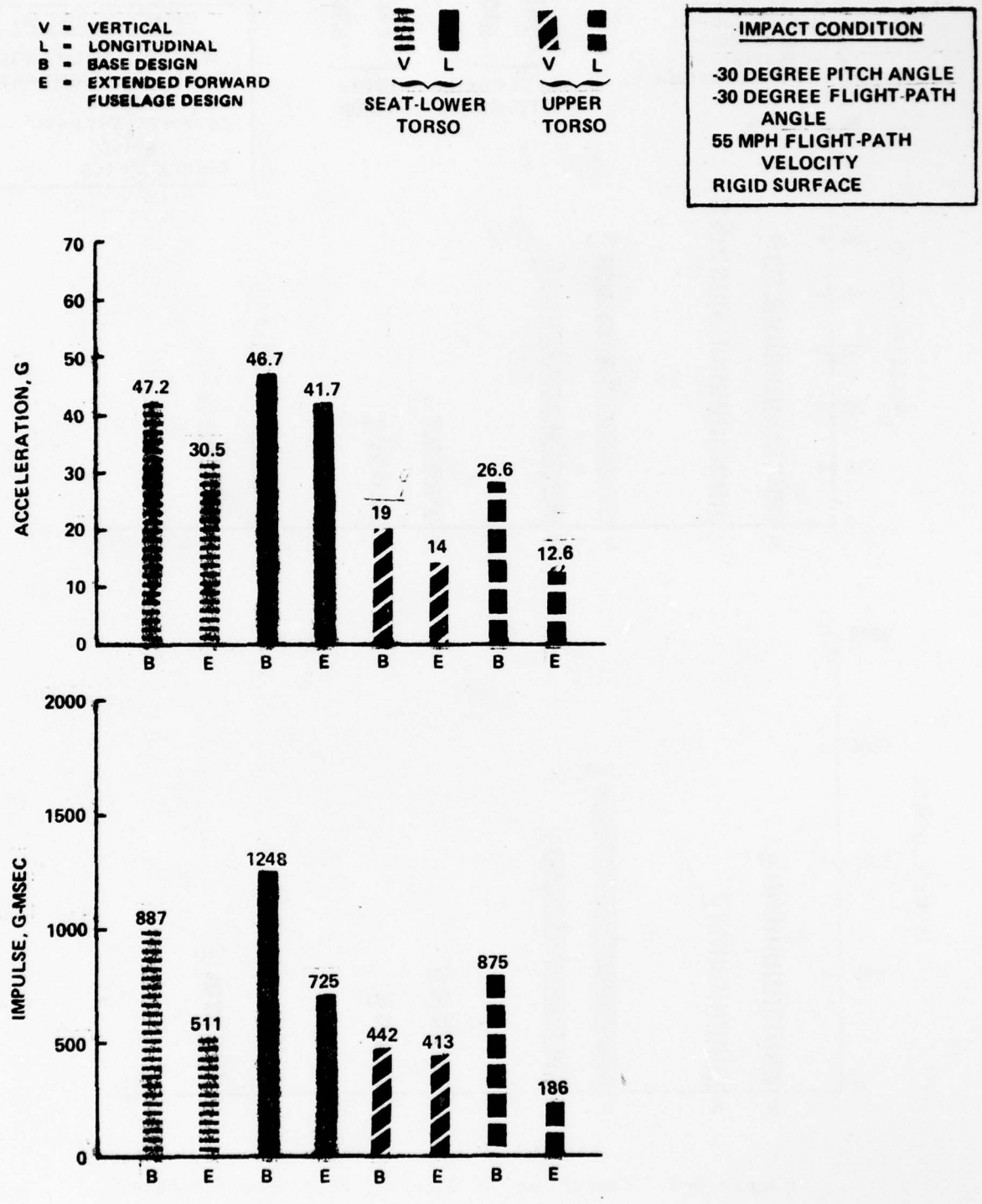

Figure 6-8. Comparison of Occupant Responses for Base versus Extended Forward Fuselage Design, 30 Degree Nose-Down Impact

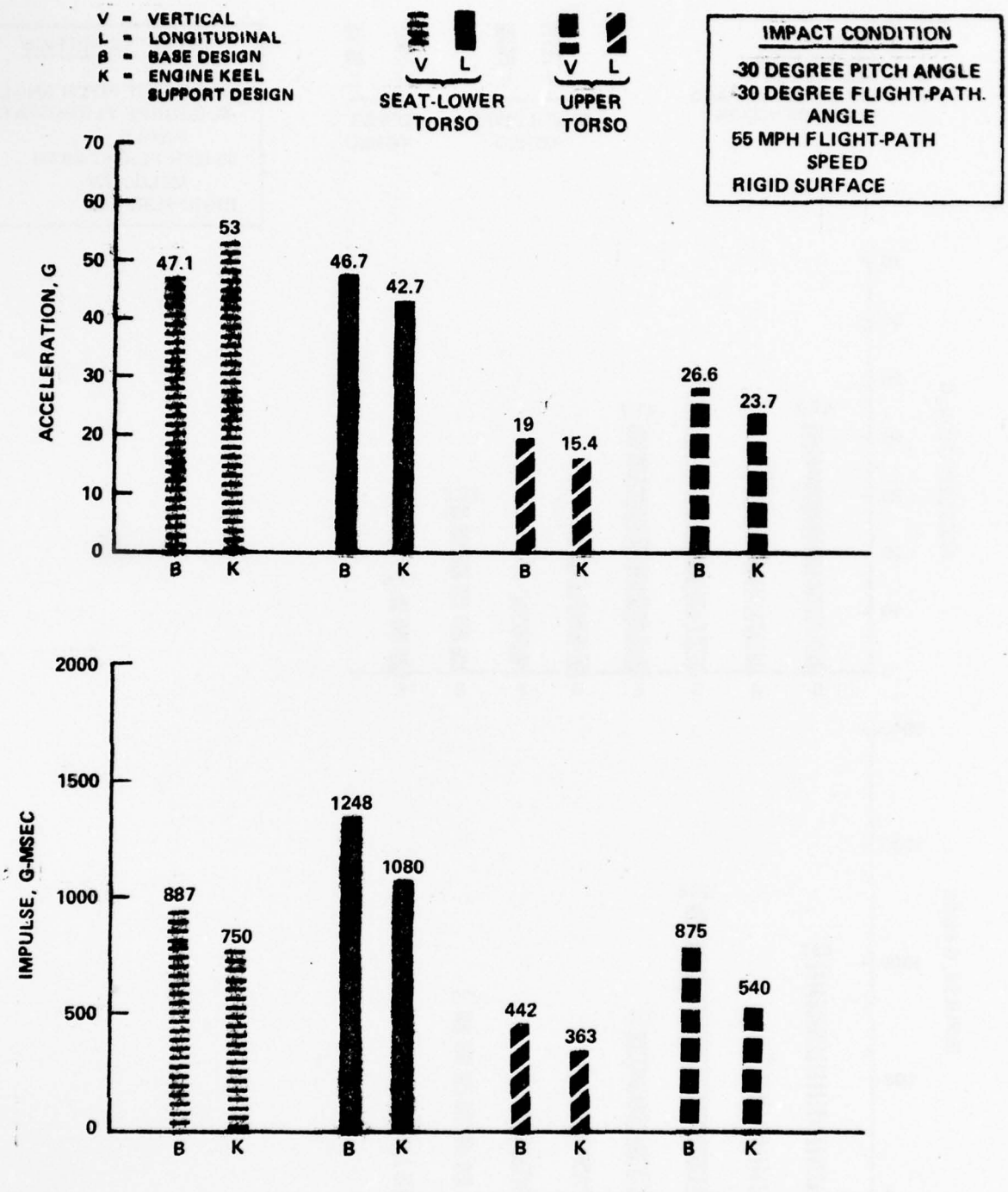

Figure 6-9. Comparison of Occupant Responses for Base versus Engine Keel Support Design Concept, 30 Degree Nose-Down Impact

in the vertical direction and from 10.7 to 52.6 percent in the longitudinal direction. In addition, the associated occupant exposures (g-msec) are correspondingly reduced significantly (39 to 79 percent) for this impact condition with the extended forward fuselage design concept. The trend observed in Figure 6-9 shows that with an engine keel mount arrangement in place of the tubular mount support, occupant peak responses decrease 10.9 and 18.9 percent for the occupant upper torso in the longitudinal and vertical directions, respectively. For the seat-lower mass representation, the peak response decreases 8.5 percent in the longitudinal direction but increases 12.5 percent in the vertical direction. The impulses which measure occupant exposure to acceleration forces decrease for both the occupant lower and upper masses by 13.5 to 38.3 percent.

Figure 6-10 shows the trend associated with the seat leg-floor intersection peak accelerations for the base design versus the extended forward fuselage and engine keel support designs. The extended forward fuselage results in a reduction in peak accelerations from 4.4 to 42.5 percent at the forward and rear locations in the vertical and longitudinal directions. The engine keel support design shows a decrease (5.9 percent) at the rear vertical location and increases (9.2 to 36.7) percent at the other floor locations and directions.

Figures 6-11 and 6-12 present trend curves for the occupant peak responses when comparing base design with the extended fuselage design for a -45 degree nose-down impact onto a rigid surface and for a -15 degree nose-down impact onto a flexible terrain, respectively. From Figure 6-11 it is computed that the occupant peak accelerations decrease by as much as 39 percent with reductions in occupant exposure as high as 71 percent. Figure 6-12 shows that the extended forward fuselage design during a nose-down soil impact generally exhibits equal or improved performance compared to the base design with regard to occupant peak response and impulses. The improvements range from 12.8 to 34.9 percent reductions in peak responses and 20 to 44 percent reductions in occupant response impulses.

Figure 6-13 shows the seat leg-floor intersection peak accelerations for the base versus extended forward fuselage designs for two impact conditions

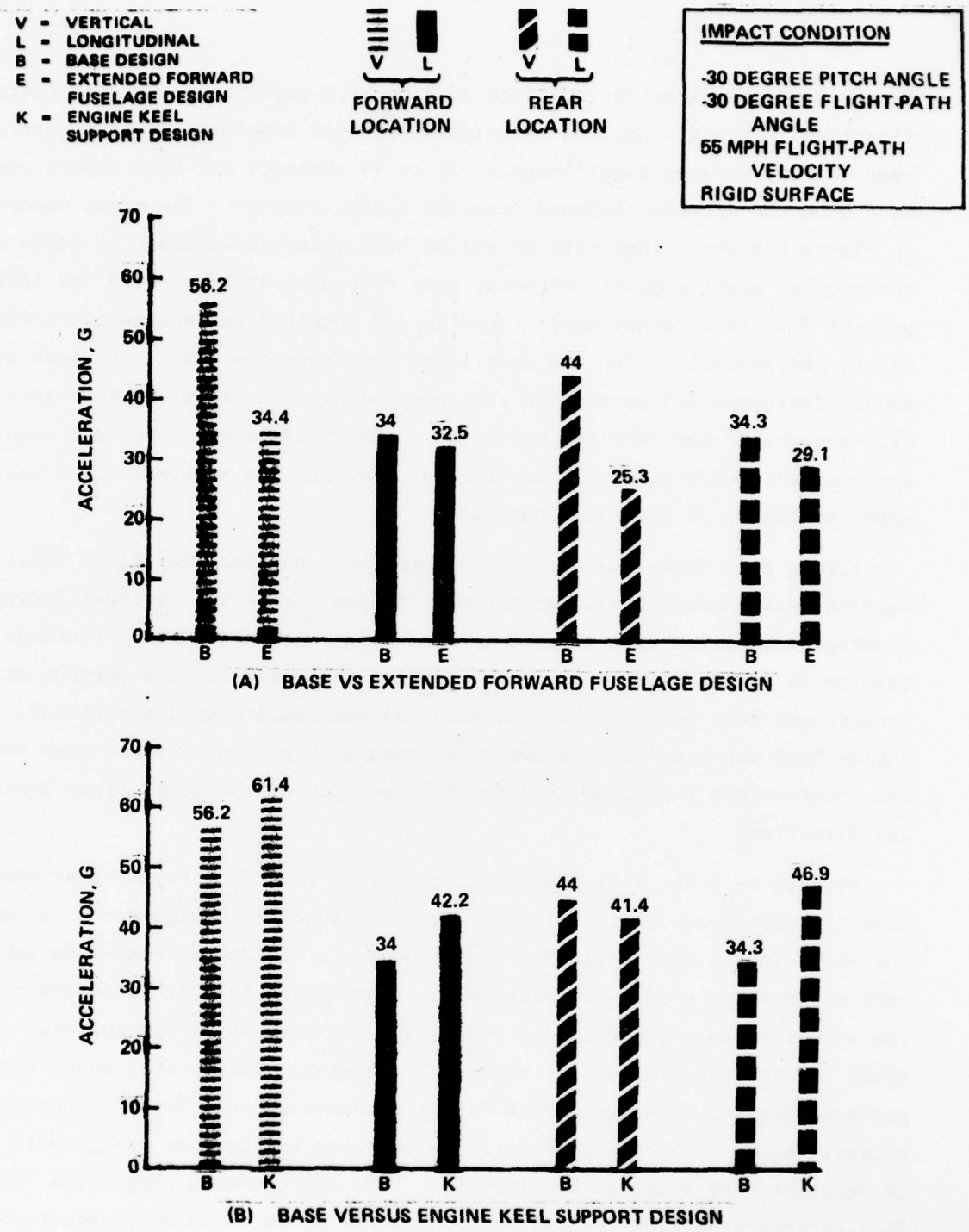

Figure 6-10. Comparison of Seat-Leg Floor Intersection Accelerations for Base versus Extended Forward Fuselage and Engine Keel Support Designs, 30 Degree Nose-Down Impact

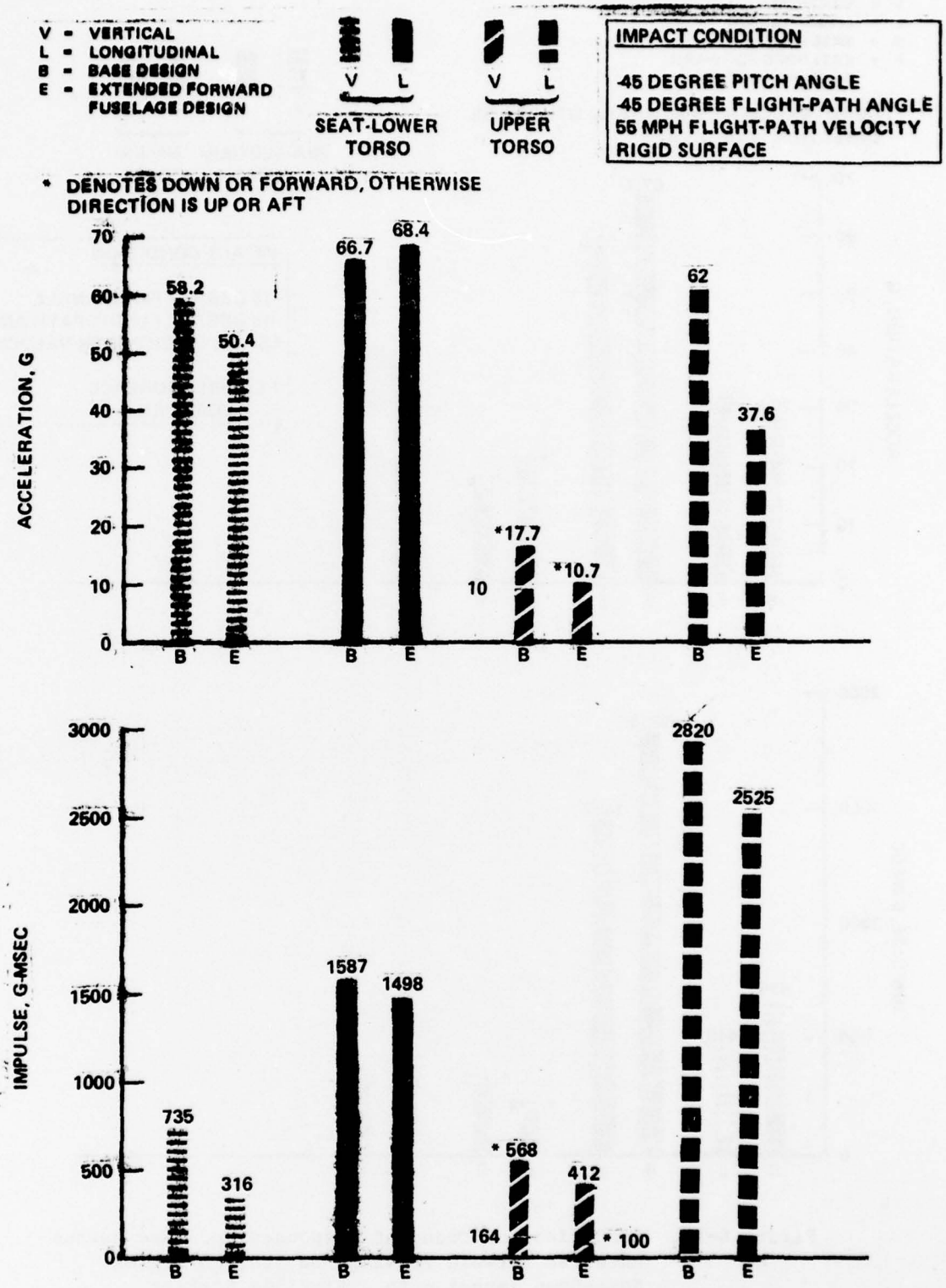

Figure 6-11. Comparison of Occupant Response for Base versus Extended Forward Fuselage Design, 45 Degree Nose-Down Impact

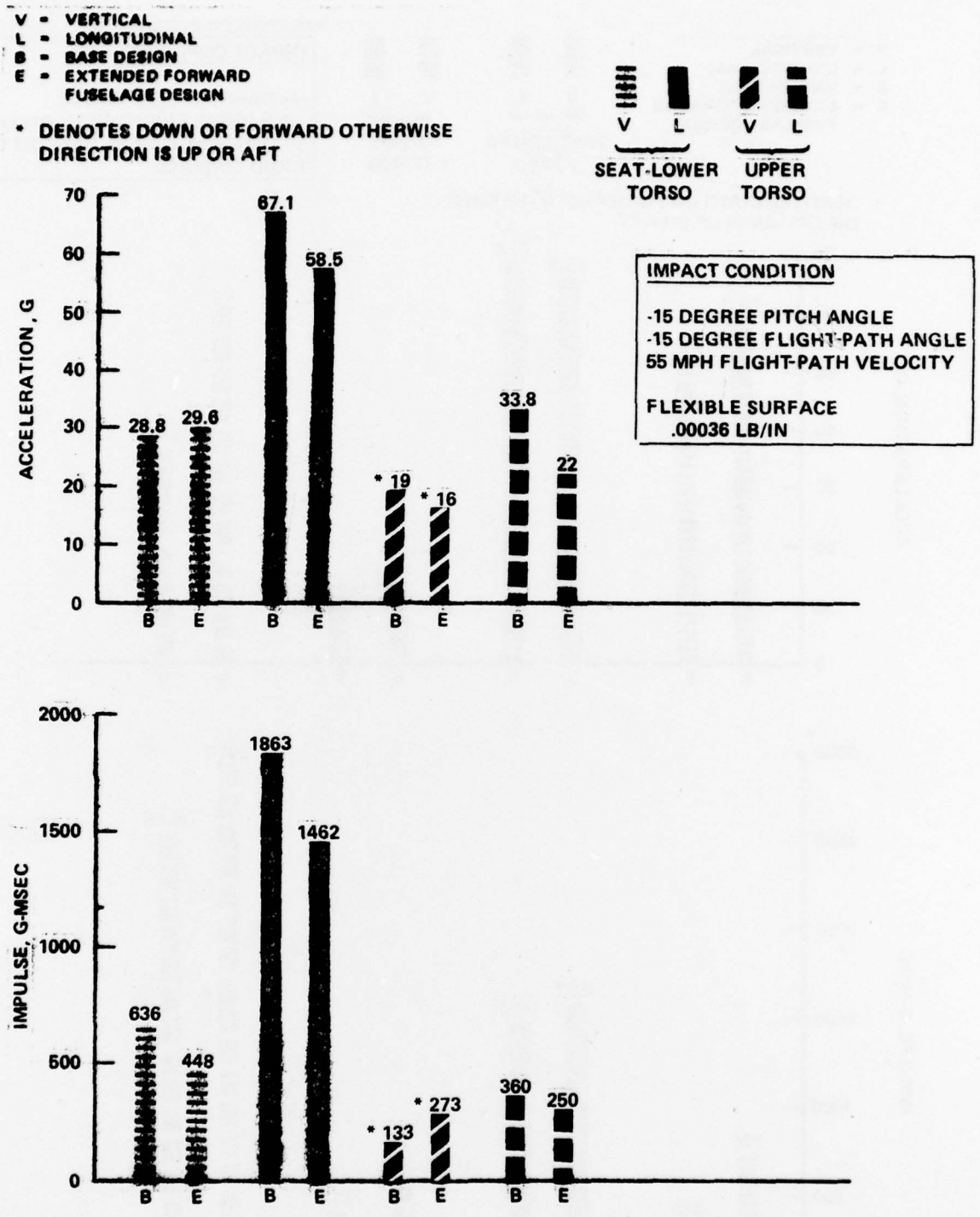

Figure 6-12. Comparison of Occupant Responses for Base versus Extended Forward Fuselage Design, 15 Degree Nose-Down Impact onto a Flexible Surface

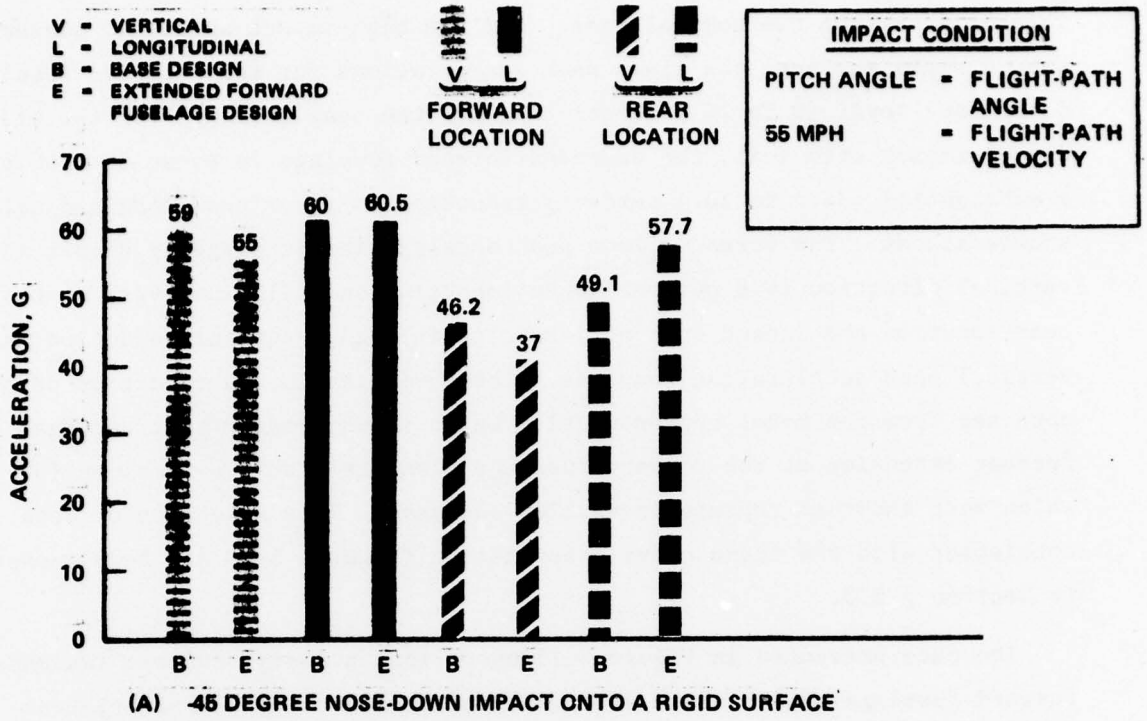

(A) -45 DEGREE NOSE-DOWN IMPACT ONTO A RIGID SURFACE

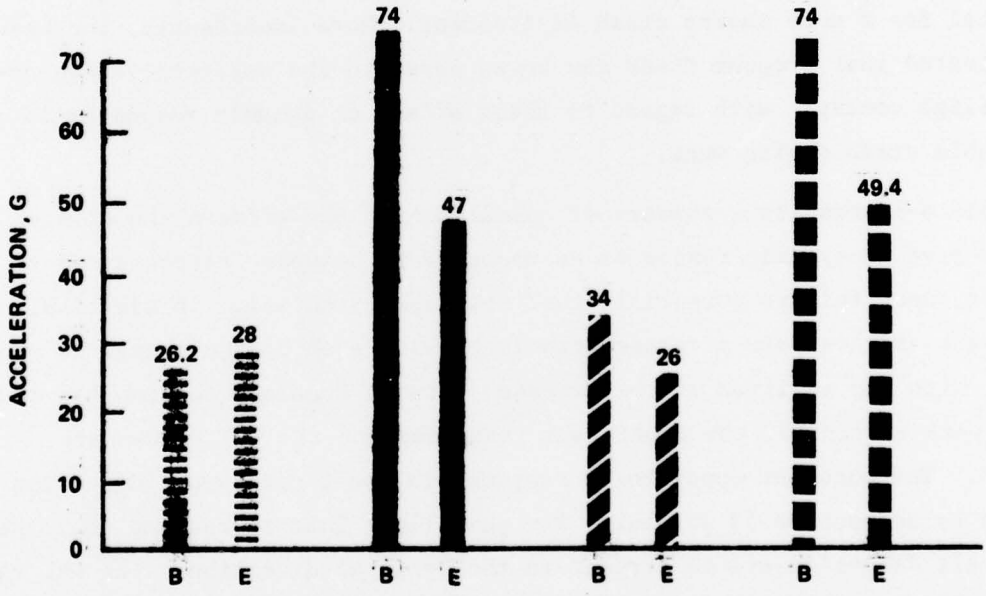

(B) -15 DEGREE NOSE-DOWN IMPACT ONTO FLEXIBLE SURFACE

Figure 6-13. Comparison of Seat-Leg Floor Intersection Accelerations for Base versus Extended Fuselage Design for Two Impact Conditions

which differ from the nominal case. For the high-impact angle (45 degrees) onto a rigid surface, the floor peak accelerations for the extended fuselage design are lower (0 to 20 percent) than for the base design. For the -15 degree impact onto soil, the extended forward fuselage is shown to result in a substantial (34.5 to 36.4 percent) reduction in floor peak longitudinal accelerations. The forward floor peak acceleration is slightly higher in the vertical direction (6.8 percent) when impacting on soil. However, at the rear location the impact onto soil results in a 23.5 percent reduction in vertical peak acceleration response. The 45-degree impact condition data is obtained from the model representation which shows greater seat strength and further extension of the forward fuselage elements (Table 6-3 column (b)), which were shown to rupture in earlier analyses. This selection of data is consistent with the trend curve presentation (Figures 5-28 and 5-29) described in Section 5.2.3.

The data presented in Figure 6-13 shows that a design concept (extended forward fuselage) which shows desirable energy-absorbing characteristics for a nominal impact condition also exhibits improved characteristics when evaluated for a more severe crash environment. More importantly, the results demonstrated that program KRASH can be an asset to the designer in evaluating design concepts with regard to their effect on dynamic responses in a survivable crash environment.

Table 6-8 presents a summary of comparison of the effects the design changes have on dynamic responses as measured by occupant response, floor response, seat failure potential, fuel spillage potential. In addition, the weight and cost per airplane associated with each design change is provided. With the addition of the extended forward fuselage section the occupant peak responses, the floor peak responses and the DRI values are reduced. The occupant upper torso response in the longitudinal direction reduces by as much as 50 percent. The peak floor load reduces up to 33 percent in the aft direction and 50 percent in the vertical direction. The DRI value reduces 23 percent. The longitudinal loads acting at the seat leg-floor intersection increase at the rear location by approximately 35 percent and change at the front location by +11 to -15 percent as compared to the base

TABLE 6-8. COMPARISON OF EFFECT OF DESIGN CHANGES ON STRUCTURAL AND OCCUPANT DYNAMIC RESPONSES AND FAILURES VERSUS INCREMENTAL WEIGHT AND COST

Design Configuration ID.	Design Change	Effect on				Weight (Pounds) per Airplane	Cost ($) per Airplane
		Occupant Response	Floor Response	Seat Failure Potential	Fuel Spillage Potential		
IA	Standard cargo pack with reinforced bulkheads	Negligible effect on occupant lower and upper torso responses and impulses. Increase DRI by 0.5 percent	Slight increase in peak loads (13 percent average)	Approximately same seat leg-floor intersection loads	None	53	2706.00
IB	Extended cargo pack with reinforced bulkheads	Maximum of 19 percent increase in peak longitudinal response. Approximately same impulse. Decrease DRI by 0.2 percent	Increase peak loads slightly (16 to 37 percent) except for the down direction (-15 to -50 percent)	Increase seat leg-floor intersection loads by 17 to 85 percent. Requires double-pin attachment	None	65	3317.00
IC	Extended forward fuselage	Decrease in lower and upper torso peak responses by 11 to 50 percent. Impulses reduced up to 68 percent in longitudinal direction and 30 percent in vertical direction. Decrease DRI by 23 percent	Decrease peak loads up to 50 percent in vertical direction and up to 50 percent in the longitudinal direction	Increase seat leg-floor intersection loads by 35 to 38 percent in rear change loads by +11 to -15 percent in front. Maximum load below single-pin attachment capability	None	33	1551.00
ID	Extended forward fuselage and cargo pack	Decrease DRI by 19 percent. Decrease upper torso peak loads by 15 to 30 percent. Change lower torso peak loads by 27.6 (longitudinal) to 18.7 percent (vertical). Decrease impulses by up to 46 percent except upper torso up direction (+75 percent) No critical load	Reduces peak loads in vertical direction (14 to 32 percent). Changes peak loads in longitudinal direction (+19.7 to -47 percent)	Increase seat leg-floor intersection loads by up to 47 percent. Maximum load below single-pin attachement capability	None	71	3612.00

TABLE 6-8. COMPARISON OF EFFECT OF DESIGN CHANGES ON STRUCTURAL AND OCCUPANT DYNAMIC RESPONSES AND FAILURES VERSUS INCREMENTAL WEIGHT AND COST (Continued)

Design Configuration ID.	Design Change	Effect on				Weight (Pounds) per Airplane	Cost ($) per Airplane
		Occupant Response	Floor Response	Seat Failure Potential	Fuel Spillage Potential		
IE	Lower rear spar tear out load design	None	None	None	Increased potential	Negligible	431
IF	Occupant Harness and seat restraint	Higher upper torso load. Higher upper torso impulse. No critical load	None	Increase seat leg-floor intersection loads 10 percent by up to 48 percent. Decrease foward intersection loads by 11 percent. Maximum load below single-pin attachment capability	None	2 per occupant	224 (with inertia reel)
IG	Change from tubular engine mount to keel type engine mount	Reduces upper torso acceleration by 11 to 19 percent. Reduce lower torso longitudinal response 8.5 percent. Increase lower torso vertical response 12 percent. Decrease DRI by 25 percent.	Increase longitudinal responses by 24 percent. Changes vertical response -63 to +8.8 percent	Increases seat leg-floor intersection loads an average of 6 percent.	None	18.7	2156

case values. However, the maximum load is 2209 pounds which is below the single-pin type attachment capability. The combination of extended forward fuselage and cargo pack results in higher occupant responses, seat leg-floor intersection loads and floor peak responses as compared to both the base case and the extended forward fuselage only configuration. Tables 6-5 and 6-6 show the results with regard to occupant responses, seat leg-floor interface loads and DRI values.

The extended forward fuselage configuration provides the greatest benefit in terms of increasing occupant potential for survival from a -30/-30/55 impact condition. The associated cost and weight for reducing the occupant responses, the DRI and floor peak response is $1551 dollars and 33 pounds per airplane. Other changes are more costly with regard to added weight and/or added cost, and do not provide clearly defined improved dynamic response capability. In fact, some changes could reduce the potential for occupant survival.

An assessment of crashworthiness capability requires consideration of energy distribution, structure peak loads and forces, occupant peak responses and acceleration histories. While not explicitly compared in the current evaluation, KRASH provides data such as structural crushing (represented by external springs) and internal member deflections, cabin deformation and energy distributions which are valuable inputs to assist in the evaluation of structural crashworthiness capability.

The assessment of the crash capability of the various design concepts requires additional analyses before decisions are finalized. For example, additional analysis should be performed to determine if the improvements obtained from the use of the extended forward fuselage will still be desirable for nose-up impacts and/or impacts onto soil. A partial demonstration of an expanded analysis encompassing more severe crash conditions was presented in the results provided in Figures 6-8 and 6-11 through 6-13. Conversely some design changes which, while not exhibiting obvious improvements for the base case impact conditions might prove beneficial for a more hazardous impact condition while not resulting in any deleterious effects for the more moderate impact conditions.

6.4 SUMMARY

The conditions analyzed demonstrate the application of program KRASH as an analytical tool for use in evaluating structural deformations and accelerations for:

- Design changes
- Potential improved crash dynamics
- Different airplane configurations
- A wide range of impact conditions

The evaluation demonstrates that: 1) not all crash design concepts will prove beneficial, from a crashworthiness standpoint; 2) improvements must be traded off against weight and cost penalties; and 3) other considerations, namely customer acceptance and operational performance along with the cost of implementation, must be weighed. On the other hand, the evaluation also shows that design changes which are desirable for utilitarian purposes, such as the standard cargo pack shell, can be evaluated for its effect on airplane post-crash behavior, dynamic response and energy absorbing characteristics.

The structural designs and impact conditions evaluated by program KRASH represent a sampling of the types of designs and conditions that can be assessed. KRASH, even considering its acknowledged limitations, has demonstrated its potential for use as an analytical tool to facilitate the future development of structural crashworthy airplanes. However, for KRASH to be an effective tool it must be part of a comprehensive procedure directed toward the development of a structural crashworthy airplane which includes:

- The definition of a survivable crash environment
- Quantitative measurements of structural crashworthiness capability
- Supporting procedures and/or substantiated data for structure nonlinear behavior
- User application and experience
- Continual updating of program KRASH and applicable modeling techniques to reflect user experience

Reference 6, Section 5 discusses the philosophy of a consistent crashworthy design and provides a general procedure for assessing a structural design with regard to a survivable crash environment.

SECTION 7

KRASH PROGRAMMER'S MANUAL

A Programmer's Manual (Reference 3) has been prepared for use with program KRASH. This manual, along with the program KRASH User's Manuals (References 4, 5, and 6), make up the documentation for the operation of the program.

In the programmer's manual, pertinent information is supplied which will facilitate bringing the program to an operational status on the user's computer system. The manual is divided into three sections, within which the program's system requirements, functional organization, and a demonstration problem are presented.

The basic core requirement for program KRASH is an equivalent 600K bytes of IBM 360 core (32-bit word and 4 bytes per word) when the overlay structure shown in Figure 7-1 is used. The program requires the use of 11 data storage units and one data storage tape unit.

Program KRASH is divided into three functional blocks. Within these blocks, computational analyses and data processing are performed, internal data storage and transfer are controlled, and external data storage and retrieval are managed. The computational analyses and data processing are performed in 22 of the 28 functional subroutines which make up the program. The other six subroutines are used for the management of the externally stored data. Internal storage and transfer of data are accomplished using the 51 common block regions included in the program.

A demonstration problem is included in the manual. The problem is designed to meet two objectives: 1) illustrate a comprehensive input data deck which exercises the commonly used options available to the user of the program, and 2) provide output data that can provide an operational and numerical check.

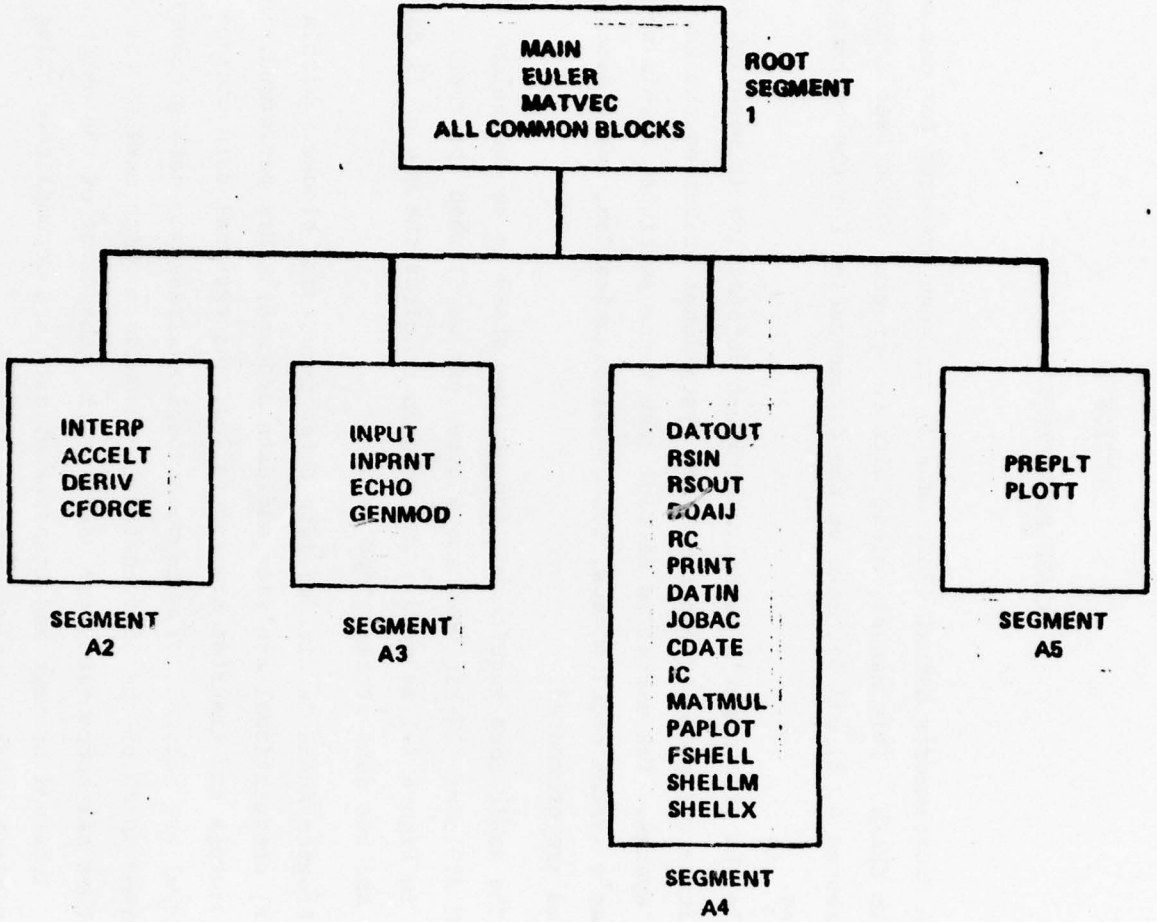

Figure 7-1. Overlay Map

SECTION 8

GENERAL AVIATION INDUSTRY WORKSHOP AND SEMINAR

As part of the Task III effort described in this report, a workshop and seminar is to be performed for the benefit of General Aviation Industry members. The purpose of the workshop and seminar is to:

- Familiarize potential users with program KRASH's capability and limitations.
- Disseminate information regarding KRASH experience and application toward structural design in a survivable crash environment.
- Provide general aviation members an opportunity to experience using program KRASH in evaluating a crash impact condition.
- Obtain feedback from poten ial users which will enhance program KRASH usage and documentation in the future.

The workshop and seminar is to be performed in two parts: instruction and workshop. The instruction portion will review the mechanics of program KRASH and the associated manuals, techniques involved in establishing models, type and source of data, selection of output data, and interpretation of results.

In the workshop, the participants will have a minimum of two crash cases to analyze. The first case will be established prior to the workshop and will be made available to all participants. The second case will be a variation of the first case and will be selected by the participants. The output from the KRASH analysis will be made available to the participants for future referral.

SECTION 9

CONCLUSIONS

Program KRASH's:

- Capability to perform satisfactory analysis to evaluate the gross behavior of general aviation airplanes exposed to a survivable crash environment has been successfully verified with experimental data from four full-scale crash tests.

- Usage as an analytical tool to assist in the evaluation of the effect of varied impact conditions, structural design changes and/or potential crash improvements on the airframe and occupant response for general aviation airplanes has been successfully demonstrated.

- Programming, modeling, data requirements, and limitations are documented in a three-volume User's Manual and a Programmer's Manual.

A computer program developed by Cessna provides the basis by which accident data can be compiled and evaluated with regard to airplane configuration and/or usage as a function of accident types, terrain, injuries, or fatalities to aid in determining crash environment design criteria.

The evaluation of light-fixed-wing airplane accident data, airplane design, and operating characteristics, along with the full-scale crash tests results indicate that:

- The basis for establishing potential crash design impact conditions is available for survivable crash conditions.

- The crash impact conditions and the occupant potential to survive the crash environment are influenced by airplane structural design and operating conditions. Thus the establishment of different airplane categories can assist in developing crash design criteria.

REFERENCES

1. Wittlin, G., Gamon, M.A. A METHOD OF ANALYSIS FOR GENERAL AVIATION AIRPLANE STRUCTURAL CRASHWORTHINESS, Lockheed-California Co., FAA-RD-76-123, U.S. Dept. of Transportation, Federal Aviation Administration, Systems Research and Development Service, Wash., D.C., Sept. 1976.

2. Wittlin, G., FULL SCALE CRASH TEST EXPERIMENTAL VERIFICATION OF A METHOD OF ANALYSIS FOR GENERAL AVIATION AIRPLANE STRUCTURAL CRASHWORTHINESS, Lockheed-California Co., FAA-RD-77-188, U.S. Dept of Transportation, Federal Aviation Administration, Systems Research and Development Service, Wash., D.C. Feb. 1978.

3. LaBarge, W.L., PROGRAM 'KRASH' PROGRAMMER's MANUAL, Lockheed-California Co., FAA-RD-78-120, U.S. Dept. of Transportation, Federal Aviation Administration, Systems Research and Development Service, Wash., D.C., (To Be Released).

4. Gamon, M.A., GENERAL AVIATION AIRPLANE STRUCTURAL CRASHWORTHINESS USER'S MANUAL - VOLUME I PROGRAM 'KRASH' THEORY, Lockheed-California Co., FAA-RD-77-189I, Federal Aviation Administration, Systems Research and Development Service, Wash., D.C., Feb. 1978.

5. Gamon, M.A., Wittlin, G., LaBarge, W.L., GENERAL AVIATION AIRPLANE STRUCTURAL CRASHWORTHINESS USER'S MANUAL - VOLUME II INPUT-OUTPUT, TECHNIQUES AND APPLICATIONS, Lockheed-California Company, FAA-RD-77-189II, Federal Aviation Administration, Systems Research and Development Service, Wash,. D.C., Feb., 1978.

6. Wittlin, G., GENERAL AVIATION AIRPLANE STRUCTURAL CRASHWORTHINESS USER'S MANUAL - VOLUME III, RELATED DESIGN INFORMATION, Lockheed-California Co., FAA-RD-71-189III, Federal Aviation Administration, Systems Research and Development Service, Wash., D.C., Feb. 1978.

7. JANE's ALL THE WORLD'S AIRCRAFT, 1975-1976, Jane's Yearbook, London, England, 1975.

8. Wullenwaber, G.E., A SUMMARY OF CRASHWORTHINESS INFORMATION FOR SMALL AIRPLANES FAA-FS-70-592-120A, FAA Aeronautical Center, Oklahoma City, Oklahoma, Feb. 1973.

9. Wilson, G.L., SELECTED CRASHWORTHINESS DATA FROM CAMI INVESTIGATIONS OF GENERAL AVIATION ACCIDENTS, FAA Project Number 74-779-120A, FAA Aeronautical Center, Oklahoma City, Oklahoma, May 1975.

10. ANNUAL REVIEW OF AIRCRAFT ACCIDENT DATA, NTSB-ARG-74-1 (1970) and NTSB-ARG-74-2 (1971), National Transportation Safety Board, Wash., D.C.

11. Snyder, DR. R.G., CRASHWORTHINESS INVESTIGATION OF GENERAL AVIATION ACCIDENTS, Presented at the Society of Air Safety Investigators, Fall Issue, 1975.

12. Bergey, K., THE DESIGN OF CRASHWORTHY GENERAL AVIATION AIRCRAFT, Univ. of Oklahoma, SAE Paper 740376, April 1974.

13. Vaughan, V., Jr., Alfaro, Bou E. IMPACT DYNAMICS RESEARCH FACILITY FOR FULLSCALE AIRCRAFT CRASH TESTING, NASA TN D-8179, April 1976.

14. Wittlin, G., Gamon, M.A., EXPERIMENTAL PROGRAM FOR THE DEVELOPMENT OF IMPROVED HELICOPTER STRUCTURAL CRASHWORTHINESS ANALYTICAL AND DESIGN TECHNIQUES, Lockheed-California Co., USAAMRDL 72-72, U.S. Army Air Mobility Research and Development Laboratory, Ft. Eustis, Va., May 1973.

15. Wittlin, G., Park K.C., DEVELOPMENT AND EXPERIMENTAL VERIFICATION OF PROCEDURES TO DETERMINE NONLINEAR LOAD-DEFLECTION CHARACTERISTICS OF HELICOPTER SUBSTRUCTURES SUBJECTED TO CRASH FORCES, USAAMRDL TR-74-12, U.S. Army Air Mobility Research and Development Laboratory, Ft. Eustis, Va., May 1, 1974.

16. Badri Nath, Y.V., MATH MODEL KRASH-CH-47A CRASHWORTHINESS, Boeing Vertol Co. Applied Technology Laboratory, U.S. Army Research and Technology Laboratory, U.S. Army Research and Technology Laboratory (AVRADCOM), Ft. Eustis, Va. (to be released).

17. Turnbow, J.W., et al, CRASH SURVIVAL DESIGN GUIDE, USAAMRDL-TR-71-22, Eustis Directorate U.S. Army Air Mobility and Research Laboratory, Ft. Eustis, Va., Oct. 1971.

18. Eiband, M.A. HUMAN TOLERANCE TO RAPIDLY APPLIED ACCELERATIONS: A SUMMARY OF LITERATURE, NASA MEMO 5-19-59E, 1959.

19. Cronkite, J.D., Winter, R.D., Singley III, G.T., INVESTIGATION OF THE CRASH IMPACT CHARACTERISTICS OF COMPOSITE AIRFRAME STRUCTURES, presented at the 34th Annual Forum of the American Helicopter Society, Washington, D.C., May 1978.

20. Laananen, D.H., DEVELOPMENT OF A SCIENTIFIC BASIS FOR ANALYSIS OF AIRCRAFT SEATING SYSTEMS, FAA-RD-74-130, U.S. Department of Transportation, Federal Aviation Administration, Systems Research and Development Service, Washington, D.C., January 1975.